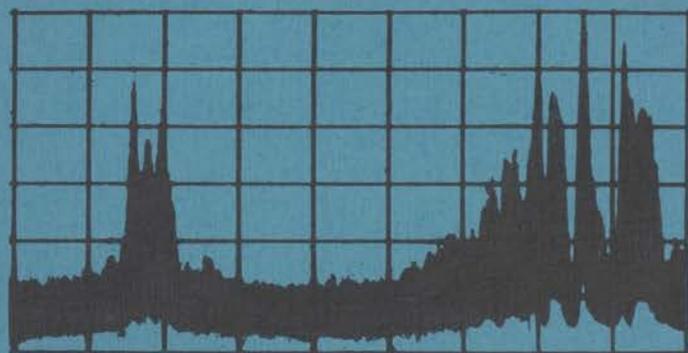


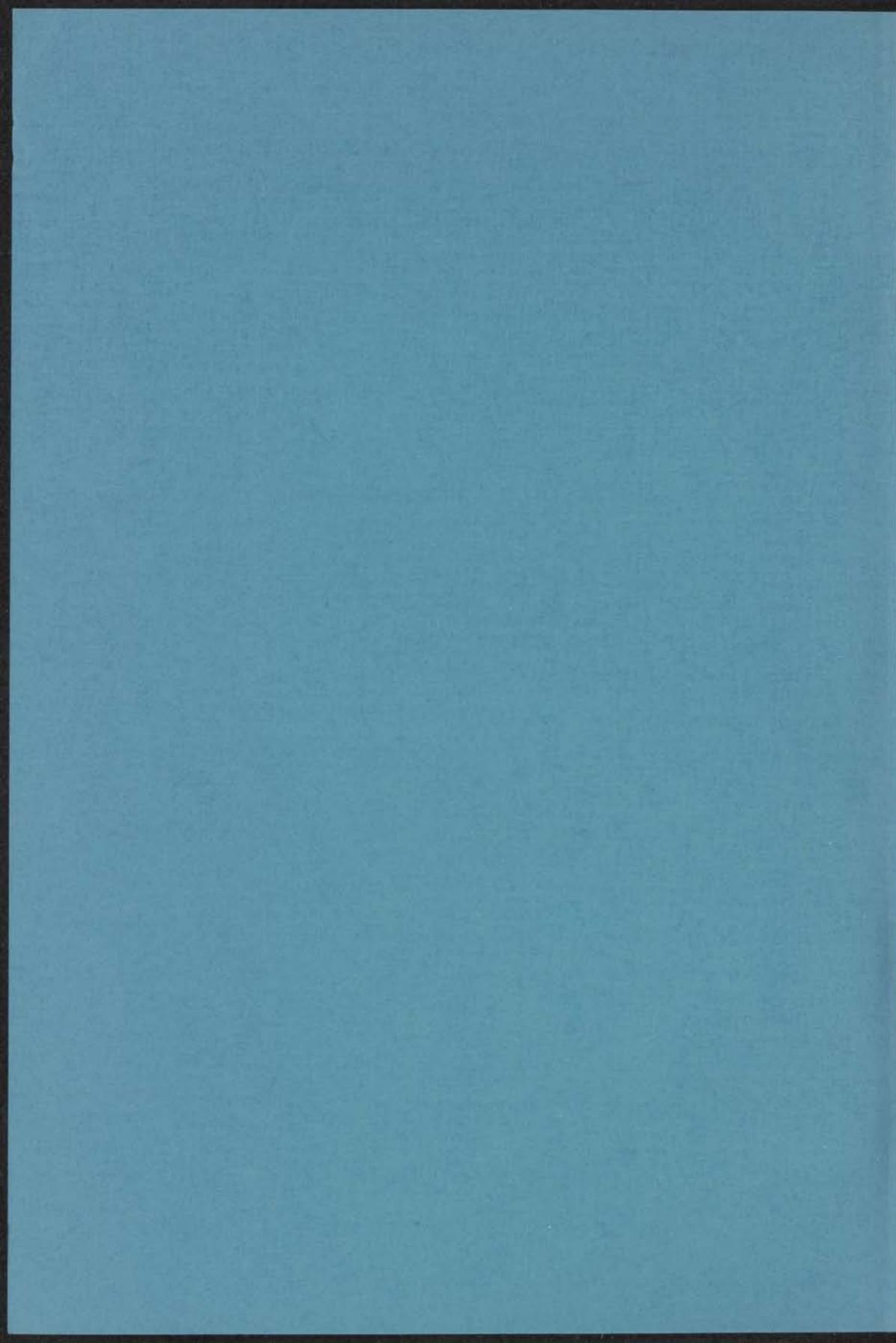
13 APR. 1971

NONLINEAR EFFECTS
IN A
BEAM-PLASMA EXPERIMENT

INSTITUUT-BORENIZ
voor theoretische natuurkunde
Nieuwsteeg 16-Leiden-Nederland



JOSÉ ARTUR DA COSTA CABRAL



NONLINEAR EFFECTS

NONLINEAR EFFECTS

IN A BEAM-PLASMA EXPERIMENT

BEAM-PLASMA EXPERIMENT

PROPOSANT

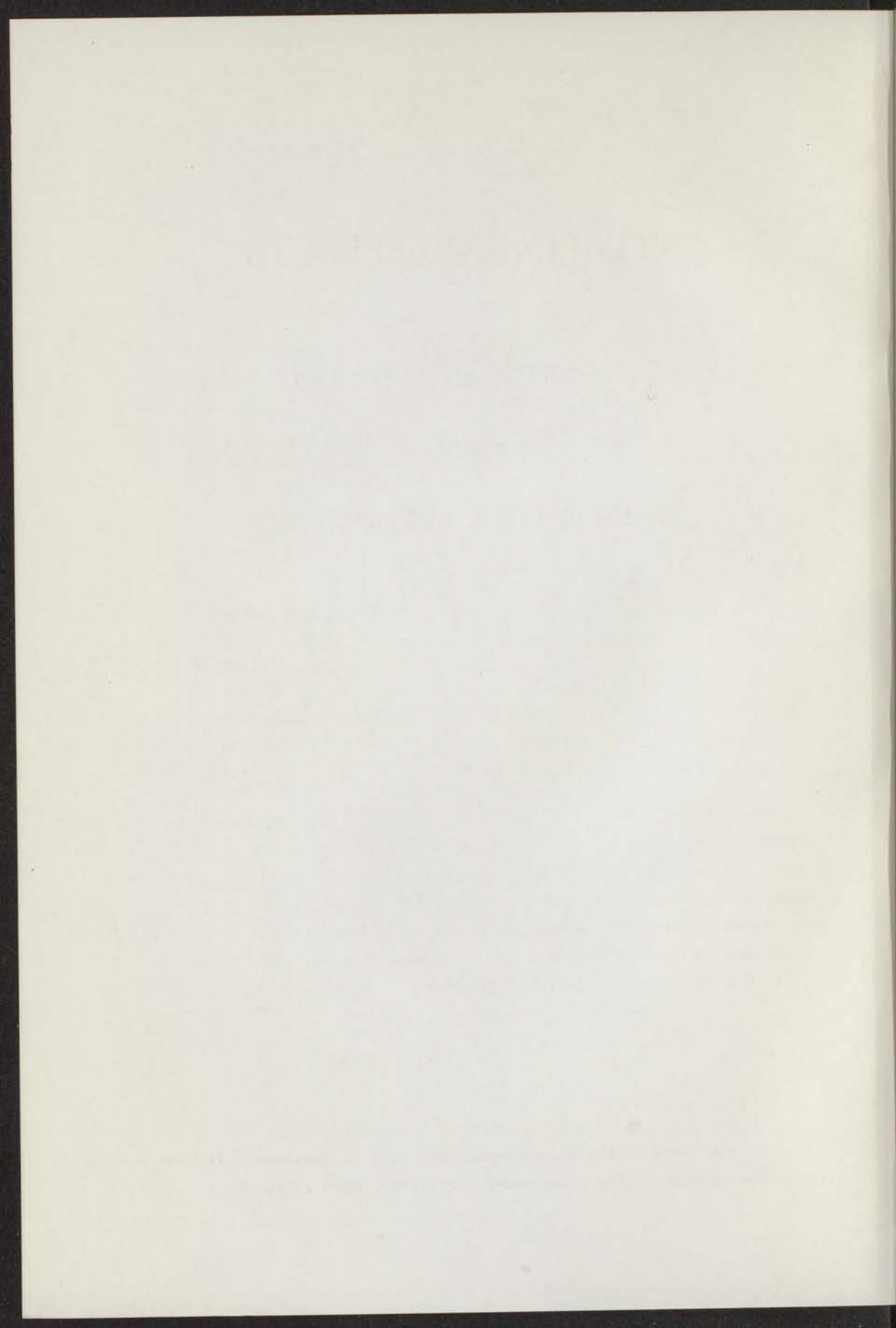
DE VERBODING VAN DE GAAST VAN GELIJK EN DE
WISSENSCHAP EN INDUSTRIE-OPVOEDING VAN DE KONING
UNIVERSITEIT TE BRUSSEL, EN GELIJK VAN DE KONING
UNIVERSITEIT DE K. WILHELMUS UNIVERSITEIT TE
EUREN EN DE UNIVERSITEIT VAN GENT
AANKOMST VAN DE WISSENSCHAP EN INDUSTRIE-OPVOEDING
TE BRUSSEL, DEN 15 DE MAART 1971

DATE

JOSE ARTUR DA COSTA CABRAL

GRADUATE IN SCIENCE OF MASSACHUSETTS INSTITUTE OF TECHNOLOGY

kast dissertatus



NONLINEAR EFFECTS
IN A
BEAM-PLASMA EXPERIMENT

PROEFSCHRIFT

TER VERKRIJGING VAN DE GRAAD VAN DOCTOR IN DE
WISKUNDE EN NATUURWETENSCHAPPEN AAN DE RIJKS-
UNIVERSITEIT TE LEIDEN, OP GEZAG VAN DE RECTOR
MAGNIFICUS DR. C. SOETEMAN, HOOGLERAAR IN DE
FACULTEIT DER LETTEREN, TEN OVERSTAAN VAN EEN
COMMISSIE UIT DE SENAAT TE VERDEDIGEN OP WOENSDAG
21 APRIL 1971 TE KLOKKE 14.15 UUR

DOOR

JOSÉ ARTUR DA COSTA CABRAL

GEBOREN TE LOURENÇO MARQUES (MOÇAMBIQUE) IN 1938

PROPOSITIONS

I

Measurements of the beam power losses which are based on the analysis of the time average velocity distribution function of the beam electrons at the beam centre, as done by Shustin et al., are not trustworthy.

- Shustin, E.G. et al. (1967), 8th Int.Conf.Phén. Ionized Gases, Vienna, p.376.

- This thesis, chapter V.

II

The essentially different shapes of the envelopes of the electron plasma and electron cyclotron instability bursts can be qualitatively explained on basis of the quasilinear theory of plasma waves with a three-dimensional k spectrum.

- This thesis, chapter V.

- Bernstein, I.B., Engelmann, F. (1966), Phys.Fluids 9, 937.

- Sagdeev, R.Z., Galeev, A.A. (1969), "Nonlinear Plasma Theory", W.A. Benjamin Inc., p.51.

III

The measurements of Levitskii et al., concerning the fine structure observed on the beam velocity distribution function can be explained by a resonant interaction between the beam electrons and a discrete set of large amplitude waves related with the boundary conditions of the system.

- Levitskii, S.M., Nuriev, K.Z. (1970), JETP Letters 12, 119.

IV

The conclusion drawn out by Cabral et al., about the interrelationship between the transverse and the axial energy of the beam electrons, is unjustified.

- Cabral, J.A. et al. (1970), 4th Europ.Conf.Contr. Fusion Plasma Phys., Rome, p.69.
- This thesis, chapter VII.

V

In beam-plasma experiments it is intrinsically more difficult to study the spatial coherence of the instability bursts than their temporal coherence.

- Yaremenko, Yu.G. et al. (1970), Soviet Phys. Techn.Phys. 14, 1158.
- Cabral, J.A., Hopman, H.J. (1970), Plasma Physics 12, 759.

VI

Kadomtsev, making some approximations, proves that the total momentum is conserved during the quasi-linear development of Cerenkov instabilities. On basis of simple arguments it can be demonstrated that the consideration of the diffusion process of the resonant electrons alone is sufficient to establish the conservation of the total energy as well as the total momentum of the system.

- Kadomtsev, B.B. (1965), "Plasma Turbulence", Academic Press, London, p.18.
- Vedenov, A.A. (1967), "Reviews of Plasma Physics", Leontovich (editor), New York, vol.3, p.229.

VII

The calculation of Bandrauk, concerning the total cross section for charge transfer between K and Br, is incorrect.

- Bandrauk, A.D. (1969), Mol.Phys. 17, 523.
- Fluendy, M.A.D. et al. (1970), Mol.Phys. 19, 659.

VIII

The arguments referred to by Cottrell et al., to prove that the vibrational relaxation time of the ν_1 mode of the NH_3 molecule is smaller than 10^{-7} s, are questionable.

- Cottrell, T.L. et al. (1966), Trans.Faraday Soc. 62, 2655.

IX

Concerning experimental communications to be published in the Proceedings of International Congresses, which are usually rather limited in extension, it is advisable that the authors should give preference to a careful presentation of the data and of the associated working conditions above the tentative of drawing out some hasty explanations of the results.

X

The presence of a relatively large percentage of guest workers, coming from under-developed countries, in the proletariat of a country of advanced capitalism can be unfavourable to the latter population group and eventually slow down the democratic evolution of that country.

J.A. da Costa Cabral

Leiden, 21 april 1971.

"Adhuc sub iudice lis est"

Horácio, "Arte Poética, 78"

AOS MEUS PAIS

À MINHA MULHER

À ISABEL

CONTENTS

	Page
1. GENERAL INTRODUCTION	11
2. LINEAR OSCILLATIONS IN A COLLISIONLESS PLASMA	15
2.1. General considerations	15
2.2. Longitudinal plasma waves - Derivation of a dispersion equation	19
2.3. Particular solutions of the dispersion equation	24
2.3.1. Dispersion of a cold plasma	24
2.3.2. Interaction between a cold electron beam and a cold plasma	25
2.3.3. Electron oscillations in a Maxwellian plasma	26
2.4. Landau damping	29
2.5. Criterium for instability	31
3. QUASILINEAR THEORY OF PLASMA WAVES	33
3.1. Introduction	33
3.2. Deduction of the quasilinear equations	34
3.3. Quasilinear development of plasma instabilities	41
3.4. Conditions of applicability of the quasilinear theory ...	46
3.5. Adiabatic contribution in the quasilinear theory	47
3.6. Relaxation time for the quasilinear interaction process .	50
3.7. Stationary solution of the quasilinear equations	53
3.8. Recent development of the quasilinear theory	56
4. NONLINEAR EFFECTS OCCURRING DURING THE DEVELOPMENT OF BEAM- PLASMA INSTABILITIES	65
4.1. Experimental set-up	65
4.2. Conventional diagnostic methods	66
4.2.1. Measurements of the plasma density	66
4.2.2. Analysis of the beam-plasma waves	67
4.2.3. Measurements of the beam axial velocity distribu- tion function	67
4.3. Dispersion equation for the beam-plasma waves under the presence of a magnetic field	69
4.4. General considerations	72
4.5. Experimental results	73

	page
4.5.1. Dependence of the beam-plasma internal parameters on the interaction length	73
4.5.2. Dependence of the beam-plasma internal parameters on the beam current and on the Helium pressure ..	81
4.6. Conclusions	86
5. STUDY OF THE 1 ST -2 ND REGIME TRANSITION IN A BEAM-PLASMA EXPERIMENT	89
5.1. Introduction	89
5.2. Correlation technique	89
5.3. Experimental results	90
5.3.1. Fast analysis of the beam-plasma instabilities ..	90
5.3.2. Beam-plasma parameters at the 1 st -2 nd regime transition	92
5.3.3. The frequency spectrum	93
5.3.4. The plasma density	94
5.3.5. Axial energy spread in the beam centre	96
5.3.6. Radial dependence of the axial energy spread in the beam	99
5.4. Interpretation of the results	102
5.4.1. Analysis of the results obtained at the beam centre	103
5.4.2. Analysis of the radial dependence of the axial energy spread in the beam	106
5.5. Moments of the beam distribution function	108
5.6. Energy considerations	110
5.7. Conclusions	113
6. NUMERICAL STUDY OF THE NONLINEAR INTERACTION BETWEEN A MONO-ENERGETIC ELECTRON BEAM AND A PLASMA WAVE IN A BEAM-PLASMA SYSTEM OF FINITE LENGTH	119
6.1. Introduction	119
6.2. Numerical determination of the axial velocity distribution function and of the power losses of the beam at the end of the interaction chamber	119
6.3. Solution in the absence of trapping	121
6.4. Solution in the presence of trapping	122
6.5. Numerical results	127

	Page
6.5.1. Results obtained without trapping	127
6.5.2. Detailed study of a particular case of wave-beam interaction when trapping occurs	131
6.5.3. Generalization of the results obtained when trap- ping occurs	136
6.6. Final considerations	140
7. MEASUREMENT OF THE TRANSVERSE ENERGY OF THE BEAM ELECTRONS ..	143
7.1. Introduction	143
7.2. Measurement of the transverse energy at the beam edge ..	144
7.2.1. General considerations	144
7.2.2. Time integrated measurements of the transverse energy of the beam electrons during the develop- ment of the beam-plasma instabilities	144
7.2.3. Correlated measurements of the transverse energy of the beam electrons at the 1 st -2 nd regime tran- sition	146
7.3. Measurement of the transverse energy at the beam centre	149
7.3.1. General considerations	149
7.3.2. Experimental results	151
7.4. Determination of the 3-dimensional velocity distribution function of the beam electrons at the beam centre	152
7.4.1. Theoretical considerations	152
7.4.2. Experimental results	156
7.4.2.1. Proof that there is no correlation be- tween the transverse and the axial beam velocities in strong second regime states of our beam-plasma system	156
7.4.2.2. Quantitative results	158
7.5. Conclusions	161
REFERENCES	164
SUMMARY	172
ACKNOWLEDGEMENTS	176
AGRADECIMENTOS	177
CURRICULUM VITAE	179

100
 101
 102
 103
 104
 105
 106
 107
 108
 109
 110
 111
 112
 113
 114
 115
 116
 117
 118
 119
 120
 121
 122
 123
 124
 125
 126
 127
 128
 129
 130
 131
 132
 133
 134
 135
 136
 137
 138
 139
 140
 141
 142
 143
 144
 145
 146
 147
 148
 149
 150
 151
 152
 153
 154
 155
 156
 157
 158
 159
 160
 161
 162
 163
 164
 165
 166
 167
 168
 169
 170
 171
 172
 173
 174
 175
 176
 177
 178
 179
 180
 181
 182
 183
 184
 185
 186
 187
 188
 189
 190
 191
 192
 193
 194
 195
 196
 197
 198
 199
 200

CHAPTER I

1. GENERAL INTRODUCTION

Nowadays it is quite unnecessary to stress the increasing importance of the new branch of science which is called plasma physics. Therefore, in this short introduction, we shall only be concerned with the development of one of its particular aspects, namely beam-plasma interaction.

During the last years, considerable attention has been paid to the problem of the interaction between a beam of charged particles and a plasma. Indeed, the understanding of the mechanics of this interaction helps to explain a number of effects appearing in several important domains of recent research. Among these effects we can name, for example, the plasma heating, the production of fast particles, the generation of microwaves, etc. Science branches which are particularly interested in the beam-plasma interaction are the astrophysics (study of the cosmic plasmas), the nuclear physics (controlled nuclear fusion) and the solid state physics.

In a beam-plasma experiment, as well as in natural plasmas, one is often faced with the fact that a small fraction of the particles of the system, possessing a relatively large velocity in comparison with the thermal velocity, can play a dominant role in the behaviour of the system. High energy cosmic particles and the so-called "runaway" electrons in the fusion experiments are examples of these minority particles.

The first experiments in which the excitation of plasma waves was detected were carried out by LANGMUIR (1925), PENNING (1926) and LANGMUIR et al., (1929). These experiments were hot cathode discharges, in which intrinsically were present beams of fast electrons. Therefore they are usually referred to as the first beam-plasma experiments.

Soon the experimental physicists became aware of the fact that in beam-plasma systems the beam particles suffer an anomalously large dissipation of energy, which could not be explained by the consideration of binary collisions (MERRILL et al., 1939). The first attempts to explain these results were made by PIERCE (1948), BOHM and GROSS (1949,1950) and AKHIEZER et al. (1949). It was, at last, proved that it is the passage of the beam through the plasma that leads to instabilities. The beam ener-

gy losses were then related with the excitation of the plasma instability. These losses were explained on basis of a coherent interaction between the beam and the plasma. The beam was assumed to be modulated in velocity by an alternating voltage existing at the plasma boundary. Due to this velocity modulation the beam would become bunched. Related with the formation of these bunches an explanation was given for the appearance of zones of intense radiation in the plasma (GABOVICH et al., 1959) and for the high energy losses, some 40 to 80 eV/cm, suffered by the beam electrons (KHARCHENKO et al., 1960, 1962). ROMANOV et al. (1961) write that it is not necessary to consider the bunch formation on the beam to explain the anomalous phenomena arising in beam-plasma experiments. It is enough to assume that the beam-plasma system is unstable. Kinetic equations describing the growth of the plasma waves and the time variation of the beam velocity distribution function began to appear in literature (KLIMONTOVICH, 1959; ROMANOV et al., 1961). A review of the theory of beam-plasma interaction was then written by CRAWFORD et al. (1961).

Gradually, the increasing number of theoretical as well as experimental publications lead to the appearance of the so-called quasilinear theory of plasma waves (VEDENOV et al., 1962; DRUMMOND et al., 1962; SHAPIRO et al., 1962). With the development of the modern nonlinear theories of beam-plasma interaction, from which a review was written by EINAUDI and SUDAN (1969), we notice a very pronounced progress in the understanding of the phenomena appearing in beam-plasma experiments. It is interesting to remark that the most recent approach in the theory of beam-plasma interaction (KADOMTSEV et al., 1970) takes again in consideration the formation of bunches in the electron beam, as the driving source of the instability. Reviews of the present research related with beam-plasma interaction were written by FAINBERG (1968) and HOPMAN (1969).

Among the most interesting experimental results of the last years we should refer to the production of very energetic electrons (SMULLIN et al., 1966; KRIVORUCHKO et al., 1968; NEIDIGH et al., 1969), the generation of harmonics of the fundamental beam-plasma instabilities (CRAWFORD, 1965; NEZLIN et al., 1966; KOGAN et al., 1968; DUSHIN et al., 1968), the nonlinear transformation of waves (MIKHAILOVSKII et al., 1966; FEDORCHENKO et al., 1967; LEVITSKII et al., 1969), the observation of the so-called plasma wave echoes (MALMBERG et al., 1968) and the generation of

very hot plasmas (JANCARIC et al., 1969; NEIDIGH et al., 1969).

Associated with all these effects, there are nowadays many theoretical studies, which as a whole constitute a rather broad and complicated domain of the modern physics.

Concluding, it is well known today that, when a beam of charged particles passes through a plasma, it gives rise to the excitation of instabilities. These instabilities, excited at the cost of part of the kinetic energy of the beam, appear under the form of growing waves. Therefore we treat, in chapter II, the problem of the linear oscillations in a collisionless plasma. We show that the frequency and the wave number of the plasma waves are in general complex quantities that satisfy the dispersion equation of the beam-plasma system. The linear theory of beam-plasma interaction is quite adequate to describe the initial stage of the development of an instability. However, as this theory predicts an unlimited exponential growth of the instabilities, we see that it loses very quickly its applicability for the study of the unstable processes occurring in real plasmas. Indeed, it is well known that the growth rate of an instability is experimentally seen to decrease with the increase in the amplitude of the instability. These instabilities, in general, occur in bursts, which means that, after an initial exponential growth, a saturation mechanism appears and is usually later followed by a decaying process. Other experimental results which can not be explained within the framework of the linear theory of beam-plasma interaction are, for example, the broadening of the excited spectrum of oscillations and the changes in both the beam and the plasma parameters, which accompany the development of the instabilities. These effects are related with nonlinear phenomena. Although restricted by a large number of conditions of applicability, the quasilinear theory of beam-plasma interaction, can anyhow explain a great part of the experimentally observed nonlinear effects. By this reason, and especially because in the quasilinear theory a rather general physical formalism is clearly presented, we make, in chapter III a review of the most salient aspects of this theory.

Chapter IV deals with measurements of the spatial development of the beam-plasma interaction and some nonlinear effects are observed, which agree with the predictions of the quasilinear theory.

In chapter V we make a detailed study of the 1st-2nd regime transition in the plasma. In this chapter we related the extension of the axial velocity spread in the beam as well as the beam power losses to the existence of a trapping mechanism in which the beam electrons become trapped in the cyclotron wave potential well.

In chapter VI a numerical study is made to test the validity of the trapping mechanism assumed in chapter V.

Finally in chapter VII we present some measurements of the transverse energy of the beam electrons. An expression, permitting the obtention of the 3-dimensional velocity distribution function at the beam centre, is derived and applied to the study of interrelationship between the transverse and the axial energy of the beam electrons.

CHAPTER II

LINEAR OSCILLATIONS IN A COLLISIONLESS PLASMA

2.1. General considerations

The plasma being a collection of particles, its state can be rather well described by a statistical theory, based on the definition, made for every type of particles, of the density of probability in phase space. For simplicity let us assume, for the moment, that the plasma can be represented by an ensemble of particles of a single type. The probability density in phase space D , is then a function of time and of the coordinates and momenta of all the N particles of the considered type. By definition we have (DELCROIX, 1963):

$$\int_{-\infty}^{\infty} D \, d\vec{r}_1 d\vec{v}_1 d\vec{r}_2 d\vec{v}_2 \dots d\vec{r}_N d\vec{v}_N = 1 \quad (2.1)$$

Because actually we can not distinguish between two particles of the same kind, we define the state of our system by the velocity distribution function $f(\vec{r}, \vec{v}, t)$ which results from the integration of the probability density D over the coordinates and momenta of all the considered particles but one. We shall use throughout this work always normalized velocity distribution functions in the sense that:

$$n_0 \int_{-\infty}^{\infty} f(\vec{r}, \vec{v}, t) \, d\vec{v} = n(\vec{r}, t) \quad (2.2)$$

Here n_0 is the average density of the particles and $n(\vec{r}, t)$ is their instantaneous density.

When we are interested in a less detailed description of the plasma (macroscopic description) it is usual to characterize it by the moments of the distribution function. Among these ones we are especially interested in:

$$- \text{The average velocity } \vec{u}(\vec{r}, t) = \frac{n_0}{n} \int \vec{v} f(\vec{r}, \vec{v}, t) \, d\vec{v} \quad (2.3)$$

$$- \text{The temperature } \kappa T(\vec{r}, t) = \frac{1}{3} \frac{n_0}{n} \int m |\vec{v} - \vec{u}|^2 f(\vec{r}, \vec{v}, t) \, d\vec{v} \quad (2.4)$$

$$- \text{The heat flux vector } \vec{q}(\vec{r}, t) = \frac{1}{2} n_0 \int m |\vec{v} - \vec{u}|^2 (\vec{v} - \vec{u}) f(\vec{r}, \vec{v}, t) \, d\vec{v} \quad (2.5)$$

where κ is the Boltzmann's constant.

Let us now consider the problem of the time evolution of the velo-

city distribution function. It is wellknown that, starting from the Liouville theorem, we can arrive to the Vlasov equation. This one is a particular case of the following general equation for the time evolution of the velocity distribution function (DELCROIX, 1963)

$$\frac{\partial f}{\partial t} + \vec{v} \cdot \frac{\partial f}{\partial \vec{r}} + \frac{\vec{F}}{m} \cdot \frac{\partial f}{\partial \vec{v}} + \int_{-\infty}^{\infty} \frac{\vec{F}_{12}}{m} \cdot \frac{\partial f_{12}}{\partial \vec{v}} d\vec{r}_2 d\vec{v}_2 = 0$$

where $f_{12}(\vec{r}, \vec{r}_2, \vec{v}, \vec{v}_2, t)$ is the double distribution function representing the correlation existing between the position of a certain particle (at \vec{r} with velocity \vec{v}) and the location of another one (at \vec{r}_2 and with velocity \vec{v}_2) which exerts on the first one a force \vec{F}_{12} . The double distribution function permits to study the macroscopic effects of the interaction among the particles.

Equation (2.6) implies that the external forces, represented by \vec{F} , satisfy the following conditions:

$$\frac{\partial \vec{F}}{\partial \vec{v}_x} = \frac{\partial \vec{F}}{\partial \vec{v}_y} = \frac{\partial \vec{F}}{\partial \vec{v}_z} = 0 \quad (2.7)$$

As the Lorentz force obeys conditions (2.7), these ones are generally satisfied in all practical cases.

Equation (2.6) expresses the fact that the time variation of the distribution function results from three different types of phenomena: Diffusion (second term), action of the external forces (third term) and interaction among the particles (last term).

Equation (2.6) cannot be solved without a prescription concerning the double distribution function. Depending upon the simplifying hypothesis made about f_{12} , (2.6) can lead to the equations of Boltzmann, Vlasov, Landau, Fokker-Planck, and so on. If we neglect the correlation between the location of the particles in phase space, then the double distribution function is simply given by

$$f_{12}(\vec{r}, \vec{r}_2, \vec{v}, \vec{v}_2, t) = f(\vec{r}, \vec{v}, t) \times f_2(\vec{r}_2, \vec{v}_2, t) \quad (2.8)$$

Under these conditions, if we admit that the force exerted among the particles is independent of the velocity, it is possible to arrive to the Vlasov equation

$$\frac{\partial f}{\partial t} + \vec{v} \cdot \frac{\partial f}{\partial \vec{r}} + \frac{\vec{F} + \vec{F}'}{m} \cdot \frac{\partial f}{\partial \vec{v}} = 0 \quad (2.9)$$

where \vec{F}' is the average force exerted on a particle by all the other ones:

$$\vec{F}'(\vec{r}, t) = \int_{-\infty}^{\infty} \vec{F}_{12} f_2(\vec{r}_2, \vec{v}_2, t) d\vec{r}_2 d\vec{v}_2 \quad (2.10)$$

But a real plasma contains at least three different species of particles: the neutral particles, the ions and the electrons. This means that in equation (2.6) we must consider new terms related with the interaction between a particle of the considered species and all the particles belonging to the other species. These additional terms are formally identical to the last one in equation (2.6) and the generalization is evident. Thus, when we write the Vlasov equation as in expression (2.9), we must consider \vec{F}' to be the total average force exerted on one particle by all the other ones. In the absence of external forces, and neglecting the influence of the neutral particles, this equation can be written as

$$\frac{\partial f}{\partial t} + \vec{v} \cdot \frac{\partial f}{\partial \vec{r}} + \frac{e}{m} [\vec{E} + \vec{v} \times \vec{B}] \cdot \frac{\partial f}{\partial \vec{v}} = 0 \quad (2.11)$$

where \vec{E} and $\vec{H} = \frac{\vec{B}}{\mu}$ are the average electric and magnetic fields produced at the point \vec{r} at time t by all the particles of the system.

With a higher accuracy equation (2.11) should still have a collisional term. Among the different types of collisions one is particularly important for the study of the plasma: - the Coulomb collision. This one is defined by the scattering of one charged particle on another. This scattering is associated with a rapid variation of the electromagnetic fields felt by these two particles. The very essence of the Vlasov equation consists in the fact that we can neglect these collisions, and let the behaviour of one particle to be determined only by the average fields \vec{E} and \vec{H} .

The neglect of the Coulomb collisions can be justified if the number of particles contributing to it is much smaller than the number of those which produce the average fields. The existence of a shielding limit on distant interactions (Debye length) reduces the former statement to the condition that the number of particles inside a Debye sphere must exceed considerably the number of those which are responsible for the Coulomb collisions. These last ones are expected to be found inside a sphere of radius $(\sigma/\pi)^{\frac{1}{2}}$, of the order of the square root of the Coulomb collision cross section σ . $(\sigma/\pi)^{\frac{1}{2}}$ being in general much smaller

than the Debye length λ_D , Coulomb collisions may therefore be neglected.

$$\sigma \approx \frac{e^4}{4\pi\epsilon_0^2 (3\kappa T)^2} \quad \lambda_D = \left(\frac{\epsilon_0 \kappa T}{n_0 e^2} \right)^{\frac{1}{2}} \quad (2.12a)$$

Indeed, the ratio between these two distances

$$\frac{\left(\frac{\sigma}{\pi}\right)^{\frac{1}{2}}}{\lambda_D} = \frac{1}{6\pi n_0 \lambda_D^3} = \frac{1}{N_D} \quad (2.12b)$$

is in all practical cases a very small number, of the order of the inverse of the number of particles inside a Debye sphere, N_D . This fact gives to the Vlasov equation a great accuracy to the study of low density high temperature plasmas. This equation, by the nature of the approximations made in its derivation, is best suited to the study of longitudinal electrostatic oscillations in a collisionless plasma.

Because we are dealing with a system of charged particles the Vlasov equation must be associated with the Maxwell equations. The following system results

$$\frac{\partial f}{\partial t} + \vec{v} \cdot \frac{\partial f}{\partial \vec{r}} + \frac{e}{m} [\vec{E} + \vec{v} \times \vec{B}] \cdot \frac{\partial f}{\partial \vec{v}} = 0 \quad (2.13)$$

$$\vec{\nabla} \cdot \vec{D} = n_0 e \int_{-\infty}^{\infty} f(\vec{v}) d\vec{v} - n_0 e = \rho \quad (2.14)$$

$$\vec{\nabla} \times \vec{E} = - \frac{\partial \vec{B}}{\partial t} \quad (2.15)$$

$$\vec{\nabla} \cdot \vec{B} = 0 \quad (2.16)$$

$$\vec{\nabla} \times \vec{H} = \frac{\partial \vec{D}}{\partial t} + n_0 e \int_{-\infty}^{\infty} \vec{v} f(\vec{v}) d\vec{v} = \frac{\partial \vec{D}}{\partial t} + \vec{J} \quad (2.17)$$

In these equations $f(\vec{v})$ is the velocity distribution function for the electrons of our system. The plasma ions are assumed at rest and uniformly distributed in space with a density n_0 , equal to the average electron density (charge neutrality). This means that we neglect the influence of the ions in the electron oscillations in which we are especially interested. The consideration of the motion of the ions would only lead to a very small correction to the results obtained with the above assumption, due to their very large relative mass.

Equations (2.13) to (2.17) constitute the self-consistent field equations or Vlasov equations. They describe the evolution of our system with the complete neglect of correlation among the particles.

2.2. Longitudinal plasma waves - Derivation of a dispersion equation

Throughout this chapter we shall only consider the case of pure longitudinal oscillations (\vec{k} parallel to \vec{E}) in the electrostatic approximation ($H=0$) in an infinite plasma. It is also supposed that there are no external fields acting on the plasma. Under these conditions the self-consistent field equations reduce to

$$\frac{\partial f}{\partial t} + \vec{v} \cdot \frac{\partial f}{\partial \vec{r}} + \frac{e}{m} \vec{E} \cdot \frac{\partial f}{\partial \vec{v}} = 0 \quad (2.18)$$

$$\vec{v} \cdot \vec{E} = \frac{n_0 e}{\epsilon_0} \left(\int_{-\infty}^{\infty} f(\vec{v}) d\vec{v} - 1 \right) \quad (2.19)$$

$$\frac{\partial \vec{E}}{\partial t} = - \frac{n_0 e}{\epsilon_0} \int_{-\infty}^{\infty} \vec{v} f(\vec{v}) d\vec{v} \quad (2.20)$$

Equations (2.19) and (2.20) are not independent as they are related through the continuity equation:

$$\vec{v} \cdot \vec{J} + \frac{\partial \rho}{\partial t} = 0 \quad (2.21)$$

To solve the system of equations (2.18) and (2.19) it is usual to decompose the velocity distribution function into a sum of a zero order term $f_0(\vec{v})$ (time independent and uniform in space) with a first order one $f_1(\vec{r}, \vec{v}, t)$ which represents the rapid fluctuations of the distribution function due to the plasma oscillations. Equations (2.18) to (2.20) are identically zero for the zero order distribution function $f_0(\vec{v})$ which obeys the following relations:

$$\int_{-\infty}^{\infty} f_0(\vec{v}) d\vec{v} = 1 \quad (2.22)$$

$$\int_{-\infty}^{\infty} f_0(\vec{v}) \vec{v} d\vec{v} = 0 \quad (2.23)$$

The last term in the Vlasov equation (2.18) is nonlinear. It contains the product of two first order quantities. When we think of

linearization we must make an assumption over the time variation of these quantities. As pointed out by SAGDEEV and GALEEV (1969) there are two fundamentally different approximations which correspond to the cases when we can hold one of the two unknowns (f and \vec{E}) constant. If the amplitude of the wave changes much more quickly than the first order distribution function, then it is allowed to replace in (2.18) $\partial f / \partial \vec{v}$ by $\partial f_0 / \partial \vec{v}$. This was the linearization procedure used by Landau. Keeping the wave amplitude constant and looking for the time evolution of the distribution function is the process used by Sagdeev and Galeev.

We shall follow the first linearization process. Then, the self-consistent equations are written as:

$$\frac{\partial f_1}{\partial t} + \vec{v} \cdot \frac{\partial f_1}{\partial \vec{r}} + \frac{e}{m} \vec{E} \cdot \frac{\partial f_0}{\partial \vec{v}} = 0 \quad (2.24)$$

$$\vec{v} \cdot \vec{E} = \frac{n_0 e}{\epsilon_0} \int_{-\infty}^{+\infty} f_1 d\vec{v} \quad (2.25)$$

To solve the Vlasov equations there are two wellknown different approaches: The method of Landau, that will be treated here, and the more recent treatment of VAN KAMPEN (1955). Both methods lead to essentially the same results.

Following LANDAU (1946) we introduce Fourier transforms in space and Laplace transforms in time:

$$f_1(\vec{k}, \vec{v}, \omega) = \int_0^{\infty} e^{j\omega t} \left(\int_{-\infty}^{\infty} f_1(\vec{r}, \vec{v}, t) e^{-j\vec{k} \cdot \vec{r}} d\vec{r} \right) dt \quad (2.26)$$

$$\vec{E}(\vec{k}, \omega) = \int_0^{\infty} e^{j\omega t} \left(\int_{-\infty}^{\infty} \vec{E}(\vec{r}, t) e^{-j\vec{k} \cdot \vec{r}} d\vec{r} \right) dt \quad (2.27)$$

We must now perform a Fourier-Laplace transformation of equation (2.24). The Laplace transform of its first term is:

$$\int_0^{\infty} e^{j\omega t} \frac{\partial f_1}{\partial t} dt = \left[e^{j\omega t} f_1 \right]_0^{\infty} - j\omega \int_0^{\infty} e^{j\omega t} f_1(\vec{r}, \vec{v}, t) dt \quad (2.28)$$

In order to proceed we must admit that for $t > 0$ there exist two numbers M and α that satisfy $|f_1(\vec{r}, \vec{v}, t)| < |M e^{\alpha t}|$ for any value of t .

In carrying out the inverse transforms we must then integrate in ω along a line with $\omega_i > \alpha$ in the complex ω plane. ω_i and ω_r are respectively the imaginary and the real parts of ω .

The inverse transforms are then:

$$f_1(\vec{r}, \vec{v}, t) = \int_{-\infty + j\alpha}^{\infty + j\alpha} e^{-j\omega t} \left(\int_{-\infty}^{\infty} f_1(\vec{k}, \vec{v}, \omega) e^{j\vec{k} \cdot \vec{r}} \frac{d\vec{k}}{(2\pi)^3} \right) \frac{d\omega}{2\pi} \quad (2.29)$$

$$\vec{E}(\vec{r}, t) = \int_{-\infty + j\alpha}^{\infty + j\alpha} e^{-j\omega t} \left(\int_{-\infty}^{\infty} \vec{E}(\vec{k}, \omega) e^{j\vec{k} \cdot \vec{r}} \frac{d\vec{k}}{(2\pi)^3} \right) \frac{d\omega}{2\pi} \quad (2.30)$$

The integration in ω along the line with $\omega_i = \alpha$ is necessary in order to assure that both f_1 and \vec{E} are zero for $t < 0$. With these assumptions the Laplace transform of the first term of (2.24) is simply given by

$$f_1(\vec{r}, \vec{v}, t=0) - j\omega f_1(\vec{r}, \vec{v}, \omega) \quad (2.31)$$

The transformation of the other terms of (2.24) is similar and we obtain

$$f_1(\vec{k}, \vec{v}, \omega) = \frac{\frac{e}{m} \vec{E} \frac{\partial f_0}{\partial \vec{v}} - g(\vec{k}, \vec{v})}{j(\omega - \vec{k} \cdot \vec{v})} \quad (2.32)$$

where $g(\vec{k}, \vec{v})$ is the Fourier transform of the initial perturbation of the distribution function $f_1(\vec{r}, \vec{v}, t=0) = g(\vec{r}, \vec{v})$.

The transformation of equation (2.25) gives:

$$\vec{E}(\vec{k}, \omega) = - \frac{j n_0 e}{\epsilon_0 k} \int_{-\infty}^{\infty} f_1(\vec{k}, \vec{v}, \omega) d\vec{v} \quad (2.33)$$

Substitution of (2.32) into the last expression leads to:

$$\vec{E}(\vec{k}, \omega) = \frac{\frac{n_0 e \vec{k}}{\epsilon_0 k^2} \int_{-\infty}^{\infty} \frac{g(\vec{k}, \vec{v})}{\omega - \vec{k} \cdot \vec{v}} d\vec{v}}{1 + \frac{n_0 e^2}{m \epsilon_0 k^2} \int_{-\infty}^{\infty} \frac{\vec{k} \cdot \frac{\partial f_0}{\partial \vec{v}}}{\omega - \vec{k} \cdot \vec{v}} d\vec{v}} \quad (2.34)$$

The physical interpretation of this mathematical treatment is that we are considering an initial value problem. At $t=0$ we admit that our system is in a state of non-equilibrium with the distribution function slightly different from the equilibrium one $f_0(\vec{v})$. The essential problem

is to deduce what are the electron oscillations which arise or, in other words, what is the response of our system to the considered perturbation $g(\vec{r}, \vec{v})$ on the distribution function.

From now on we will consider a one-dimensional problem. For simplicity we choose the \vec{z} -axis to be in the \vec{k} -direction. So hereafter v will be the \vec{z} -component of the velocity and $f_0(v)$ will be the partial integral of the distribution function over the other two components of the velocity (\vec{v}_x and \vec{v}_y). By the same way

$$g(k, v) = \int_{-\infty}^{\infty} g(k, \vec{v}) d\vec{v}_x d\vec{v}_y \quad (2.35)$$

and equation (2.34) becomes

$$E(k, \omega) = \frac{-\frac{n_0 e}{\epsilon_0 k} \int_{-\infty}^{\infty} \frac{g(k, v)}{kv - \omega} dv}{1 - \frac{n_0 e^2}{m \epsilon_0 k} \int_{-\infty}^{\infty} \frac{\frac{\partial f_0}{\partial v}}{kv - \omega} dv} \quad (2.36)$$

Equation (2.36) permits to compute the Fourier-Laplace transform of the electric field of the plasma oscillations. The transform of the first order distribution function is then determined by (2.32).

Inverse transformations of $E(k, \omega)$ and $f_1(k, v, \omega)$, according to equations (2.29) and (2.30), represent the complete solution of the initial value problem considered.

We recall that, integrating along the Bromwich contour in the ω -plane, as implicit in (2.29) and (2.30), both integrals in (2.36) are free from singularities arising from the term $(kv - \omega)$ because we use values of ω_1 that exceed the highest value associated with all the singularities of E .

An easier way to perform the inverse transformations is to carry the integration in the complex ω plane along an equivalent contour introduced by LANDAU (1946). The contribution to the integral from all parts of the new contour can be neglected except in the neighbourhood of the poles of $E(k, \omega)$. But this last contribution is nothing more than the sum of the residues of these poles that we denote by ω_α .

$$E(k, t) = \sum_{\alpha} e^{-j\omega_{\alpha} t} \text{Res}_{\omega_{\alpha}} [E(k, \omega)] \quad (2.37)$$

However, the integrals involved in the Laplace transformations are only meaningful for $\omega_i \geq \alpha$, as we admitted when deriving equation (2.32). Anyhow it is possible to use the Landau contour for the integration in ω provided that we define the proper analytic continuation of the function $E(k, \omega)$ defined previously only for $\omega_i \geq \alpha$.

This question of the analytic continuation of the function $E(k, \omega)$ has been extensively treated in literature (STIX, 1962; SIMON, 1965; BRIGGS, 1964), since the appearance of the work of LANDAU (1946). This procedure requires that the integrals in v in equation (2.36), which could (for $\omega_i \geq \alpha$) be taken along the real axis, must now be performed along a special contour. This one avoids lack of continuity in the final solution of the considered problem for $t > 0$, resulting from the poles, which eventually cross the real v axis when we move in ω from $\omega_i \geq \alpha$ to $\omega_i < 0$. This means that above this new contour in the complex v plane there must appear all the poles which, for $\omega_i \geq \alpha$, were found with $v_i > 0$ and only these ones.

The final expression for the electric field of the plasma oscillations can now be written:

$$E(k, \omega) = \frac{-\frac{n_0 e}{\epsilon_0 k} \int_c \frac{g(k, v)}{k v - \omega} dv}{1 - \frac{n_0 e^2}{m \epsilon_0 k} \int_c \frac{\partial f_0}{\partial v} \frac{1}{k v - \omega} dv} \quad (2.38)$$

where subscript c indicates integration along the Landau contour in the velocity plane.

Under these conditions, the time variation of the electric field is completely determined by its poles in the complex ω plane as expressed in (2.37). If there is a pole ω_M which possesses the greatest value of ω_i then the contribution of all the other poles will be, for any finite value of t , exponentially small compared with its own contribution and the response of the plasma to the initial value problem will be of the form (STIX, 1962):

$$\lim_{t \rightarrow \infty} E(k, t) \sim e^{-j \omega_M t} [(\omega - \omega_M) E(k, \omega)]_{\omega = \omega_M} \quad (2.39)$$

If $g(k, v)$ and $\partial f_0 / \partial v$ are both analytic functions of v and in particular entire functions, the integrals in (2.38) are both entire

functions of the complex variable ω (integration along contour c). Equation (2.38) is, under these conditions, the ratio of two entire functions, and so the singularities of $E(k, \omega)$ are all due to the zeros of the denominator of this equation.

But the poles contributed by the denominator of (2.38) are independent of the initial perturbation on the distribution function. They depend only on the details of the zero order distribution function $f_0(v)$. These poles occur when

$$1 = \frac{n_0 e^2}{m \epsilon_0 k} \int_c \frac{\partial f_0}{k v - \omega} dv \quad (2.40)$$

and, by the last considerations, they represent the natural modes of oscillation of the plasma electrons. This fact justifies that we call to (2.40) the dispersion equation for longitudinal electron plasma waves.

Due to the analytic continuation of $E(k, \omega)$ an equivalent dispersion equation can be easily derived by partial integration of (2.40) and the result is

$$1 = \frac{n_0 e^2}{m \epsilon_0} \int_c \frac{f_0(v)}{(kv - \omega)^2} dv \quad (2.41)$$

2.3. Particular solutions of the dispersion equation

With equations (2.40) or (2.41) we can now study some particular cases of dispersive propagation of longitudinal electrostatic plasma waves.

2.3.1. Dispersion of a cold plasma

A particular solution of the dispersion equation can be easily obtained for the case of a zero temperature plasma. In this case no singularities arise, for any finite value of ω , as $v=0$. So we can write $f_0(v) = \delta(v)$ and equation (2.41) immediately gives:

$$1 = \frac{n_0 e^2}{m \epsilon_0 \omega^2} \quad \text{or} \quad \omega^2 = \omega_p^2 = \frac{n_0 e^2}{m \epsilon_0} \quad (2.42)$$

We see that the result of a perturbation made on an electron gas at zero temperature, immersed in a neutralizing ion gas, is an oscil-

lation at the so-called electron plasma frequency ω_p . This one is independent of the wave number k and so there is no propagation of the perturbation along the space as the group velocity ($d\omega/dk$) is zero.

2.3.2. Interaction between a cold electron beam and a cold plasma

A second particular solution of the dispersion equation corresponds to the case in which we have two groups of electrons with zero temperature and average velocities respectively equal to zero and to v_b . This case is a theoretical limit of the experimental situation resulting from the passage of a monoenergetic electron beam through a cold plasma. In this case the combined electron distribution function can be written as

$$f_o(v) = \frac{1}{n_o} [n_p \delta(v) + n_b \delta(v - v_b)] \quad (2.43)$$

where n_p is the density of the electrons at rest (plasma electrons) and n_b is the density of the electrons with average velocity equal to v_b (beam electrons). n_o is of course the total electron density ($n_o = n_p + n_b$).

Substitution of (2.43) into the dispersion equation (2.41) leads to

$$1 = \frac{\omega_p^2}{\omega^2} + \frac{\omega_{pb}^2}{(\omega - kv_b)^2} \quad (2.44)$$

where ω_p and ω_{pb} are respectively the plasma frequencies of the corresponding groups of electrons.

This is the wellknown linear dispersion equation for an infinite beam-plasma system. This equation has, for real k , complex conjugate solutions for ω . This means that, for certain values of k , the beam-plasma system is unstable. KLIMONTOVICH (1967) gives an approximate solution for waves with a phase velocity $v_{ph} = \omega/k$ very close to the beam velocity v_b . This solution is:

$$\omega = (k v_b) \left[1 \pm \frac{\omega_{pb}}{\sqrt{[(k v_b)^2 - \omega_p^2]}} \right] \quad (2.45)$$

From this equation it is clear that, if the wave number k satisfies the following condition

$$(k v_b)^2 < \omega_p^2 \quad (2.46)$$

there are two complex-conjugate roots of (2.45) revealing instability. This means that due to the presence of the beam the propagation of plasma waves with frequencies below ω_p becomes possible. Expression (2.45) is a good approximation to the dispersion equation only for long wavelengths and when the beam density n_b is much smaller than the main plasma density n_p . A dispersion diagram (plot of k against ω) representing the complete solution of equation (2.44) can be found in BRIGGS (1965).

A slightly modified dispersion relation

$$1 = \frac{\omega_p^2}{\omega^2 - 3k^2 v_T^2} + \frac{\omega_{pb}^2}{[\omega - (\vec{k} \cdot \vec{v}_b)]^2} \quad (2.47)$$

is referred by ALLIS (1967) for the case of the passage of a monoenergetic beam through a plasma with finite temperature. Here $v_T = (\kappa T/m)^{1/2}$ is the thermal velocity of the plasma electrons.

2.3.3. Electron oscillations in a Maxwellian plasma

The third particular case we will treat is the one in which the zero order distribution function is Maxwellian, with temperature T :

$$f_0(v) = \left(\frac{m}{2\pi\kappa T}\right)^{3/2} e^{-mv^2/2\kappa T} \quad (2.48)$$

Substitution of this expression into (2.40), leads to the following equation (SIMON, 1965; KLIMONTOVICH, 1967)

$$1 + k^2 \lambda_D^2 + \frac{z}{\sqrt{\pi}} \int_c \frac{e^{-t^2}}{t-z} dt = 0 \quad (2.49)$$

where $z = \frac{\omega}{k} (m/2\kappa T)^{1/2}$, $t = v (m/2\kappa T)^{1/2}$, and λ_D is the Debye length.

In the limit of long wavelengths this equation leads to the following solution:

$$(\omega_r)^2 = \omega_p^2 + 3 \frac{\kappa T}{m} k^2 = \omega_p^2 (1 + 3\lambda_D^2 k^2) \quad (2.50)$$

$$(\omega_i) = -\sqrt{\pi/8} \frac{\omega_p}{(k\lambda_D)^3} e^{-\frac{1}{2(k\lambda_D)^2}} \quad (2.51)$$

These are the famous results obtained by LANDAU (1946). The imaginary part of the frequency is negative and so the obtained solution corresponds to damping. Simon proves that in the other extreme limit (short wavelengths) equation (2.49) leads to heavily damped modes, with the logical conclusion that collective oscillations with wavelengths much shorter than the Debye length can not be maintained in the plasma.

Equations (2.50) and (2.51) were obtained with the assumption that the damping coefficient (ω_i) was much smaller than the real part of the frequency. From these equations we verify that this happens when $k\lambda_D \ll 1$.

Under these conditions the phase velocity of the plasma waves is approximately given by

$$v_{ph} \approx \frac{\omega_p}{k} \left(1 + \frac{3}{2} \lambda_D^2 k^2\right) \approx \frac{\omega_p}{k} \quad (2.52)$$

and is so considerably greater than the electron thermal velocity $v_T = \omega_p \lambda_D$. From (2.52) we see that the plasma is a dispersive medium as the phase velocity depends on the wavelength.

It can be proved (KLIMONTOVICH, 1967), that when $k\lambda_D \sim 1$ the imaginary part of the frequency ω_i becomes comparable with its real part ω_r , and equations (2.50) and (2.51) are no longer valid.

Equation (2.50) can be directly obtained from (2.41) if we expand its denominator in terms of the small parameter k . The result, valid of course only for large wavelengths, is

$$\omega^2 = \omega_p^2 + k^2 \int v^2 f_0(v) dv + O(k^4) \quad (2.53)$$

For a Maxwellian plasma with temperature T we obtain (2.50) neglecting the term of the order of k^4 .

Differentiating (2.53) we can see that the product of the group velocity ($v_g = d\omega/dk$) by the phase velocity ($v_{ph} = \omega/k$), for small k , is equal to $\langle v^2 \rangle$ the mean square velocity of the zero order distribution function f_0 .

$$\frac{d\omega}{dk} \frac{\omega}{k} = \langle v^2 \rangle = \int v^2 f_0(v) dv \quad (2.54)$$

As the phase velocity of the plasma waves is much greater than the electron thermal velocity we see from (2.54) that these waves are characterized by relatively small values of the group velocity.

We have thus seen that perturbations made in a plasma in thermodynamic equilibrium lead to oscillations at frequencies close to the plasma frequency. These oscillations are found to be damped. This damping mechanism, which would absorb energy in a collisionless plasma, has been the subject of large controversy. Indeed how can a damping process be derived from the Vlasov equation, which, as it is, wellknown, has the property of conserving the entropy of the system? VAN KAMPEN (1955) writes that it may be surprising to find a damping process resulting from the Vlasov equation which is invariant for time reversal. But he also states that this apparent irreversibility has its foundations on the incomplete definition of the assumed initial state.

ALLIS (1958) points out that it is delicate to apply perturbation techniques to an arbitrary solution of the Vlasov equation written as zero order. With the simultaneous neglect of collisions and of the zero order electric field the Boltzmann equation is degenerate and the Maxwell-Boltzmann distribution is only one of the multiple solutions of this equation.

A similar reasoning is referred by KLIMONTOVICH (1967) which says that the selection of a definite solution of the Vlasov equation goes out of the framework of the first moment equations, which means that this choice makes use of higher moments or of correlations among the particles. Indeed the Maxwell-Boltzmann distribution is quite attached to the existence of binary collisions.

The answer to this question seems to be that there is no contradiction between the damping of a macroscopic parameter of our system (like the electric field or the first order density perturbation) and the conservation of the entropy. VAN KAMPEN et al. (1967) clearly explain the apparent paradox of the Landau damping. According to them only the distribution function must follow a reversible transformation. Due to the fact that collisions are completely neglected in the Vlasov theory there are no linear differential equations for the macroscopic quantities characterizing a Vlasov plasma. So, these macroscopic quantities are allowed to suffer irreversible or dissipative processes.

SIMON (1965) makes a detailed study of this problem. From equation (2.32) we see that for large values of the time, when the electric field of the oscillations had decayed to zero due to Landau damping, the first order distribution function can be written as:

$$f_1(\vec{k}, \vec{v}, \omega) = - \frac{g(\vec{k}, \vec{v})}{j(\omega - \vec{k} \cdot \vec{v})} \quad (2.55)$$

representing the existence of a pure oscillating term. We see that, although the electric field damps away, the first order perturbation in the distribution function does not. By inverse transformation of (2.55) Simon finds that

$$f_1(\vec{r}, \vec{v}, t) = f_1(\vec{r} - \vec{v}t, \vec{v}, t=0) \quad (2.56)$$

meaning that the distribution function, after the decay to zero of the electric field, settles down to the value it would have if only free streaming of the plasma electrons had occurred. Since all the initial information of the problem was contained in the distribution function (Landau initial value treatment) we see that this information has been conserved. Thus the Landau damping conserves the entropy of the system.

2.4. Landau damping

A simplified derivation of the Landau damping decrement can be done starting with the linearized Vlasov equation written in the first order (2.24). We do not consider anymore an initial value problem and so we are allowed to take Fourier transforms of the form $e^{j(kz - \omega t)}$ in time and space. If we remember the considerations presented before for the way of performing the inverse transformations, we obtain easily an expression for the perturbed distribution function:

$$f_1(k, v, \omega) = \frac{-\frac{e}{m} E \frac{\partial f_0}{\partial v}}{j(kv - \omega)} \quad (2.57)$$

The perturbed electron current density is simply given by $n_0 e v f_1$ and so

$$J = j \frac{n_0 e^2}{m} E \frac{v \frac{\partial f_0}{\partial v}}{kv - \omega} \quad (2.58)$$

In this way it is possible to calculate the partial work done on the particles by the electric field per second and unit of volume:

$$(E \cdot J)_v = j \frac{n_0 e^2}{m} E^2 \frac{v \frac{\partial f_0}{\partial v}}{kv - \omega} \quad (2.59)$$

An integration over the electron velocity leads to the total power density

$$(E \cdot J) = j \frac{n_o e^2}{m} E^2 \int_c \frac{v \frac{\partial f_o}{\partial v}}{kv - \omega} dv \quad (2.60)$$

where the subscript c refers to the integration contour c in the velocity plane.

If we assume that the damping rate is much smaller than the oscillation frequency $\omega_i \ll \omega_r$, the imaginary part of the velocity is also much smaller than the real part ($v = \omega/k$) and we can admit that the pole lies close to the real v axis. Then, the integral in (2.60) can be written as the sum of a real principal part with a pure imaginary contribution from the residue of the referred pole. We see that the principal part of the integral leads to reactive power and that the only real contribution to the work comes from the residue term and is given by

$$(E \cdot J)_r = - \frac{\pi n_o e^2}{mk} E^2 \frac{\omega}{k} \left(\frac{\partial f_o(v)}{\partial v} \right)_{v=\omega/k} \quad (2.61)$$

We see that the work done by the electric field on these resonant particles ($\dot{v} = \omega/k$) is proportional to the wave energy and to the velocity derivative of the distribution function taken at the point where v is equal to the wave phase velocity. This result is given by SIMON (1965).

Writing now the expression for the Poynting theorem in the absence of applied fields and in the electrostatic approximation

$$\int \left[(E \cdot J) + 2 \frac{\partial}{\partial t} \left(\frac{\epsilon_o E^2}{2} \right) \right] d\vec{r} = 0 \quad (2.62)$$

it is possible to find an expression for the time variation of the electrostatic energy and so for the damping rate. The factor 2 in equation (2.62) comes from the virial theorem which states that if we give to an electrostatic wave a certain amount of energy one half of it goes into its electrostatic energy and the other half goes into kinetic energy of the bulk of particles which sustain the wave. Using (2.61) we obtain

$$\frac{\partial E^2}{\partial t} = 2\omega_i E^2 \quad (2.63)$$

where

$$\omega_i = \frac{\pi}{2} \frac{\omega_p^2}{k^2} \omega \left(\frac{\partial f_0}{\partial v} \right)_{v=\omega/k} \quad (2.64)$$

The derived results agree with the usual expression for the Landau damping (DAWSON, 1961)

$$\omega_i = \gamma = \frac{\pi}{2} \frac{\omega_p^3}{k|k|} \left(\frac{\partial f_0}{\partial v} \right)_{v=\omega/k} \left(1 - \frac{k}{\omega} \frac{d\omega}{dk} \right) \quad (2.65)$$

for the case of waves with group velocity much smaller than the phase velocity, a characteristic of the electron plasma oscillations.

Expression (2.64) for the rate of change of the wave energy has a simple physical interpretation. If a wave propagates with a phase velocity v_{ph} it exchanges energy preponderantly with those electrons which travel with velocities around v_{ph} (Cerenkov effect). Now, due to the action of its electric field, the wave has a tendency to accelerate electrons with velocities slightly smaller than v_{ph} and to retard the ones which travel a little faster than the wave itself. Then if $\partial f_0 / \partial v$ is negative, this means that the number of electrons which absorb, in this way, energy from the wave exceeds the number of those which give up energy to it. By this reason the wave is forced to damp. By a similar reasoning we can see that distributions with $\partial f_0 / \partial v > 0$ can lead to growing waves.

2.5. Criterium for instability

We have seen that one of the particular solutions of the dispersion equation given in section 2.3 showed for certain values of k complex conjugate solutions for ω . This means that the Vlasov equations can, under certain conditions, describe unstable states of our system. Inspecting equation (2.65) we can verify that if we can create distribution functions which show for some range of velocities a positive slope, the Landau coefficient γ is positive and the wave will grow instead of being damped. From (2.64) we see that a necessary condition for the presence of an instability in our system is the existence of a rising part ($v \partial f_0 / \partial v > 0$) on the velocity distribution function. However, we shall see that this condition alone is not sufficient to lead to instabilities.

As we know the natural oscillation modes of our system are completely determined by the zero order velocity distribution function. It

is therefore interesting to have a criterium to distinguish the stable from the unstable distribution functions.

One of these criteria is due to PENROSE (1960). To derive it we can write the dispersion equation (2.40) in the following form:

$$\frac{k^2}{\omega_p^2} = \int_c \frac{df_o/dv}{(v - \frac{\omega}{k})} dv = Z(\frac{\omega}{k}) \quad (2.66)$$

Now, if an unstable root exists for some real value of k , the frequency must be complex and with a positive imaginary component. Because k^2/ω_p^2 is positive (k is real) a necessary and sufficient condition for instability is that the function $Z(\frac{\omega}{k})$ defined in (2.66) has a positive real value for some ω in the positive imaginary ω plane (SIMON, 1965). The existence of such roots can be predicted by applying to this problem the wellknown Nyquist criterium (PENROSE, 1960; STIX, 1962; SIMON, 1965). The result of this procedure is the so-called Penrose criterium. This one states that if a distribution function $f_o(v)$ characterizes a system which is unstable, then there must exist a certain value v_R of the velocity v for which the following conditions are satisfied:

$$\left(\frac{\partial f_o}{\partial v}\right)_{v=v_R} = 0 \quad \left(\frac{\partial^2 f_o}{\partial v^2}\right)_{v=v_R} > 0 \quad (2.67)$$

From these relations we can conclude that the presence of a minimum in the distribution function is a necessary, although not sufficient, condition for instability. The complete condition for instability also requires that the following relation must be satisfied:

$$\int_{-\infty}^{\infty} \frac{f_o(v) - f_o(v_R)}{(v - v_R)^2} dv > 0 \quad (2.68)$$

From (2.67) we can conclude that only distribution functions which are double-humped can lead to instabilities. As a corollary of this criterium one can immediately say that a single humped distribution function, even when it shows for some values of v a positive slope, can not originate instabilities. We still notice that not all the double-humped distributions represent unstable states. Indeed condition (2.68) expresses that a considerable separation between the two maxima in $f(v)$ is required for the system to attain an unstable state.

CHAPTER III

QUASILINEAR THEORY OF PLASMA WAVES

3.1. Introduction

In chapter 2, treating the problem of the linear oscillations in a collisionless plasma, we were able to see how important is the knowledge of the electron velocity distribution function. Indeed, if we know the average (or zero order) distribution function, equation (2.40) permits to determine the dispersion characteristics of the plasma waves. However, in cases in which unstable situations arise, we must inquire about the validity of linearization. In the last chapter we linearized the Vlasov equation (2.18) assuming that the wave amplitude varies much quicker than the velocity distribution function. We now remember that the wave growth rate γ depends (equation 2.64) on the details of the average velocity distribution function at the so-called resonance region ($\omega = kv$). As the wave grows, electrons which possess velocities around the wave phase velocity can become trapped in the wave potential well. This means that, in this resonant velocity region, the distribution function will be considerably modified due to the action of the wave. The time for this change to occur is of the order of the oscillation period τ of an electron in the wave potential well (DAWSON, 1965). Thus, a necessary condition for the validity of the linearization procedure referred in chapter II, is that τ must be much larger than the inverse of the wave growth rate, and so we have

$$\gamma\tau \gg 1 \quad (3.1)$$

Condition (3.1) imposes a limit on the amplitude of the instability electric field, as the period τ is approximately given by (STIX, 1962; WHARTON et al., 1968):

$$\tau = 2\pi (-m/eEk)^{\frac{1}{2}} \quad (3.2)$$

Thus (3.1) becomes:

$$E \ll \frac{4\pi^2 m \gamma^2}{-ek} \quad (3.3)$$

When the electric field does not satisfy condition (3.3) the linear solution of the Vlasov equations is no longer valid. In the other extreme situation $\gamma\tau \ll 1$ the linearization procedure referred to by SAGDEEV and GALEEV (1969) becomes applicable. When $\gamma\tau \sim 1$ the problem is essentially nonlinear.

If we want to follow the development of the plasma instabilities to amplitudes which approach the limit value given by (3.3), we must consider a nonlinear solution of the Vlasov equations. The question of the search for a general nonlinear solution of the self-consistent field equations is far from being solved. One can only obtain particular solutions of this system of equations, making some special assumptions, which lead to certain plasma models not always easy to compare with real plasmas. One of these particular solutions was obtained almost simultaneously by VEDENOV, VELIKHOV and SAGDEEV (1962) and DRUMMOND and PINES (1962). This approach is known as quasilinear theory of plasma waves and describes the interaction between the resonant electrons ($v = \omega/k$) and the plasma waves.

3.2. Deduction of the quasilinear equations

The quasilinear approximation in the dynamics of a collisionless plasma is based on the assumption of weak turbulence. By weak turbulence we mean the state of the plasma in which the total wave electrostatic energy density ($Q_W = \sum_k W_k$ with $W_k = \frac{1}{2} \epsilon_0 |E_k|^2$) is small compared with the thermal energy density ($W_T = n_0 \kappa T$) but much greater than the value related with the fluctuating fields in thermal equilibrium

$$(W_N = \frac{-n_0^{3/2} e^3}{\epsilon_0^{3/2} (\kappa T)^{1/2}})$$

(EINAUDI and SUDAN, 1968).

Essential in the quasilinear theory is the existence of a broad spectrum of oscillations, constituting an almost continuum of modes. The phases of these plasma modes are assumed to be randomly distributed, so that the electron velocity can not become coherently related with the electric field of any particular mode. With this assumption, usually known as "random phase approximation", the resonant electrons are expected to perform a kind of "Brownian" motion in velocity space, due

to the simultaneous and incoherent action of the different plasma modes.

Using now (2.12) for the Debye length, the condition for weak turbulence can be written as

$$1 \gg \frac{Q_W}{n_o \kappa T} \gg \frac{1}{N_D} \quad (3.4)$$

where N_D is the number of electrons inside a Debye sphere.

One can ask why is the condition of weak turbulence necessary. To answer this question we note that the Vlasov equation (2.18) is not exact. Indeed its validity was based on the assumption that N_D was a large number. So, N_D^{-1} is a small parameter in terms of which we can expand the exact motion equations for the particles. But in the case of weak turbulence there exists another small parameter, namely $Q_W/n_o \kappa T$. Zero order in these two small parameters lead to the Vlasov equations (2.18) to (2.20). First order in the expansion in N_D^{-1} leads to the appearance of Fokker-Planck type collisional terms in (2.18), which contribute to a slow diffusion of particles in velocity space due to binary collisions. However, the plasma electrons are submitted to the random effect of the electric field of the different plasma waves and this fact also leads to their diffusion in velocity space. The rate of diffusion of the particles due to the action of these waves is proportional, as we shall later see, to the wave energy density. Then the "collisional diffusion" can be neglected in comparison with the "wave diffusion" if our second small parameter $Q_W/n_o \kappa T$ is much greater than N_D^{-1} , as expressed in (3.4). Therefore, the reason for considering the plasma in a state of weak turbulence is this: - In the quasilinear theory we intend to neglect the binary collisions and only take into account the diffusion effect due to the plasma waves. If the plasma would be in a state close to thermodynamic equilibrium the two referred diffusion processes (wave and collisional) could not be treated separately, and collisions could not be neglected.

In the derivation of the quasilinear equations we will follow very closely the work of VEDENOV (1963, 1967). We begin by considering the self-consistent field equations. As in the second chapter we will only consider the case of longitudinal electrostatic waves in the absence of external fields. The plasma is assumed to be infinite and the ions constitute a neutralizing background for the electron oscillations. Again

we consider a one-dimensional problem with the notations introduced in the last chapter. So, in what follows, k will be parallel to the electric field E and both directed along z . Under these conditions the Vlasov equations are:

$$\frac{\partial f}{\partial t} + v \frac{\partial f}{\partial z} + \frac{eE}{m} \frac{\partial f}{\partial v} = 0 \quad (3.5)$$

$$\vec{\nabla} \cdot \vec{E} = \frac{n_0 e}{\epsilon_0} \left(\int_{-\infty}^{\infty} f(v) dv - 1 \right) \quad (3.6)$$

$$\frac{\partial E}{\partial t} = - \frac{n_0 e}{\epsilon_0} \int_{-\infty}^{\infty} v f(v) dv \quad (3.7)$$

In the last chapter we derived a general equation (2.40) for the dispersion of the longitudinal waves starting with (3.5) and (3.6). However, we can also use (3.5) and (3.7) to derive quickly an equation describing linear plasma oscillations in the particular case of long wavelengths ($k \rightarrow 0$). Indeed if we linearize (3.5) and if we expand both f and E in a Fourier series

$$f = f_0 + \sum_k f_k e^{jkz} \quad (3.8)$$

$$E = \sum_k E_k e^{jkz} \quad (3.9)$$

we arrive, neglecting $v \frac{\partial f_k}{\partial z} \sim jkv f_k$ in comparison with $\frac{\partial f_k}{\partial t} \sim -j\omega f_k$ as allowed by the long wavelength assumption ($k \ll \omega/v$), at

$$\frac{\partial f_k}{\partial t} = - \frac{e}{m} E_k \frac{\partial f_0(v)}{\partial v} \quad (3.10)$$

$$\frac{\partial E_k}{\partial t} = - \frac{n_0 e}{\epsilon_0} \int_{-\infty}^{\infty} v f_k dv \quad (3.11)$$

These last two equations when combined permit to obtain the wellknown linear harmonic oscillator equation,

$$\frac{\partial^2 E_k}{\partial t^2} + \frac{n_0 e^2}{m \epsilon_0} E_k = 0 \quad (3.12)$$

which describes undamped oscillations occurring at the electron plasma frequency.

Let us assume that at $t=0$ our plasma is in a state of weak turbulence, manifested by the presence of the different plasma waves consistent with the random phase approximation. If the electron velocity distribution function shows a rising part ($v \partial f / \partial v > 0$) at the resonance region ($v = \omega/k$), the plasma becomes unstable and a mechanism of energy exchange takes place between the resonant electrons and the plasma waves. This mechanism leads to the following two effects: 1) the average energy of the plasma waves varies in time and 2) the distribution function of the resonant electrons changes.

To obtain equations describing these phenomena we suppose that the resonant electrons constitute a very small minority group in the electronic population of our system. So, it is assumed that their presence does not modify any of the macroscopic plasma parameters as well as any of the wave properties, exception being made for the growth or damping rates. In other words this assumption means that the waves are supposed to be sustained by the non-resonant electrons alone and that the presence of the resonant electrons has no other effect than to modify the wave amplitude. Then, the distribution function of the non-resonant electrons can be represented by the Fourier series (3.8). For the resonant electrons the distribution function f_r can be written as the sum of a rapidly varying term f_{1r} (following the different waves) with a slowly varying one $f_{0r}(t, v)$. For the electric field we assume that its mean value is zero and that the amplitudes of the Fourier modes $E_k(t)$ also vary slowly in time.

$$f_r = f_{0r}(t, v) + \sum_k f_{kr} e^{jkz} = f_{0r}(t, v) + f_{1r} \quad (3.13)$$

$$E = \sum_k E_k(t) e^{jkz} \quad (3.14)$$

With this approximation the quasilinear equations will only be accurate within a term of the order of γ/ω . γ/ω is the small expansion parameter of the quasilinear theory and it is related in a certain way with the ratio between the respective number of resonant and non-resonant electrons in the system.

Given the smallness of γ/ω it is adequate to assume that the plasma oscillates in frequencies around its electron plasma frequency. So, for the oscillating part of the distribution function and of the electric

field, an average in time over periods much greater than the period of the plasma oscillation (or in space over distances much greater than the wavelength) leads to a zero value. Thus, an average in time and space of the Vlasov equation, written for the resonant electrons, leads to

$$\frac{\partial f_{0r}(t,v)}{\partial t} = \left\langle -\frac{eE}{m} \frac{\partial f_{1r}}{\partial v} \right\rangle = -\frac{1}{2} \frac{\partial}{\partial v} \frac{e}{m} (\sum_k E_k^* f_{kr} + E_k f_{kr}^*) \quad (3.15)$$

Subtracting (3.15) from the Vlasov equation we get

$$\frac{\partial f_{1r}}{\partial t} + v \frac{\partial f_{1r}}{\partial z} + \frac{eE}{m} \frac{\partial f_{0r}(t,v)}{\partial v} = -\frac{e}{m} \frac{\partial}{\partial v} (E f_{1r} - \langle E f_{1r} \rangle) \quad (3.16)$$

In this equation all the terms at the left are first order and the ones at the right are clearly second order and represent the interaction of the waves with themselves. In the case of weak turbulence the difference between these second order terms can be neglected (DRUMMOND and PINES, 1962) and we have by (3.13) and (3.14):

$$\frac{\partial f_{kr}}{\partial t} + jkv f_{kr} = -\frac{e}{m} E_k \frac{\partial f_{0r}(t,v)}{\partial v} \quad (3.17)$$

Equation (3.15) is the first of the two starting equations necessary to the construction of the quasilinear theory. To obtain the second one we take the time derivative of the Maxwell equation (3.7), considering separately the contribution of the resonant and non-resonant electrons. Using (3.10) for these last ones we can arrive to (VEDENOV, 1967)

$$\frac{\partial^2 E_k}{\partial t^2} + \omega_p^2 E_k = \frac{n_0 e}{\epsilon_0} \int_{-\infty}^{\infty} v \frac{\partial f_{kr}}{\partial t} dv \quad (3.18)$$

which still represents plasma oscillations but differs from (3.12) in the fact that the new term introduces the time variation of their amplitude.

To obtain the quasilinear equations we begin by integrating (3.17) in time. The result is:

$$f_{kr}(t) = f_{kr}(0) e^{-j kv t} - \frac{e}{m} \int_0^t E_k(t') \frac{\partial f_{0r}(t',v)}{\partial v} e^{-j kv(t-t')} dt' \quad (3.19)$$

Still following VEDENOV (1967), we substitute this result in (3.15) and (3.18). The equation which results from (3.18) is then multiplied by $\partial E_k^*/\partial t$, and to both sides of the resulting equation we add the respective complex conjugate abbreviated by C.C. Then we get:

$$\frac{\partial f_{Or}(t, v)}{\partial t} = -\frac{1}{2} \frac{e}{m} \frac{\partial}{\partial v} \sum_k E_k^* \{ f_{kr}(0) e^{-jkvt} - \int_0^t E_k(t') \frac{\partial f_{Or}(t', v)}{\partial v} e^{-jkv(t-t')} dt' \} + C.C. \quad (3.20)$$

$$\begin{aligned} \frac{\partial E_k^*}{\partial t} \left\{ \frac{\partial^2 E_k}{\partial t^2} + \omega_p^2 E_k \right\} + C.C. &= \frac{d}{dt} \left\{ \left| \frac{\partial E_k}{\partial t} \right|^2 + \omega_p^2 |E_k|^2 \right\} = \\ &= \frac{n_0 e}{\epsilon_0} \frac{\partial E_k^*}{\partial t} \int_{-\infty}^{\infty} v \{ -jkv f_{kr}(0) e^{-jkvt} + \frac{e}{m} jkv \cdot \\ &\cdot \int_0^t E_k(t') \frac{\partial f_{Or}(t', v)}{\partial v} e^{-jkv(t-t')} dt' - \\ &- \frac{e}{m} E_k \frac{\partial f_{Or}(t, v)}{\partial v} \} dv + C.C. \quad (3.21) \end{aligned}$$

In these last equations we can now make explicit the time dependence by substituting E_k by $|E_k| e^{-j\omega_k t}$. ω_k is the frequency associated with the wavenumber k . For long wavelength oscillations, which is the case we are considering, the frequency ω_k is approximately equal to the electron plasma frequency (expression 2.53). After this substitution we can take the assumed slowly varying functions of time ($|E_k|$ and $\partial f_{Or}(t, v)/\partial v$) out of the integrals over t' .

In the resulting equations we can now look for the limit $t \rightarrow \infty$, and this procedure leads to (VEDENOV, 1967):

$$\frac{\partial f_{Or}(t, v)}{\partial t} = \frac{\partial}{\partial v} \left\{ \frac{e^2}{m^2} \sum_k |E_k|^2 \pi \delta(\omega_k - kv) \frac{\partial f_{Or}(t, v)}{\partial v} \right\} \quad (3.22)$$

$$\frac{\partial |E_k|^2}{\partial t} = |E_k|^2 \pi \omega_p^2 \int_{-\infty}^{\infty} v \frac{\partial f_{Or}(t, v)}{\partial v} \delta(\omega_k - kv) dv \quad (3.23)$$

We can write these equations in the simplified form

$$\frac{\partial f_{0r}(t, v)}{\partial t} = \frac{\partial}{\partial v} \left\{ D_k(t) \frac{\partial f_{0r}(t, v)}{\partial v} \right\} \quad (3.24)$$

$$\frac{\partial |E_k|^2}{\partial t} = 2 \gamma_k(t) |E_k|^2 \quad (3.25)$$

where the values of the parameters D_k (diffusion coefficient) and γ_k (growth rate) are given by:

$$D_k(t) = \frac{\pi e^2}{m} \sum_k |E_k|^2 \delta(\omega_k - kv) \quad (3.26)$$

$$\gamma_k(t) = \frac{\pi}{2} \omega_p^2 \int_{-\infty}^{\infty} v \frac{\partial f_{0r}(t, v)}{\partial v} \delta(\omega_k - kv) dv \quad (3.27)$$

(3.22) and (3.23) are the fundamental quasilinear equations. The first one has the form of a diffusion equation with a time dependent diffusion coefficient. In (3.23) we recognize the formulas of the linear theory (2.63) and (2.64) with the only difference that the growth rate is now a slowly varying function of time.

The quasilinear equations constitute a closed system in the sense that the diffusion coefficient in velocity space depends linearly on the wave energy density, which in turn depends on the details of the distribution function of the diffusing resonant electrons.

Let us now consider the time variation of the total energy density Q in our plasma. This energy is made up of contributions from the kinetic energy of the resonant electrons, the electrostatic energy of the plasma waves and the kinetic energy of the nonresonant electrons. Due to the relatively small number of the resonant electrons, the electrostatic energy associated with the wave is, by the virial theorem, approximately equal to the kinetic energy of the nonresonant electrons which, as we supposed, sustain the wave by their coherent motion. Then we can write

$$\frac{dQ}{dt} = \frac{d}{dt} \left\{ \int_{-\infty}^{\infty} \frac{n_0 m v^2}{2} f_{0r}(t, v) dv + 2 \sum_k \frac{\epsilon_0 |E_k|^2}{2} \right\} \quad (3.28)$$

If we now use the quasilinear equations (3.24) and (3.25) for the time derivative of both the average distribution function of the resonant electrons and the electrostatic energy density, it is easy to find, integrating by parts, that the total energy in our system is conserved

$$\frac{dQ}{dt} = 0 \quad (3.28a)$$

3.3. Quasilinear development of plasma instabilities

The quasilinear equations can be used to study several processes occurring in a plasma. Among these processes we are especially interested in the growth of perturbations arising in an unstable plasma. Before specifying the type of unstable situation let us first simplify the quasilinear equations for the case of a one-dimensional problem. If the wave spectrum is one-dimensional the wave number k and the velocity of the resonant electrons v , that coincides with the wave phase velocity (Cerenkov effect), are simply related by $v = v_{ph} = \omega_k/k \approx \omega_p/k$.

Then, the quasilinear coefficients can be simplified to

$$D_k(v,t) = \frac{[1]e^2 |E_k|^2}{2m^2 v} \quad (3.26a)$$

$$\gamma_k(t) = \frac{\pi}{2} \frac{\omega_p^3}{k^2} \left(\frac{\partial f_{0r}(t,v)}{\partial v} \right)_{v=\omega/k} \quad (3.27a)$$

where $[1]$ represents an unit of length, arising from the passage from the sum in k to an integral in $dk/2\pi$.

The quasilinear equations can now be written as

$$\frac{\partial f_{0r}}{\partial t} = \frac{\partial}{\partial v} \left\{ \underline{B} W \frac{\partial f_{0r}}{\partial v} \right\} \quad (3.29)$$

$$\frac{\partial W}{\partial t} = \underline{A} W \frac{\partial f_{0r}}{\partial v} \quad (3.30)$$

where the coefficients \underline{A} and \underline{B} are given by (equation 2.42):

$$\underline{A} = \pi \omega_p^2 v^2 \quad (3.31)$$

$$\underline{B} = \frac{[1] \omega_p^2}{n_0 m v} \quad (3.32)$$

and W is the wave electrostatic energy density, $W = \frac{1}{2} \epsilon_0 |E_k|^2$.

Hereafter, it is more convenient to consider $W(t, v)$ as a function of the wave phase velocity $v = \omega_p/k$ rather than as a function of k .

In (3.29) and (3.30) f_{Or} and W are both slowly varying functions of time. The quasilinear coefficients \underline{A} and \underline{B} are time independent.

The system of quasilinear equations possesses an interesting property. If we substitute $W \partial f_{Or} / \partial v$ obtained from (3.30) into (3.29) we obtain

$$\frac{\partial}{\partial t} [f_{Or} - \frac{\partial}{\partial v} (\underline{BA}^{-1} W)] = 0 \quad (3.33)$$

and we verify that the quantity $\{f_{Or}(t, v) - \partial/\partial v [\underline{BA}^{-1} W(t, v)]\}$ is conserved during the interaction between the resonant electrons and the plasma waves. This fact permits to determine the final amplitude of the plasma oscillations. From (3.33) we can write

$$f_{Or}(\infty, v) - \frac{\partial}{\partial v} [\underline{BA}^{-1} W(\infty, v)] = f_{Or}(0, v) - \frac{\partial}{\partial v} [\underline{BA}^{-1} W(0, v)] \quad (3.34)$$

and an integration over the velocity leads to

$$W(\infty, v) - W(0, v) = \underline{AB}^{-1} \int_{-\infty}^v [f_{Or}(\infty, v') - f_{Or}(0, v')] dv' \quad (3.35)$$

If we now consider waves with a phase velocity equal to v , we see that the final energy density $W(\infty, v)$ can be determined from (3.35) if we are able to know the final average distribution function for the resonant electrons $f_{Or}(\infty, v)$. Both the initial wave energy density $W(0, v)$ and the distribution function $f_{Or}(0, v)$ are supposed to be known, as they are the main parameters which characterize the state of the plasma at $t=0$. For a certain initial distribution function (a given ω_p) the coefficients \underline{A} and \underline{B} are only functions of the velocity v .

So, we are faced with the question of how to determine the final distribution function for the resonant electrons. A physical picture for the interaction process must then be given. As we are dealing with an unstable situation, the initial distribution function ($t=0$) must exhibit a rising part for some range of velocities. An example of such an unstable distribution, known as "bump on the tail" distribution is represented in figure 3.1, where v_1 and v_2 are assumed to be considerably greater than the thermal velocity of the plasma electrons.

The noise level at the beginning of the quasilinear development of the instabilities ($t=0$) is assumed to be of thermal origin everywhere except in the small range of velocities comprised between v_1 and v_2 where it is large enough to satisfy the condition of weak turbulence of the plasma.

Under these circumstances the plasma waves which have phase velocities in the resonance region ($v_1 \leq v \leq v_2$) will begin to increase in amplitude due to Landau growth ((2.63) and (2.64)).

At the same time the diffusion process begins to flatten the distribution function in this resonance region (3.29) and this leads to a decrease of the wave growth rate (3.27a). However the waves still continue to grow, increasing the diffusion coefficient in velocity space (3.26a). This means that the flatning process on the distribution function becomes quicker and this results in a faster decrease of the wave growth rate. The process goes on until we attain the saturation of the wave amplitude ($\gamma=0$). At the end of the quasilinear relaxation process both the wave energy and the diffusion coefficient attain their maximum value. Anyhow due to the uniformity of the distribution function in the resonance region ($\partial f_{Or} / \partial v = 0$) the quasilinear equations (3.29) and (3.30) are identically zero.

Thus the system has attained a stationary state in which the average distribution function is forced to be constant in the resonance region. Due to the thermal character of the wave energy density outside the resonance region it can be assumed that the average distribution function for the nonresonant electrons does not change during the quasilinear relaxation process. This last assumption is only approximately correct and we will return to this point when treating the so-called adiabatic contribution in the quasilinear theory.

The considerations just presented permit to compute $f_{Or}(\infty, v)$. We now know that the average distribution function will only be different from the initial one inside the resonance region, where it is forced to change to a plateau. Then the determination of the height of the plateau is simply based on the expression for the conservation of the density of the plasma electrons.

$$f_{Or}(\infty, v) = \frac{1}{v_M - v_m} \int_{v_m}^{v_M} f_0(0, v) dv \quad (3.36)$$

v_M and v_m are the extreme values of the range of velocities where the plateau has been formed. These limits are easily obtained stating that (figure 3.1)

$$f_0(0, v_m) = f_{0r}(\infty) = f_0(0, v_M) \quad (3.37)$$

In other words v_m and v_M constitute the only pair of velocities, possessing the same value of f_0 , which makes the establishment of the plateau compatible with density conservation.

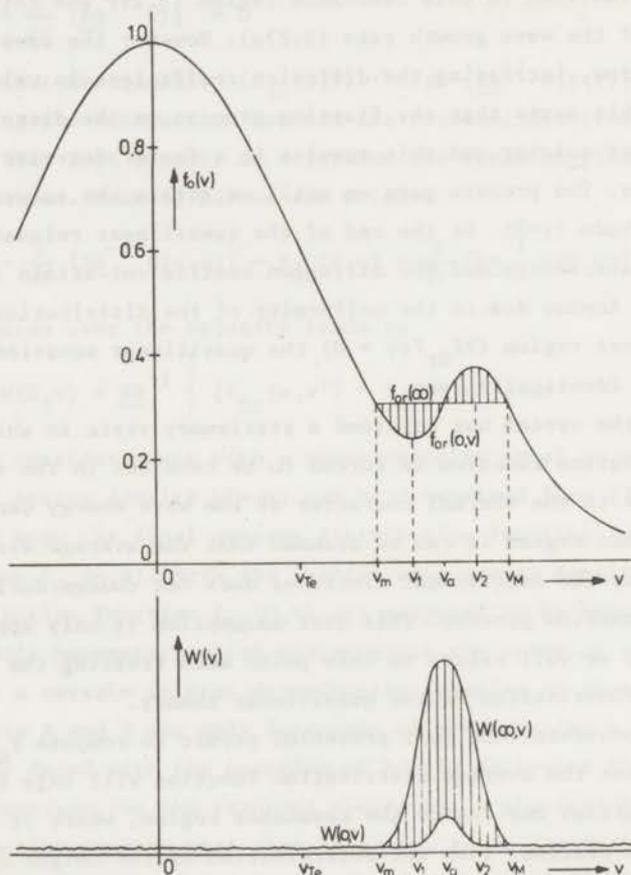


Fig. 3.1. - Initial and final velocity dependence of both the average velocity distribution function and the wave electrostatic energy density under the excitation of the electron plasma instability.

With the knowledge of $f_{Or}(\infty)$, equation (3.35) completely determines the final value of the wave energy density as a function of the phase velocity v or equivalently as a function of the wavenumber $k = \omega_p/v$. In a more explicit form (3.35) can be written as

$$W(\infty, v) = \frac{\pi n_o m v^3}{[1] \cdot \omega_p} \int_{v_m}^v [f_{Or}(\infty) - f_{Or}(0, v')] dv' + W(0, v) \quad (3.38)$$

In figure 3.1 we present the initial ($t=0$) and final ($t=\infty$) velocity dependences of both the average distribution function and the wave electrostatic energy density. We notice that the wave energy is maximum for phase velocities near the centrum of the resonance region. We also notice that due to the interaction process the resonance region broadens in the course of time.

As a result of the quasilinear development of the plasma instabilities we see that some electrons are transferred from regions of higher to regions of lower velocity. This means that the resonant electrons lose a certain amount of energy which is necessary to the build up of the final supra-thermal spectrum of plasma oscillations. From (3.38) we can write

$$2 \int_{\omega_p/v_M}^{\omega_p/v_m} [W(\infty, v) - W(0, v)] \frac{dk}{2\pi} = \int_{v_m}^{v_M} n_o m v \int_{v_m}^v [f_{Or}(\infty) - f_{Or}(0, v')] dv' dv \quad (3.39)$$

Integration by parts of the right hand side of this equation leads to an energy conservation relation (VEDENOV, 1967):

$$2 \int_{\omega_p/v_M}^{\omega_p/v_m} [W(\infty, v) - W(0, v)] \frac{dk}{2\pi} = - \int_{v_m}^{v_M} \frac{n_o m v^2}{2} [f_{Or}(\infty) - f_{Or}(0, v)] dv \quad (3.40)$$

We see that the energy lost by the resonant electrons equals twice the increase in the electrostatic energy of the plasma waves.

3.4. Conditions of applicability of the quasilinear theory

As we wrote before, the quasilinear equations, as deduced here following VEDENOV (1967), are only approximately correct. Indeed they can be looked upon as being the lowest order expressions in the expansion on the small parameter γ/ω . Before considering the necessary corrections let us now make a brief résumé of the conditions of applicability of these equations.

First of all the plasma must be in a state of weak turbulence.

In deriving the quasilinear equations, use was made of time and space averages. If these averages are to be valid, the resonant electrons are not allowed to undergo fast processes. This means that this resonance interaction must be rather slow, and that the trapping of the resonant electrons in the potential well of any individual wave is therefore forbidden to occur. Then, the spread in the wave phase velocity must be greater than the capture velocity (as determined in the wave reference frame) of the highest amplitude wave. This condition can be expressed by (VEDENOV et al., 1963; EINAUDI et al., 1969):

$$\Delta\left(\frac{\omega}{k}\right) = \Delta v > (-eE/km)^{\frac{1}{2}} \quad (3.41)$$

where E is the amplitude of the electric field of an individual wave.

Another condition assumed when deriving the quasilinear equations requires that the changes in the average distribution function and in the wave amplitude must be very small over several plasma oscillations. This implies that the growth rate and the reciprocal of the relaxation time (equation 3.50), must both be much smaller than the oscillation frequency.

The quasilinear theory applies only for the situations where the wave growth rate depends on the velocity gradient of the electron distribution function (velocity space instabilities). As, in the exposed theory, the growth rate depends linearly on $\partial f_{0r}/\partial v$, this derivative is not allowed to take very large values in order to avoid violation of the adiabaticity of the interaction.

Fundamental is the condition which states that the wave-particle interaction must be rather sharp in velocity space. In other words, this means that the interaction of a particular wave with the resonant electrons must take place in a narrow band in the total resonance velo-

city region (VEDENOV, 1963; IVANOV et al., 1967.a; KLOZENBERG et al., 1970). This condition can be expressed by

$$\Delta v \gg \frac{\gamma_k}{k} \quad (3.41a)$$

This is equivalent to say that the value of the velocity distribution function at the resonance region must vary weakly over a velocity interval equal to γ_k/k . Only so can we go over from (3.20) and (3.21) to (3.22) and (3.23), the fundamental quasilinear equations.

Because the final supra-thermal spectrum of oscillations is rather broad it is also essential that the plasma dispersion equation (2.40) must not allow any kind of resonant mode coupling or, by other words, that neither the sum nor the difference of two excited frequencies can be equal to the natural frequency of another plasma mode.

3.5. *Adiabatic contribution in the quasilinear theory*

As we have seen, the simplified derivation of the quasilinear equations leads to the conclusion that the distribution function changes only inside the resonance region where it becomes a plateau. In this way, we immediately see that the plasma electrons lose energy as well as momentum. Anyhow, by the virial theorem, we could prove that energy was conserved during the interaction process, as the energy lost by the resonant electrons was found in the total energy associated with the plasma waves. The fact that one half of this energy must appear under the form of kinetic energy of the nonresonant electrons (which constitute the bulk of particles which sustain the wave) is quite in contradiction with the invariance of the average distribution function of these electrons. Further, even with the problem of energy conservation solved, we can verify that the quasilinear equations, as we presented them, do not conserve momentum.

To analyse this problem we need to consider a less restrictive deduction of the quasilinear equations. DRUMMOND and PINES (1962) arrive to formally the same equations as VEDENOV et al. (1962). Equation (3.23) remains unchanged and the diffusion equation (3.22) differs only in the fact that the diffusion coefficient is written with more generality.

In the treatment of Drummond and Pines the equivalent of (3.26) is written as

$$D_k(t) = \frac{e^2}{m^2} \sum_k |E_k|^2 \frac{\gamma_k(t)}{(\omega_k - kv)^2 + \gamma_k^2} \quad (3.42)$$

However, in the resonance region we have $v = \omega_k/k$ and, due to the fact that $\gamma_k \ll \omega_k$, we see that the denominator in (3.42) displays a characteristic resonance behaviour. So we can write

$$\frac{\gamma_k(t)}{(\omega_k - kv)^2 + \gamma_k^2} = \pi \delta(\omega_k - kv) \quad (3.42.a)$$

which transforms (3.42) into the simplified expression (3.26).

The approximate diffusion coefficient is quite adequate to describe the interaction between the resonant electrons and the plasma waves.

However, when considering the nonresonant electrons, (3.42.a) is no longer valid and we must take for D_k the value given by (3.42). From this expression we see that the diffusion coefficient is strongly peaked at the resonance region and that it decays with the increase in $|(\omega_k - kv)|$. Because for the nonresonant electrons $(\omega_k - kv)^2 \gg \gamma_k^2$ we verify that their diffusion coefficient is much smaller than the corresponding one for the resonant electrons. But the number of nonresonant electrons being much greater than the number of the resonant ones, their diffusion can not be ignored.

These two diffusion processes (resonant and nonresonant or thermal) are essentially different in character (SAGDEEV and GALEEV, 1969). The diffusion of the resonant electrons leads to the establishment of the plateau in the distribution function and constitutes an irreversible process. The diffusion of the nonresonant electrons, or adiabatic diffusion, is responsible for the increase in the oscillatory kinetic energy of these electrons when the plasma waves increase in amplitude. This last diffusion process is reversible.

KADONTSEV (1965), making use of the diffusion coefficient for the nonresonant electrons arrives to

$$f_o(v, v) - f_o(0, v) = \frac{[1]e^2}{2m^2} \int E_k^2 (t=\infty) \frac{\partial}{\partial v} \left[\frac{1}{(\omega - kv)^2} \frac{\partial f_o}{\partial v} \right] \frac{dk}{2\pi} \quad (3.43)$$

This equation permits to determine the final shape of the average distribution function of the nonresonant electrons. Kadomtsev writes that all the momentum and one half of the energy lost by the resonant electrons for the growth of the plasma waves are transferred to the thermal electrons and this results in the distortion of their distribution function. According to Kadomtsev the final shape of the distribution function will be similar to that presented in figure 3.2. Due to momentum conservation the final distribution function is slightly shifted to the right in relation to $f_0(0,v)$ and so it has the maximum for some small positive value of the velocity.

It can be proved (GALEEV and SAGDEEV, 1969) that, as a result of the quasilinear interaction between the resonant electrons and the waves, the nonresonant particles (or the main plasma) appear to be heated. The increase in the plasma temperature is given by:

$$\Delta T = \sum_k \frac{\epsilon_0 |E_k|^2}{2 n_0 \kappa} \quad (3.44)$$

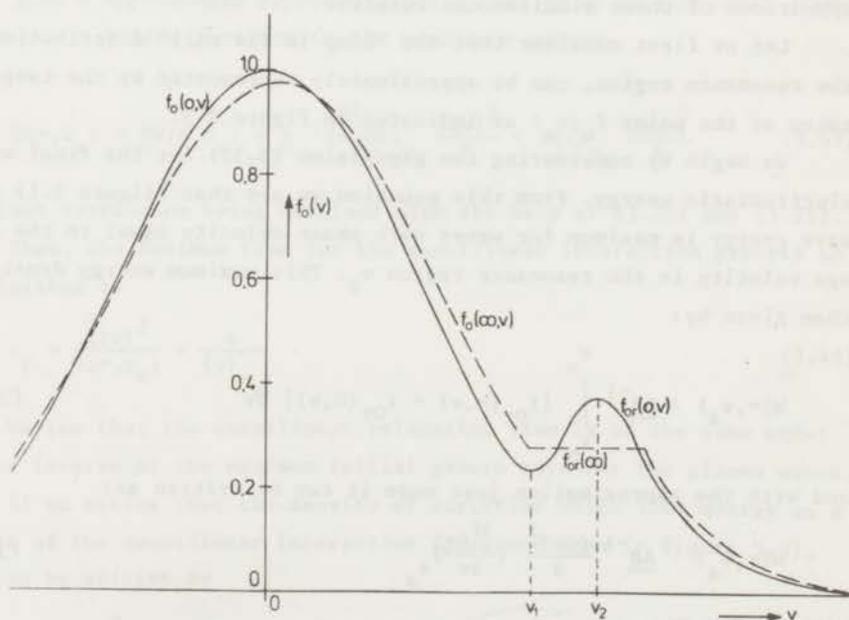


Fig. 3.2. - Initial and final average velocity distribution function related with the excitation of the electron plasma instability.

The quasilinear theory is of course only valid if (equation 3.4) the increase in temperature is negligible when compared with the initial plasma temperature. This heating is attained without increase in the entropy of the system, as the adiabatic diffusion process is a reversible one. In other words if the waves will later be damped by any other mechanism, the plasma temperature will accordingly also decrease.

This adiabatic contribution from the thermal electrons to the diffusion process can be quite important for the study of processes occurring in a plasma in which no resonant interaction exists (EINAUDI and SUDAN, 1969) or for example when considering the enhanced diffusion in a plasma (KADOMTSEV, 1965).

3.6. Relaxation time for the quasilinear interaction process

We have seen that the quasilinear development of the plasma instability leads to the establishment of a plateau in the distribution function and to the saturation of the wave amplitude. We are now interested in obtaining the order of magnitude of the time needed for the appearance of these simultaneous results.

Let us first consider that the "bump in the tail" distribution, in the resonance region, can be approximately represented by the tangent taken at the point $f_0(v_a)$ as indicated in figure 3.3.

We begin by considering the expression (3.35) for the final wave electrostatic energy. From this equation we see that (figure 3.1) the wave energy is maximum for waves with phase velocity equal to the average velocity in the resonance region v_a . This maximum energy density is then given by:

$$W(\infty, v_a) = \frac{AB}{8}^{-1} \int_{v_m}^{v_a} [f_{0r}(\infty, v) - f_{0r}(0, v)] dv \quad (3.45)$$

and with the approximation just made it can be written as:

$$W(\infty, v_a) = \frac{AB}{8}^{-1} \frac{(\Delta v)^2}{8} \left(\frac{\partial f_{0r}}{\partial v} \right)_{v_a} \quad (3.46)$$

with $\Delta v = v_M - v_m$.

The maximum value of the diffusion coefficient is then given (3.29) by:

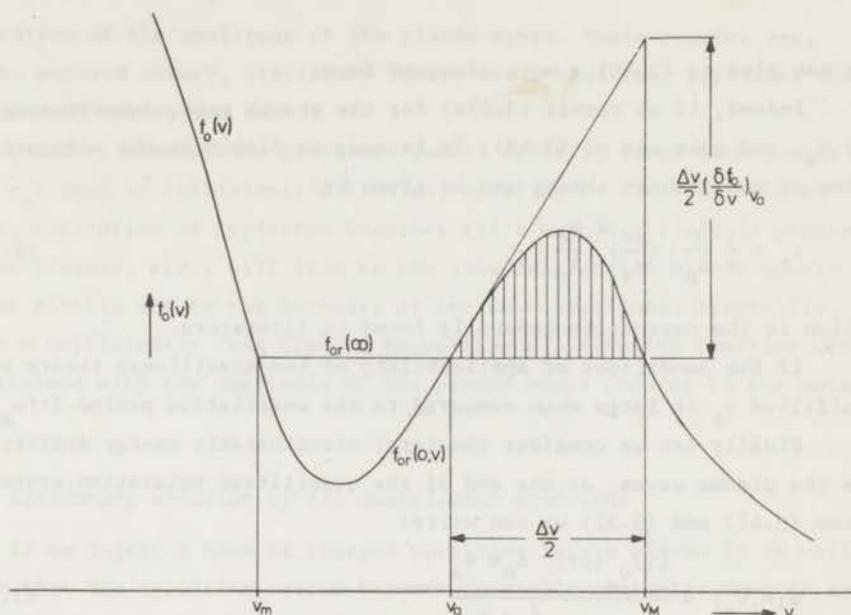


Fig. 3.3. - Approximate representation of the "bump in the tail" distribution function in the resonance region.

$$D(\infty, v_a) = \underline{B}W(\infty, v_a) \approx \underline{A} \left(\frac{\partial f_{0r}}{\partial v} \right)_{v_a} \frac{(\Delta v)^2}{8} \approx 2(\gamma)_{v_a} \frac{(\Delta v)^2}{8} \quad (3.47)$$

the last expression being obtained with the help of (3.30) and (3.25).

Then, the minimum time for the quasilinear interaction process to be finished is

$$\tau_r \approx \frac{(\Delta v)^2}{D(\infty, v_a)} \approx \frac{4}{(\gamma)_{v_a}} \quad (3.48)$$

We see that the quasilinear relaxation time is of the same order as the inverse of the maximum initial growth rate for the plasma waves.

If we notice that the density of particles which lost energy as a result of the quasilinear interaction (darkened area in figure 3.3), δn , can be written as

$$\delta n = n_o \int_{v_a}^{v_M} [f_{0r}(0, v) - f_{0r}(\infty, v)] dv = n_o \frac{(\Delta v)^2}{8} \left(\frac{\partial f_{0r}}{\partial v} \right)_{v_a} \quad (3.49)$$

we can give to (3.48) a more adequate form.

Indeed, if we recall (3.27a) for the growth rate, substituting ω/k by v_a , and make use of (3.49), it is easy to find that the relaxation time of quasilinear theory can be given by:

$$\tau_r \approx \frac{1}{\pi} \frac{1}{\omega_p} \left\{ \frac{\Delta v}{v_a} \right\}^2 \frac{n_o}{\delta n} \quad (3.50)$$

which is the expression generally found in literature.

If the conditions of applicability of the quasilinear theory are fulfilled τ_r is large when compared to the oscillation period $2\pi/\omega_p$.

Finally let us consider the total electrostatic energy density Q_w in the plasma waves, at the end of the quasilinear relaxation process. From (3.47) and (3.32) we can write:

$$W(\infty, v_a) = \frac{(\gamma)_{v_a} (\Delta v)^2 n_o m v_a}{4 \omega_p^2 [1]} \quad (3.51)$$

An integration in k leads approximately ($\Delta k \approx -\frac{\omega_p}{2} \frac{\Delta v}{v_a}$) to

$$Q_w = \sum_k W_k \approx \frac{1}{2\pi} W(\infty, v_a) \Delta k \approx \frac{1}{8\pi} \left\{ \frac{\Delta v}{v_a} \right\}^3 \frac{(\gamma)_{v_a}}{\omega_p} n_o m v_a^2 \quad (3.52)$$

In order to compare Q_w with the thermal energy density of the plasma electrons $W_T = n_o m v_T^2 = n_o kT$, we can write (3.52) under the form

$$Q_w = \frac{1}{8\pi} \frac{\Delta v}{v_a} \left\{ \frac{\Delta v}{v_T} \right\}^2 \frac{(\gamma)_{v_a}}{\omega_p} W_T \quad (3.52a)$$

Thus, even at the end of the quasilinear interaction process, the condition of weak turbulence (3.4) is fulfilled as the total energy of the final spectrum is rather small (of order γ/ω) compared with the thermal energy of the plasma electrons.

In the quasilinear theory, as we have seen, the only nonlinear effect considered was the reaction of the plasma oscillations in the zero order velocity distribution function. The average quadratic effects produced by the rapidly varying part of the distribution function on the development of the instability lead, as we verified, to the establishment of the plateau in the velocity distribution function and to the

saturation of the amplitude of the plasma waves. These results are, in the exposed theory, stationary in the sense that they represent the response of our system when $t \rightarrow \infty$.

However, slow plasma processes (which occur in times much longer than τ_r) such as collisional diffusion, coupling of different plasma modes, excitation of cyclotron branches (if a magnetic field is present in the plasma), etc., will lead to the slow destruction of the quasilinear plateau and to the decrease of the wave amplitude. Eventually, after a sufficiently long time, a Maxwellian distribution function will be attained with the amplitude of the plasma waves reduced to the noise level.

3.7. Stationary solution of the quasilinear equations

If we inject a beam of charged particles into a plasma it is well known that the resulting system becomes generally unstable. However the resulting beam-plasma interaction has a different character in the two extreme situations: 1) when the beam is dense and almost monoenergetic the instability frequency and the associated growth rate must be determined with the consideration of the entire beam-plasma system (BRIGGS, 1964); 2) but when the beam has a rather low density and exhibits a relatively large velocity spread, it can be expected that the result of its passage through the plasma will be the excitation of the natural plasma oscillations with a small growth rate ($\gamma \ll \omega_r$) determined by the beam (SEIDL, 1970). In other words the plasma oscillations are assumed to satisfy the dispersion equation of the plasma alone and the beam has no other property than to modify the wave amplitude by resonant interaction.

The quasilinear theory, as presented here, applies only to the study of the interaction of the second type of beams with a plasma. Indeed the derivation of the quasilinear equations (3.22) and (3.23) is only valid if the extension of the resonance region in velocity is larger than $1/k\tau_r$ (equations 3.41a and 3.48), where τ_r is the quasilinear relaxation time. Using (3.50) this fundamental condition can be written as

$$\left(\frac{\Delta v}{v_b}\right) \gg \left(\frac{n_b}{n_p}\right)^{1/3} \quad (3.53)$$

where the beam density n_b is here identified with δn , the density of the fraction of the resonant electrons which lose energy in the quasilinear wave-particle interaction (figure 3.3). So this theory can not be used to study the interaction of monoenergetic beams with a plasma.

The combined beam-plasma electron velocity distribution function is assumed to be similar to the one presented in figure 3.1, the so-called "bump in the tail" distribution. In section 3.3 we analyzed the homogeneous solution of the quasilinear equations. We are now interested in obtaining their stationary solution, as, when treating problems of injection of beams, it is more adequate to consider the spatial variation of the beam-plasma interaction. We assume that we inject our beam in the z -direction and again we consider a one-dimensional problem. The initial conditions are now associated with $z=0$, the coordinate of the plane of injection of the beam into the assumed infinite plasma. The limit $t \rightarrow \infty$ becomes $z \rightarrow \infty$ and all the derivations made in the last section are valid leading to similar results.

In this case a new system of quasilinear equations can be written using the obvious substitutions

$$\frac{\partial f_{Or}}{\partial t} \rightarrow v \frac{\partial f_{Or}}{\partial z} \quad \text{and} \quad \frac{\partial W}{\partial t} \rightarrow v_g \frac{\partial W}{\partial z} \quad (3.54)$$

where v_g is the group velocity of the plasma waves:

$$v \frac{\partial f_{Or}}{\partial z} = \frac{\partial}{\partial v} \left(\underline{B} W \frac{\partial f_{Or}}{\partial v} \right) \quad (3.55)$$

$$v_g \frac{\partial W}{\partial z} = \underline{A} W \frac{\partial f_{Or}}{\partial v} \quad (3.56)$$

The consideration of a one-dimensional model is justified as, in practice, the most unstable modes always travel in the direction of the beam. The physical picture for the interaction is similar to the one presented in section 3.3 and so we conclude that when $z \rightarrow \infty$ a plateau is established on the distribution function in the resonance region. The essential difference between this spatial treatment and the former temporal analysis lies in the fact that the quasilinear interaction conserves now another quantity. Instead of (3.33) we have

$$\frac{\partial}{\partial z} \left[v f_{0r} - \frac{\partial}{\partial v} (BA^{-1} v_g W) \right] = 0 \quad (3.57)$$

Thus the final energy density for the plasma waves is computed from

$$W(\infty, v) = W(0, v) + \frac{AB^{-1}}{v_g} \int_{-\infty}^v v' [f_{0r}(\infty, v') - f_{0r}(0, v')] dv' \quad (3.58)$$

The plateau is established between v_m and v_M which are now given by

$$\int_{v_m}^{v_M} v f_{0r}(\infty) dv = \int_{v_m}^{v_M} v f_{0r}(0, v) dv \quad (3.59)$$

which states the conservation of the current density (DRUMMOND, 1964). So, the height of the plateau is determined by

$$f_{0r}(\infty) = \frac{2}{v_M^2 - v_m^2} \int_{v_m}^{v_M} v f_{0r}(0, v) dv \quad (3.60)$$

together with equations (3.37).

Energetic considerations are identical and we can see that, at $z=\infty$ the energy density of the plasma waves must be much greater than at $z=0$, as the beam loses part of its kinetic energy during its passage through the plasma. Multiplying (3.58) by the group velocity v_g we can, integrating by parts, arrive at

$$2 v_g \int_{\omega_p/v_M}^{\omega_p/v_m} [W(\infty, v) - W(0, v)] \frac{dk}{2\pi} + n_0 \int_{v_m}^{v_M} v \frac{mv^2}{2} [f_{0r}(\infty) - f_{0r}(0, v)] dv = 0 \quad (3.61)$$

This equation represents the conservation along the space of the total energy flux.

Comparing (3.58) with (3.35) we verify that, roughly speaking, the final electrostatic energy density in this case is a factor v_b/v_g greater

ter than in the homogeneous case. This is due to the fact that kinetic energy is quickly transported to a certain region by the beam electrons, while the electrostatic energy is rather slowly taken out from this region by the plasma waves (small value of the group velocity).

3.8. Recent development of the quasilinear theory

In the last 5 years a considerable number of theoretical publications appeared in literature related with the quasilinear theory. Generally speaking, the authors of these publications intended to make the use of this theory less restrictive. In the last sections we derived the quasilinear equations making a large number of assumptions. Among these ones we remember: 1) The instability frequency is very close to the electron plasma frequency; 2) There are no external fields acting on the plasma; 3) The plasma is assumed to be infinite; 4) The plasma is assumed to be homogeneous; 5) The beam has a relatively large velocity spread; 6) The excited spectrum of oscillations must be rather broad and consistent with the "random phase approximation"; 7) The spectrum is one-dimensional.

With all these assumptions it is not surprising that the theoreticians have been trying to extend the quasilinear theory to cases in which one or more of these conditions is not fulfilled. In this way the quasilinear theory has been extended to:

1) the study of other types of instabilities. For example SIZONENKO et al. (1966) and KOVRISHNYKH (1967) consider the quasilinear relaxation occurring under the presence of ion-acoustic waves; ROWLANDS et al. (1966) treat the case of the ion cyclotron instability. VÖLK (1967) develops the quasilinear theory for the two-stream instability. IVANOV et al. (1967.b) treat the case of potential drift waves with the electron temperature exceeding the ion temperature. SHAPIRO et al. (1968) mention the quasilinear relaxation process occurring due to the excitation of cyclotron instabilities due to the anomalous Doppler effect ($\omega - kv = -\omega_{ce}$). RYUTOV (1967) introduces the quasilinear theory of runaway electrons. ZASLAVSKII et al. (1968) apply the quasilinear approximation to the study of the stochastic instabilities of trapped particles.

2) The consideration of the presence of a magnetic field in the plasma has been reported by SHAPIRO et al. (1962), DRUMMOND (1964),

SIZONENKO et al. (1966), BASS et al. (1966), ROWLANDS et al. (1966) and SHAPIRO et al. (1968).

3) Semi-infinite plasmas are considered in the works of DRUMMOND (1964), FAINBERG et al. (1965), IVANOV et al. (1967-a) and CARNEVALE et al. (1967). Drummond also considers the case in which the plasma is immersed in a magnetic field and possesses a cylindrical symmetry with a density gradient perpendicular to the magnetic axis.

4) The quasilinear relaxation of an electron beam in an inhomogeneous plasma is studied by IVANOV et al. (1967-b), RYUTOV (1970) and BREIZMAN et al. (1970).

5) The interaction of almost monoenergetic beams with a plasma is considered by SHAPIRO (1963), FAINBERG et al. (1965,1970) and IVANOV et al. (1967.a).

6) The consideration of a narrow spectrum of oscillations (almost monochromatic waves) is made by AL'TSHUL' and KARPMAN (1966).

7) The quasilinear relaxation process under the presence of a three-dimensional spectrum is studied in detail by BERNSTEIN et al. (1966).

With all these different new approaches in the quasilinear theory, a rapid progress is noticed in the understanding of the interaction between charged particles and waves in beam-plasma systems.

From all the referred publications we shall now select and present, without great details, the most important contributions. These ones have, in one way or another, influenced the measurements done in our beam-plasma experiment.

Perhaps, the main disagreement between the exposed theory and our experimental situation lies in the fact that we inject an almost monoenergetic beam into the plasma. But, following FAINBERG and SHAPIRO (1965), when a monoenergetic beam is injected into a plasma, it loses very quickly its monoenergeticity and becomes sufficiently spread out in velocity space so that its subsequent interaction with the plasma can be followed within the framework of the quasilinear theory. So, let us follow with a little more detail the work of these authors.

When an electron beam is almost monoenergetic, it is clear that it will resonate, as a whole, with any plasma wave which will have a phase velocity close to the beam initial velocity v_b . Thus in the first stage of its interaction with a plasma the nonlinear effects will appear much

sooner in the beam than in the plasma. This means that the plasma waves are rather well described by the linear theory to which the beam only contributes through its macroscopic parameters (density, average velocity and temperature).

So, during this first phase of the interaction, the evolution of the beam-plasma system will be determined by the evolution of the beam. This one can be followed within a hydrodynamic description based on the moments of the beam velocity distribution function (equations 2.3 to 2.5). These quantities obey the conservation laws derived from the kinetic equation for the distribution function. Such an analysis leads to the conclusion that, in the interaction with the plasma waves, the beam average velocity decreases slightly and the beam temperature increases. These changes occur in times of the order of $\omega_p^{-1} (n_p/n_b)^{1/3}$ and so rather small compared with the quasilinear relaxation time τ_r (expression 3.50).

After this short time the interaction can be followed with the quasilinear equations. In their paper, Fainberg and Shapiro consider the non-stationary inhomogeneous solution of the equations (3.22) and (3.23), with the obvious substitutions

$$\frac{\partial f_{0r}}{\partial t} \rightarrow \frac{\partial f_{0r}}{\partial t} + v \frac{\partial f_{0r}}{\partial z} \quad \text{and} \quad \frac{\partial |E_k|^2}{\partial t} \rightarrow \frac{\partial |E_k|^2}{\partial t} + v_g \frac{\partial |E_k|^2}{\partial z} \quad (3.62)$$

They also assume that at $t=0$ the electron beam begins to be continuously injected at $z=0$ into a semi-infinite plasma. The problem is one-dimensional.

Due to the continuous injection of the beam (the same happens in our experiment) the excitation of the plasma waves takes place continuously as new electrons are injected in the plasma. If the wave group velocity is much smaller than the initial beam velocity, as expected in the case of the excitation of the electron plasma instability, the energy lost by the beam during the quasilinear relaxation process accumulates in a transition layer near to the plasma boundary.

Fainberg and Shapiro consider from now on two regions in the plasma: - the region of large z ($z \gg v_b \tau_r$) attained by the beam electrons in a time large compared with the relaxation time, and in which

the boundary effects are unimportant; - and the region of small z ($z \lesssim v_b \tau_r$) in which the distribution of the electric field intensity is highly inhomogeneous. In the region of large z nothing new is obtained and the results of the presented quasilinear theory are applicable.

In the region of small z the change in the total wave energy is equal to the energy transported by the beam into this region. Thus the wave energy, during the first stages of the quasilinear interaction, increases with time due to the continuous injection of the beam. Therefore, as the field amplitude increases, the relaxation of the beam becomes more rapid and the relaxation length is reduced. In this way a high intensity layer is formed which is seen to be displaced, in the course of time, towards the plasma boundary.

An approximate expression for the relaxation length is given by

$$z_r(t) = v_b \tau_r e^{-t/\tau_r} + v_g \tau_r [1 - e^{-t/\tau_r}] \quad (3.63)$$

The minimum value for this relaxation length is then attained for $t \rightarrow \infty$ and is

$$z_r(t \rightarrow \infty) = v_g \tau_r \quad (3.64)$$

The maximum wave energy density is reached at this distance and is given by

$$W(z_r)_{t \rightarrow \infty} = \frac{\pi n_0 m v^3 v}{\omega_p v_g [1]} \int_{-\infty}^{\infty} v' [f_{0r}(\infty) - f_{0r}(0, v')] dv' \quad (3.65)$$

This value coincides with the one given by expression (3.58) obtained for the stationary case.

At $z = z_r(t \rightarrow \infty)$ the quasilinear plateau is established in the distribution function and the instability amplitude attains its maximum value. For larger values of z , and for times of the order of the relaxation time, the field amplitude must decrease, as the beam does not carry anymore any transferrable kinetic energy ($\partial f_{0r} / \partial v = 0$) and the waves have not yet had time to transport to these large distances the associated energy, due to the smallness of their group velocity.

Related with the first stage of the beam-plasma interaction, namely the loss of the monoenergeticity of the beam, another layer of intense fields is predicted by Fainberg and Shapiro. This one is anyhow

less intense and it appears naturally closer to the plasma boundary. In conclusion, it is proved that the relaxation process of a monoenergetic beam in a plasma leads to the appearance of two high intensity field layers in the plasma. These layers are expected to be formed in a time of the order of the quasilinear relaxation time.

Another important publication was written by IVANOV and RUDAKOV (1967-a). These authors consider the evolution of the quasilinear relaxation process towards equilibrium. They investigate the temporal variation of the distribution function of a weak beam, satisfying the quasilinear requirements, which is injected into a plasma. The beam initial distribution function is shown in fig. 3.4. As we see, the beam initial velocity is assumed to be much larger than the thermal velocity of the plasma electrons. Also a region exists in velocity space where f_0 is zero.

The quasilinear theory is applied by these authors who start the study of the relaxation of this beam with equations (3.22) and (3.23). The frequency of the instability is assumed to be the electron plasma frequency and the problem is one-dimensional.

Dimensionless variables and functions are introduced according to:

$$F = \pi \frac{n_b}{n_p} v_b f \quad \tau = \omega_p \frac{n_p}{n_b} t \quad (3.66)$$

$$w = \frac{W_k \omega_p}{n_p m v^3} \quad V = \frac{v}{v_b}$$

With these new symbols the quasilinear equations become

$$\frac{\partial F}{\partial \tau} = \frac{\partial}{\partial V} (wV^2 \frac{\partial F}{\partial V}) \quad (3.67)$$

$$\frac{\partial w}{\partial \tau} = wV^2 \frac{\partial F}{\partial V} \quad (3.68)$$

where F is normalized to:

$$\int F dV = \pi \quad (3.69)$$

Substituting $wV^2 \frac{\partial F}{\partial V}$ from (3.68) into (3.67) and integrating in τ we get

$$F - F_0 = \frac{\partial}{\partial V} (w - w_0) \quad (3.70)$$

F_0 and w_0 represent the distribution function and the wave energy at $t = 0$. Using (3.70) we can eliminate F from (3.68) and obtain an equation which only contains $w(V, \tau)$.

$$\frac{\partial w}{\partial \tau} = V^2 w \frac{\partial^2 (w - w_0)}{\partial V^2} + V^2 w \frac{\partial F_0}{\partial V} \quad (3.71)$$

In the region separating, in velocity space, the zones occupied by the beam and the plasma, F_0 is zero and so $\partial F_0 / \partial V$ is also zero. Then equation (3.71) is, for that region, written as

$$\frac{\partial w}{\partial \tau} = V^2 w \frac{\partial^2 (w - w_0)}{\partial V^2} \quad (3.72)$$

Equation (3.72) remotely resembles the equation describing the propagation of heat in space when the thermal conductivity is a power function of the amount of heat. By similarity with this type of heat propa-

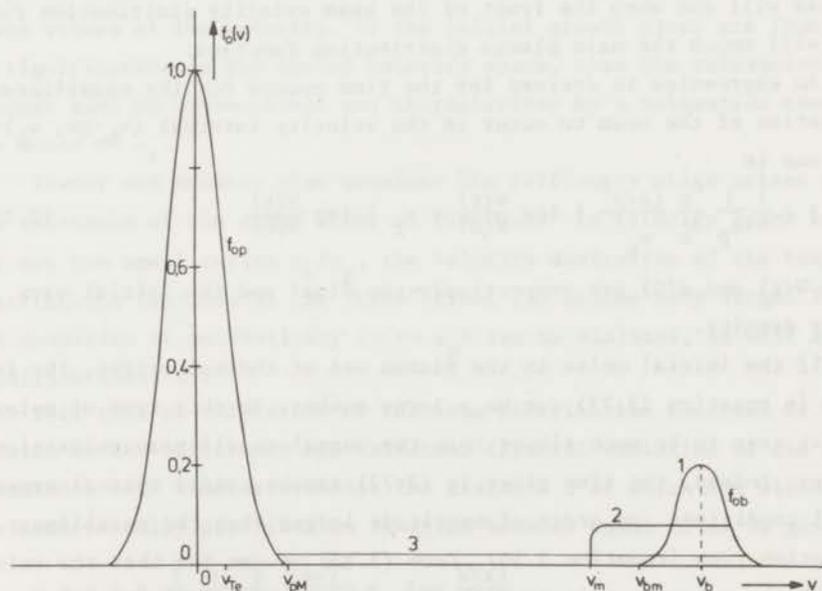


Fig. 3.4. - Evolution of the beam velocity distribution function according to Ivanov and Rudakov.

gation along space, the authors state that the beam distribution function will move in velocity space as a "wave" with a steep front, as indicated in figure 3.4. It is also stated that the diffusion of the beam electrons in velocity space will depend on the fine details of the distribution function only at the very beginning of the interaction process, when the distribution function begins to flatten. For the later phases of the interaction, the evolution of the beam distribution function will depend only on the total beam initial energy density. This is based on the fact that in the similar problem of the heat conduction, the front of the thermal wave at large distances from an explosion does not depend on the temporal history of the explosion but rather on the amount of heat released in it.

A very important result of this self-similar study is thus the fact that it is predicted that the beam velocity distribution function will always show a plateau during the course of the interaction process. The height of this plateau will depend on time, decreasing while the plateau extends towards lower velocities. The quasilinear relaxation process will end when the front of the beam velocity distribution function will touch the main plasma distribution function.

An expression is derived for the time needed for the quasilinear relaxation of the beam to occur in the velocity interval $(v_b - \Delta v, v_b)$. This one is

$$t \approx \frac{1}{\pi} \frac{1}{\omega_p} \frac{n_p}{n_b} \frac{(\Delta v)^2}{v_b^2} \frac{1}{2} \log \frac{W(t)}{W(0)} = \tau_r \frac{1}{2} \log \frac{W(t)}{W(0)} \quad (3.73)$$

where $W(t)$ and $W(0)$ are respectively the final and the initial wave energy density.

If the initial noise in the plasma was of thermal origin, the logarithm in equation (3.73) can be a large number. So this type of relaxation is seen to be much slower than the normal quasilinear relaxation process. Indeed, the time given in (3.73) can be, under typical experimental conditions, an order of magnitude larger than the quasilinear relaxation time (equation 3.50). From (3.73) we can see that the velocity of the wave front is determined by the wave growth rate.

The physical picture for this type of interaction, given by Ivanov and Rudakov, is the following: - After a time of the order of τ_r the "wave" front has traversed a path in velocity space approximately

equal to $2\Delta v/\log\{W(\tau_r)/W(0)\}$, and a plateau is formed on the distribution function behind the "wave" front. At the same time supra-thermal noise is excited in the same resonance velocity interval. If the noise level ahead of the front was null this situation would be definitive, and the relaxation process was then finished. But the existence of thermal noise near to the "wave" front continues the interaction process until that $\partial f/\partial v$ becomes negative or zero for all values of the velocity. This only happens when the two distribution functions (beam and plasma) are joined together (case 3 of figure 3.3), finishing the quasilinear relaxation of the beam.

This type of relaxation is then stated by the authors to be reasonably applicable to a broad class of initial beam distribution functions, even when there is no separation in velocity space between the beam and the plasma. The generalization of this theory to other cases is demonstrated to be valid if the plasma waves will firstly grow in the vicinity of the initial beam velocity, where the linear growth rate is maximum. In the other velocity regions it is expected that the noise will keep its initial thermal character until the "wave" front will reach these values of the velocity. If the initial growth rates are found to be significative in the entire velocity space, then the relaxation process must be conventional and characterized by a relaxation time of the order of τ_r .

Ivanov and Rudakov also consider the difficulty which arises from the existence of the steep front on the "wave" in velocity space because, for not too small ratios n_b/n_p , the velocity derivative of the beam distribution function at the "wave" front can become very large. Then, the condition of adiabaticity ($\gamma \ll \omega_p$) can be violated, as well as condition (3.41.a).

This type of relaxation of the beam distribution function is then treated in the stationary approximation (spatial variation of the interaction) with similar results. The distance z at which the width of the beam velocity distribution function becomes equal to Δv is given by

$$z = v_g t = \frac{1}{2\pi} \frac{1}{\omega_p} \frac{n_p}{n_b} \frac{(\Delta v)^2}{v_b^2} v_g \log \frac{W(z)}{W(0)} \quad (3.74)$$

where v_g is naturally the wave group velocity.

To finish this chapter we should shortly refer the work of SHAPIRO and SHEVCHENKO (1968). In this paper it is stated that, when a strong magnetic field is present in a plasma, the quasilinear plateau which results from the excitation of Cerenkov instabilities ($\omega = kv$) is unstable against the excitation of oscillations due to the anomalous Doppler effect ($\omega - kv = -\omega_{ce}$).

When $\omega_{ce} \gg \omega_p$ the quasilinear relaxation of the electron beam takes place in two phases. The first one leads to the growth of the Cerenkov instability up to the saturation level and to the concomitant establishment of the plateau in the distribution function. The second and slower phase of the interaction leads to the excitation of the anomalous Doppler effect instability.

As a result the resonant electrons diffuse along the lines

$$v_{\perp}^2 + v_z^2 - 2 \int \frac{\omega_k}{k_z} dv_z = \text{const.} \quad (3.75)$$

On these lines we have

$$\frac{dv_{\perp}}{dv_z} = - \frac{v_z - \omega_k/k_z}{v_{\perp}} = - \frac{\omega_{ce}}{k_z v_{\perp}} < 0 \quad (3.76)$$

and so we see that the diffusion is accompanied by an increase of the transverse energy in the beam and by a decrease of its longitudinal energy. This leads to an inclination of the plateau and the axial distribution function becomes everywhere a decreasing function of the velocity.

When $\omega_{ce} \rightarrow \infty$ these effects are expected to be negligible. Indeed it is predicted that the time in which this second phase of the beam relaxation takes place will be an increasing function of ω_{ce}/ω_p .

The theoretical statement that, under the excitation of instabilities brought about by the anomalous Doppler effect, the energy lost by the beam goes over essentially into the increase of the beam transverse temperature was already advanced by these authors in (1962).

CHAPTER IV

NONLINEAR EFFECTS OCCURRING DURING THE DEVELOPMENT OF BEAM-PLASMA
INSTABILITIES

4.1. Experimental set-up

Our beam-plasma experiment, schematically drawn in figure 4.1, was described in detail in former publications (VERMEER et al., 1966; VERMEER, 1968). Essentially it consists of a cylindrical interaction chamber ($\phi = 8$ cm) with a length variable from 25 to 80 cm, where the background pressure amounts to 3×10^{-7} Torr. The interaction chamber is filled with Helium at pressures of the order of 10^{-4} Torr. The axial magnetic field is constant along the experimental tube (within 1%) and can be varied between 0.01 and 0.1 Wb m^{-2} . An electron gun continuously injects a beam of 1500 eV and current variable up to 20 mA. In general the beam has a diameter of a few mm. The injection is parallel to the magnetic field. The beam, after interacting with its own created plasma,

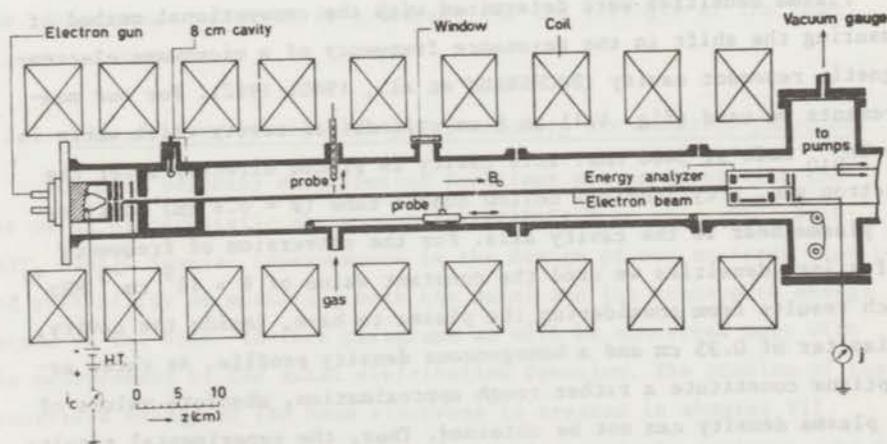


Fig. 4.1. - Schematic drawing of the experimental set-up.

is collected on the external wall of an electrostatic energy analyser which permits the measurement of velocity distribution functions. An electromagnetic resonant cavity for density measurements and several probes are also available in the experiment.

For a given set of the fixed external parameters (beam potential V_b , beam current i_b , Helium pressure p , magnetic field B and interaction length L), the state of the beam-plasma system can be reasonably described if we are able to measure some important internal parameters. Among these ones we are specially interested in the plasma density n_p , the plasma temperature T_p , the beam energy spread and the excited spectrum of oscillations arising from the beam-plasma instabilities. Spatial variation of these quantities provide extra information about the state of the beam-plasma system. Indeed, all the internal parameters depend on the axial distance from the electron gun z , as well as on the radius r , at which they are measured (LEVITSKII et al., 1967.a).

A brief summary of the diagnostic methods is given in the following paragraphs.

4.2. Conventional diagnostic methods

4.2.1. Measurements of the plasma density

Plasma densities were determined with the conventional method of measuring the shift in the resonance frequency of a microwave electromagnetic resonant cavity (BUCHSBAUM et al., 1960; 1962). For our measurements we used (fig. 4.1) an 8 cm cylindrical cavity which works in the TM_{010} mode at 3460 MHz. This cavity is placed directly after the electron gun. A cylindrical hollow quartz tube ($\varnothing = 0.8$ cm) confines the plasma near to the cavity axis. For the conversion of frequency shifts into densities we used the constant value of $8 \times 10^9 \text{ cm}^{-3} \text{ MHz}^{-1}$, which results from considering the plasma to have, inside the cavity, a diameter of 0.35 cm and a homogeneous density profile. As these assumptions constitute a rather rough approximation, absolute values of the plasma density can not be obtained. Thus, the experimental results are only to be considered in a relative way. However, we believe that they agree in order of magnitude with the real values of the plasma density.

4.2.2. Analysis of the beam-plasma waves

The beam-plasma instabilities are studied analysing the r.f. signals taken out from the plasma by Langmuir probes. The fundamental description of these instabilities is based on the analysis of the excited frequency spectrum. Frequency spectra are measured on a "Polarad" Spectrum analyser which covers a band extending from 10 to 4000 MHz. These measurements, which are time integrated, present the frequency dependence of the amplitude of the beam-plasma waves. For a given instability, the time dependence of the amplitude of its electric field can be measured by selecting, with the use of an adequate filter, only this instability from the total signal captured by the probe and using a fast detection system. This technique reveals the existence of bursts and provides information about their duration and growth as well as decay rates. The only disadvantage of this technique is the loss of the exact value of the frequency of the bursts. However, the use of a "Tektronix" sampling oscilloscope permits the observation of the temporal variation of the instability field down to the nanosecond. Bursts with frequencies as high as 1000 MHz can be clearly recorded giving a complete time definition (figure 5.1.c). The total integrated microwave power received by the probe can also be measured on a "Hewlett-Packard" Microwave Power Meter (bolometer) in the entire band extending from 10 to 10.000 MHz. This amount of power is a measure for the strength of the beam-plasma interaction.

4.2.3. Measurements of the beam axial velocity distribution function

The beam velocity distribution functions are measured with the use of an electrostatic energy analyser (BEREZIN et al., 1964; ETIEVANT, 1964). Several improvements in the design of our analyser lead to the possibility of measuring both the axial and the transverse energy spread in the beam. In this paragraph we will be concerned only with the measurement of the axial distribution function. The problem of the transverse energy of the beam electrons is treated in chapter VII.

Figure 4.2 presents a scheme of our electrostatic analyser, which, as we remember, terminates the interaction chamber. The electron beam is therefore collected on the analyser's external wall, which has a very small entrance hole ($\phi = 0.2$ mm). This wall is kept at earth po-

tential. As the beam diameter, at the end of the interaction chamber, is of the order of 3 - 10 mm, we see that only a very small fraction of the beam is analysed. The first internal electrode (plate 2) is kept at a positive potential (100 V) to reflect the plasma ions. The second electrode (plate 3) receives the variable retarding potential (0 to -2.000 V) necessary to determine the beam velocity spread. Plate 4 can eventually be used for an extra velocity modulation of the parallel electron velocity but it is in general kept on earth during these measurements. Electrons which were able to pass the analyser's potential barrier are then collected on the assembly of plates 5 and 6. These two collectors have adequate positive potentials to avoid the effects of the secondary electron emission in the measured currents.

As a complementary instrument we used a "Tektronix" oscilloscope. Its horizontal amplifier operates with a small fraction of the retarding potential in the analyser, in order to create a linear energy scale. This retarding potential is continuously varied (50 Hz) from 0 to -2.000 V. The vertical amplifier of the oscilloscope detects the current collected by the two plates (5 and 6) of the analyser through a load of 1 k Ω which permits a fast analysis (RC better than 100 ns) with sufficiently large amplitude signals. In this way we obtain the so-called energy analyser characteristic, that is to say, the plot of the collected current j as a function of the retarding potential V .

In a measurement of the beam distribution function with the help of an electrostatic energy analyser we obtain the current density of electrons with an axial energy equal or greater than $U = eV = \frac{1}{2} mv^2$, with V being the applied retarding potential on plate 3 of the analyser. This collected current density, measured at a distance r from the beam axis, is given by

$$j(v,r) = n_0(r) e \int_v^{\infty} f(v',r) v' dv' \quad (4.1)$$

where $n_0(r)$ is the total electron density in the beam-plasma system. The distribution function, which is, as usual, normalized to unity, is then determined by differentiation with respect to v :

$$f(v,r) = - \frac{m}{n_0(r)e} \frac{dj(v,r)}{mv dv} = - \frac{m}{n_0(r)e} \frac{dj(U,r)}{dU} \quad (4.2)$$

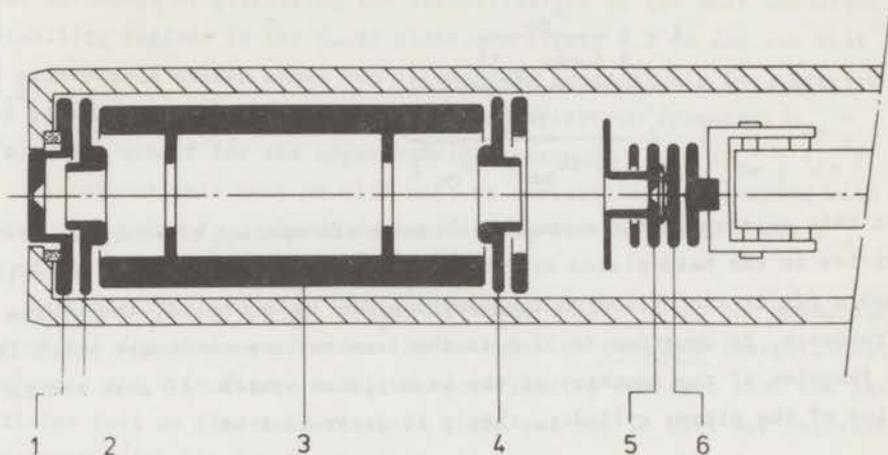


Fig. 4.2. - Scheme of the electrostatic energy analyser.

So, the beam velocity distribution function is directly obtainable from the energy analyser characteristic $j = j(U, r)$ by differentiation with respect to the energy.

4.3. Dispersion equation for the beam-plasma waves under the presence of a magnetic field

In the previous chapters we only considered the excitation of the electron plasma instability resulting from the Cerenkov effect. But, when a finite magnetic field is present in the plasma, a new type of resonance appears, namely the cyclotron resonance. This one usually leads to the excitation of both the ion cyclotron and the electron cyclotron instabilities. Thus, we need to consider a dispersion equation, more general than (2.40), which will describe the linear stage of the electron plasma as well as the electron cyclotron instabilities. For cylindrical geometry, which is the most adequate to our experimental situation, the dispersion equation for the case of a cold beam-plasma system is given by (ETIEVANT, 1964; BRIGGS, 1964; HOPMAN, 1969):

$$p^2 + k^2 D(\omega, k) = 0 \quad (4.3)$$

where $D(\omega, k)$ is

$$D(\omega, k) = \frac{1 - \sum \frac{\omega_p^2}{\alpha (\omega - kv_{oz})^2}}{1 - \sum \frac{\omega_p^2}{\alpha [(\omega - kv_{oz})^2 - \omega_{c\alpha}^2]}} \quad (4.4)$$

In this expression the summation is over all species of charged particles in the beam-plasma system. v_{oz} is the zero order axial velocity and $\omega_c/2\pi$ is the cyclotron frequency. $\omega_p/2\pi$ is, as usual, the plasma frequency. In equation (4.3) p is the transverse wave number which is a function of the geometry of the beam-plasma system. If a is the radius of the plasma cylinder, then p is determined by

$$p = J_{nm}/a \quad (4.5)$$

where J_{nm} is the n -th zero of the Bessel function $J_m(p r)$.

If we neglect the influence of the plasma ions on the electron oscillations, then we can consider that in our system we have only two types of particles, namely the plasma electrons, with a zero average velocity, and the beam electrons with an average velocity equal to v_b , directed along z , the direction of the magnetic field lines. In this case equation (4.3) can be written as

$$p^2 \left\{ 1 - \frac{\omega_p^2}{\omega^2 - \omega_{ce}^2} - \frac{\omega_{pb}^2}{(\omega - kv_b)^2 - \omega_{ce}^2} \right\} + k^2 \left\{ 1 - \frac{\omega_p^2}{\omega^2} - \frac{\omega_{pb}^2}{(\omega - kv_b)^2} \right\} = 0 \quad (4.6)$$

This is the wellknown dispersion equation for a cold beam-plasma system, in a magnetic field. We notice that if the transverse dimensions of the plasma are infinite ($p=0$) then the longitudinal oscillations of the beam-plasma system are characterized by the formerly derived dispersion equation (2.44). Also, if there is no magnetic field in the plasma ($\omega_{ce}=0$), then, even for finite transverse dimensions of the system, the non-trivial solution of (4.6) is given by (2.44).

Equation (4.6) can be numerically solved, giving either ω as a function of the real variable k or conversely the complex value of k for real ω . In figure 4.3 we present a solution of this equation

(dispersion diagram) for a set of parameters similar to the ones we used in some measurements. This dispersion diagram has, at least, the great advantage of permitting the identification of the most important instability regions in the (ω, k) plane. In figure 4.3 we can see that the beam-plasma system shows two resonances, respectively for the electron plasma frequency and for the electron cyclotron frequency ($\omega_{ce} = eB/m$), and a cutoff for the upper hybrid frequency, $f_{uh} = (f_{pe}^2 + f_{ce}^2)^{1/2}$.

Throughout this work we will call to instabilities appearing with frequencies below f_{pe} , plasma instabilities, Instabilities above f_{ce} are called cyclotron instabilities.

Instabilities are also frequently named according to the mechanism responsible for their excitation. So we have: 1- Cerenkov instabilities (regions 1 and 4 in figure 4.3), characterized by the fact that the beam particles feel an almost DC electric field and can in this way interact effectively with the longitudinal plasma waves ($\omega - kv \approx 0$); 2- Anomalous

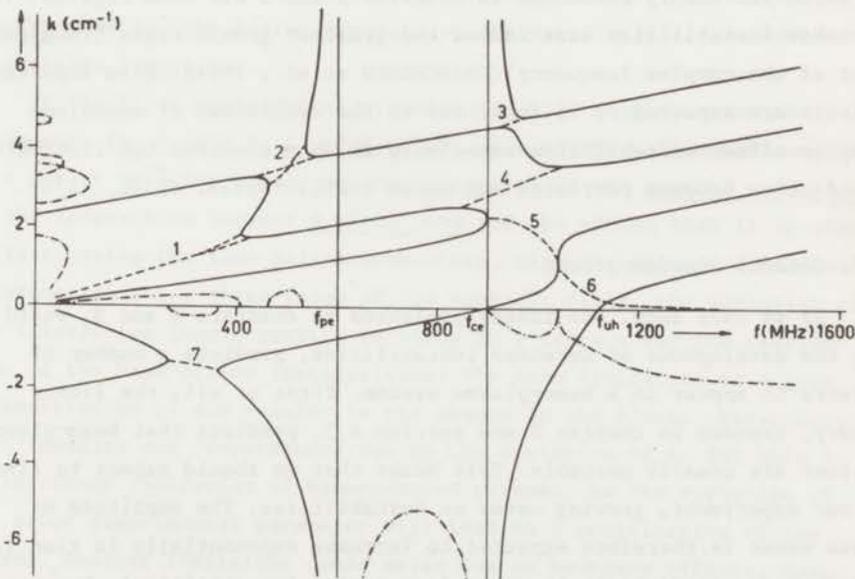


Fig. 4.3. - Dispersion characteristics of a cold beam-plasma system. Parameters are: $f_{pb} = 300$ MHz; $f_{pe} = 600$ MHz; $f_{ce} = 900$ MHz; $v_b = 2.5 \times 10^9$ cm s⁻¹; $p = 2$ cm⁻¹. Dashed lines represent the real part of the frequency as well as of the wave number. Dot-dash lines represent the imaginary parts of f and k .

Doppler effect instabilities (regions 2 and 3) characterized by the fact that, during their Larmor gyrations around the magnetic lines, the beam electrons will feel the transverse electric field almost in phase so that a considerable gain of transverse energy can be achieved ($\omega - kv \approx -\omega_{ce}$).

3- Normal Doppler effect instabilities ($\omega - kv \approx \omega_{ce}$) are generally not excited in normal beam-plasma systems as region 6 represents a situation of heavy damping and region 7 leads to an instability which can only be excited at the cost of a decrease in the transverse energy of the beam. If initially the beam possesses a rather high amount of transverse energy, then the excitation of this last instability becomes possible and, as a result, the beam will lose part of its transverse energy and at the same time will gain axial energy, as the instability phase velocity is negative (SHAPIRO et al., 1962).

A look at figure 4.3 indicates that in our beam-plasma system we expect to have mainly instabilities brought about by the Cerenkov effect, to which the theory presented in chapters 2 and 3 has been derived. These Cerenkov instabilities have indeed the greatest growth rates (imaginary part of the complex frequency) (KHARCHENKO et al., 1964). Also important effects are expected to be found due to the excitation of Anomalous Doppler effect instabilities especially in what concerns the transverse interaction between particles and waves (APEL, 1969.a; SEIDL, 1970).

4.4. General considerations

As we have seen, the theory presented in chapters 2 and 3, valid for the development of Cerenkov instabilities, predicts a number of effects to appear in a beam-plasma system. First of all, the linear theory, exposed in chapter 2 and section 4.3, predicts that beam-plasma systems are usually unstable. This means that we should expect to find, in our experiment, growing waves or instabilities. The amplitude of these waves is therefore expected to increase exponentially in time (absolute instabilities) or in space (convective instabilities). However, the quasilinear theory predicts the saturation of the instability amplitude at a rather low level (weak turbulence). This saturation of the wave amplitude is expected to be accompanied by an increase of the energy spread in the beam and by an enlargement of the excited spectrum of oscillations due to the increase in the extension of the resonance

velocity region (figures 3.1 and 3.4). We have also learned that the quasilinear relaxation process can be followed in space if we inject a beam through a plasma (sections 3.7 and 3.8). Further it was predicted that the relaxation of the beam would take place in a time large compared to the oscillation period (and so in a distance large compared to the wavelength) and this fact indicates that we should be able to follow these processes experimentally in a beam-plasma experiment.

4.5. Experimental results

4.5.1. Dependence of the beam-plasma internal parameters on the interaction length

We will begin this study by considering the spatial variation of the experimental parameters which partially characterize a beam-plasma interaction. We will keep throughout this work the beam energy always equal to $U_b = 1500$ eV. The main external parameters will then be the beam current i_b , the Helium pressure p , the magnetic field B and the interaction length L .

In the first experimental situation we will keep constant the beam parameters ($V_b = 1500$ V, $i_b = 16$ mA) as well as the Helium pressure ($p = 4.8 \times 10^{-4}$ Torr. Thus we are interested in the spatial evolution of the interaction between a given beam and the plasma that it creates while crossing the same Helium atmosphere, with the magnetic field as a parameter. For a given value of the magnetic field, the variation of the interaction length permits to study in a certain way the development of the beam-plasma instabilities. The main limitation to a good interpretation of the results is the change in the plasma characteristics (density and temperature) due to the variation of L . But this is an intrinsic limitation of beam-created plasmas, as the variation of any other experimental parameter will lead to a modification of the plasma. Another limitation could arise due to boundary effects, namely the reflection of the beam-plasma waves by the energy analyser wall which terminates the interaction chamber. However, as no resonant interaction can take place for the reflected wave, we expect that, exception made for the immediate vicinity of the collector, the boundary effects will not lead to any new phenomena. Further it has been experimentally verified that the reflected wave is strongly damped (HOPMAN et al., 1969; LEVITSKII et al., 1967.b).

The beam-plasma system is characterized, for every set of values of L and B , by measurements of the plasma density, the excited spectrum of oscillations, the radiated power, and by the beam energy spread. These experimental quantities were determined with the formerly referred diagnostic methods.

Figures 4.4 and 4.5 present, as a function of the interaction length, the excited spectrum of oscillations, the energy spread in the beam and the plasma density, measured respectively for $B = 0.0325$ and $B = 0.0540 \text{ Wb m}^{-2}$. We define in this chapter the beam energy spread by the width of the energy range in which the collected current due to the beam electrons decreases from 95% to 5% of its maximum value.

In figures 4.4 and 4.5 it can be seen that the behaviour of the beam-plasma system is essentially different for low and high magnetic fields. In the case of low magnetic field (figure 4.4) there is a sudden jump in the beam-plasma characteristics, at a certain value of the interaction length, representing the so-called 1st-2nd regime transition (SMULLIN et al., 1962; KHARCHENKO et al., 1964; KOGAN et al., 1968). At high magnetic fields the transition of regimes in the plasma takes place gradually (figure 4.5). By first regime in a beam-plasma experiment we mean the states in which the plasma is mainly created by the inelastic collisions between the beam electrons and the neutral atoms. These states usually represent weak beam-plasma interactions and they are characterized by thin and rather quiescent plasma columns with diameters of the order of the beam diameter. The transition 1st-2nd regime is defined by the onset of another ionization process in which the neutral atoms are ionized by the plasma electrons. These ones were heated by the beam-plasma instabilities. This last ionization process is usually referred to as high frequency ionization. Second regime states are characterized by the fact that the dominant ionization mechanism is the high frequency one. These states have in general high densities, compared with the first regime ones.

Returning to figure 4.4 we can observe that, until $L = 43$ cm, only the cyclotron instability is present, the density does not exhibit significant fluctuations and the beam has a narrow energy spread.

Between $L = 43$ and $L = 48$ cm the only new feature is the appearance of the plasma instability accompanied by a small increase in the beam energy spread and the onset of density fluctuations. After the

transition ($L = 49$ cm) the plasma density has a much higher value due to the high frequency ionization of the Helium (HOPMAN et al., 1968), the beam is almost completely spread out in energy and the spectrum attains its maximum width, with a plasma peak extending from 0 to 1000 MHz. The cyclotron peak also jumps to higher frequencies in agreement with the fact that it occurs near the upper hybrid frequency. For the next 10 cm the state of the system remains the same. After $L = 60$ cm we notice a decrease in density, in the beam energy spread, and in the width of the spectrum.

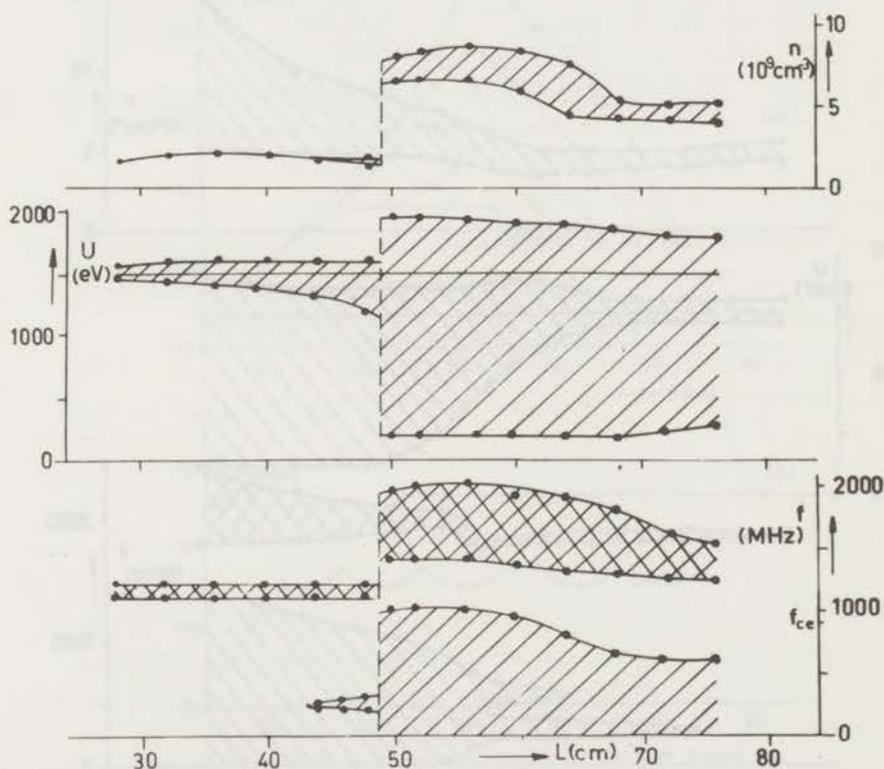


Fig. 4.4. - Variation of the plasma density, axial energy spread and excited spectrum of oscillation with the interaction length for a case of low magnetic field. Conditions: $V_b = 1500$ V; $i_b = 16$ mA; $p = 4.8 \times 10^{-4}$ Torr; $B = 0.0325$ Wb η^{-2} .

Similarly, figure 4.5 presents the results for a case of high magnetic field. Again the system only shows the cyclotron instability for small L . The plasma instability appears sooner (in L) and is followed at $L = 46$ cm by its second harmonic. At $L = 53$ cm these two plasma peaks join together and we notice an increase in the plasma density and the steepest increase in the beam energy spread. For still larger values of L the beam-plasma interaction continues to gain in strength, opposite to the case of low B .

In figure 4.6 we made a plot of the total time integrated radiated

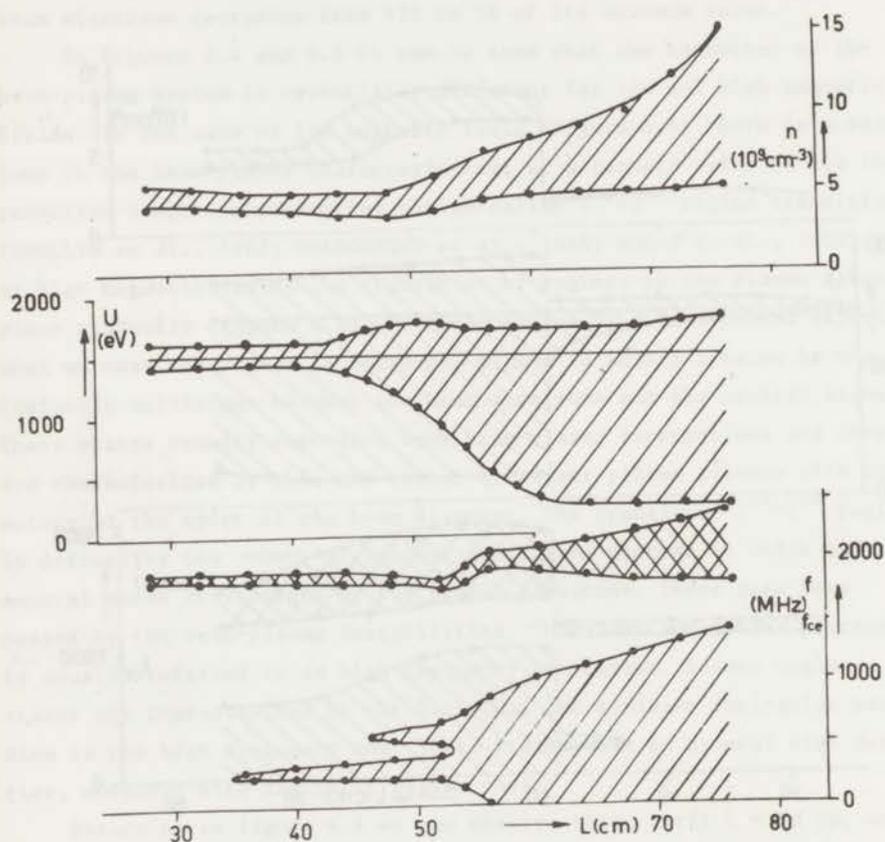


Fig. 4.5. - Variation of the plasma density, axial energy spread and excited spectrum of oscillations with L , for a case of high magnetic field. Conditions: $V_b = 1500$ V; $i_b = 16$ mA; $p = 4.8 \times 10^{-4}$ Torr; $B = 0.0540$ Wb m^{-2} .

power collected by an axially movable pin probe, as a function of the distance z from the electron gun, for different values of the interaction length. In the lower part of this figure we can see that the radiated power, for the case of low magnetic field, remains practically constant along the experimental tube. The amount of power was independent of the collector position. In the upper part of figure 4.6 we have the results obtained for $B = 0.0540 \text{ Wb m}^{-2}$, and we notice that the power be-

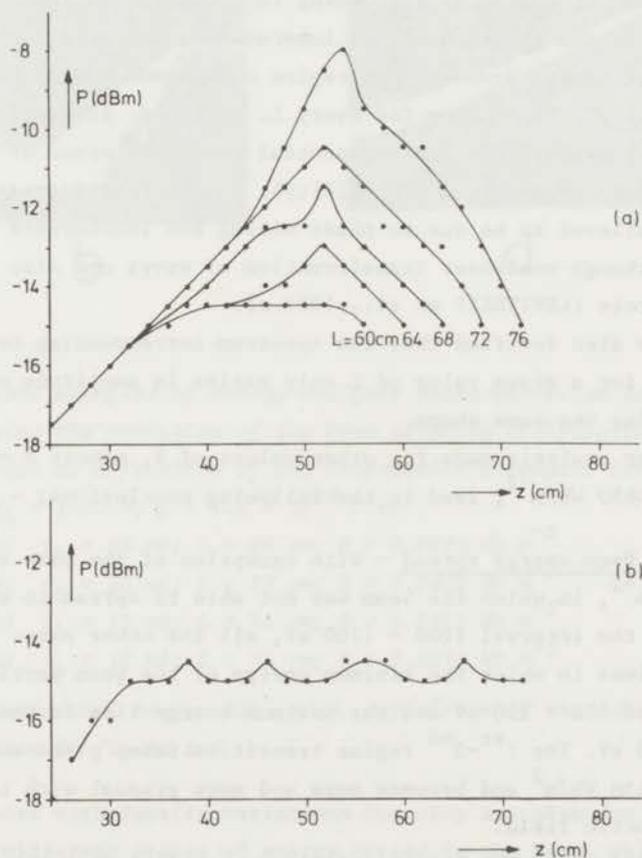


Fig. 4.6. - Plot of the total radiated high frequency power as a function of the distance from the electron gun at which it is measured, for different values of L and under the conditions presented in figures 4.4 and 4.5.

(a) - $B = 0.0540 \text{ Wb m}^{-2}$; (b) - $B = 0.0325 \text{ Wb m}^{-2}$.

gins to increase exponentially with z , attains a maximum and then decreases with z (SHASHURIN, 1967; ARTEMOV et al., 1968; MALMBERG et al., 1969). The maximum power is measured at $z = 53$ cm, the place occupied by the collector when, in the study of the spectrum as a function of L , the two plasma peaks merged. To analyse if this region of maximum power was eventually related with the boundaries of the system, we varied L and repeated the power measurement. The conclusion was clear: -For $z < 36$ cm the radiated power is completely independent of the collector position. Of course by shortening the interaction length we expect a decrease of the strength of the interaction, and so a decrease in the radiated power. However, the region of maximum plasma radiation was found at $z = 52 - 53$ cm for every L . We found, in the first half of the experimental tube, an exponential growth in space of the total radiated power (convective instability). The further decrease of the power is believed to be due to phase mixing and incoherence (APEL, 1969.a) although nonlinear transformation of waves can also play an important role (LEVITSKII et al., 1967.c).

It was also verified that the spectrum corresponding to the radiated power for a given value of L only varies in amplitude with z , but maintains the same shape.

Similar analysis made for other values of B , namely $B = 0.0215$, 0.0430 , 0.0650 Wb/m⁻², lead to the following conclusions: -

(a) - Beam energy spread - With exception of the case of $B = 0.0215$ Wb/m⁻², in which the beam was not able to spread to energies outside of the interval 1200 - 1700 eV, all the other cases lead to second regimes in which the minimum energy of the beam particles is of the order of 100 - 200 eV and the maximum energy lies in the range 1800 - 2000 eV. The 1st-2nd regime transition takes place abruptly for $B < 0.0430$ Wb/m² and becomes more and more gradual with the increase in the magnetic field.

Independent of the magnetic field we verified that the beam velocity distribution function (equation 4.2) suffers always the same type of evolution. In the first regime (figure 4.7.a) the energy spread is small, and there are no significant fluctuations. At the 1st-2nd regime transition (figures 4.7.b and 5.6.a) there are strong fluctuations in the energy analyser characteristics. These fluctuations are

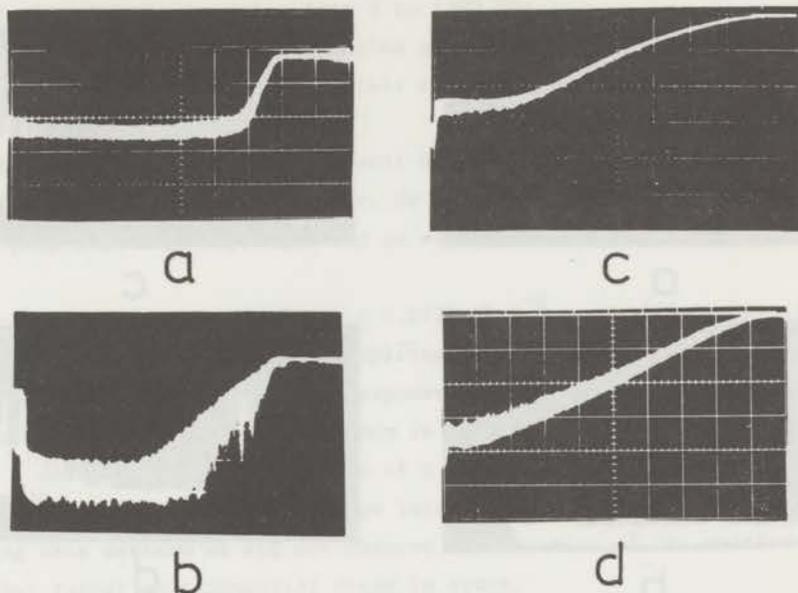


Fig. 4.7. - Some examples of energy analyser characteristics representing the evolution of the beam velocity distribution function as a function of the interaction strength. Conditions: $V_b = 1500$ V; $p = 4.8 \times 10^{-4}$ Torr.

- a) $i_b = 10$ mA; $L = 46$ cm; $B = 0.0540$ Wb m⁻²
 b) $i_b = 10$ mA; $L = 73$ cm; $B = 0.0405$ Wb m⁻²
 c) $i_b = 12$ mA; $L = 73$ cm; $B = 0.0405$ Wb m⁻²
 d) $i_b = 16$ mA; $L = 73$ cm; $B = 0.0270$ Wb m⁻²

Horizontal scale: 200 eV/cm. Definition of the axes can be seen in figure 5.6.

not only related with density variations but they are also due to the existence of different states of energy spread in the beam, which appear in correlation with the different beam-plasma instabilities, as we shall see in chapter 5.

Going into a moderate second regime (figure 4.7.c) the fluctuations disappear and the energy spread is large. Deep second regimes are characterized by an almost complete relaxation of the beam (figure 4.7.d) with velocity distribution functions which have a "plateau-like" character in the energy range between 200 and 1800 eV.

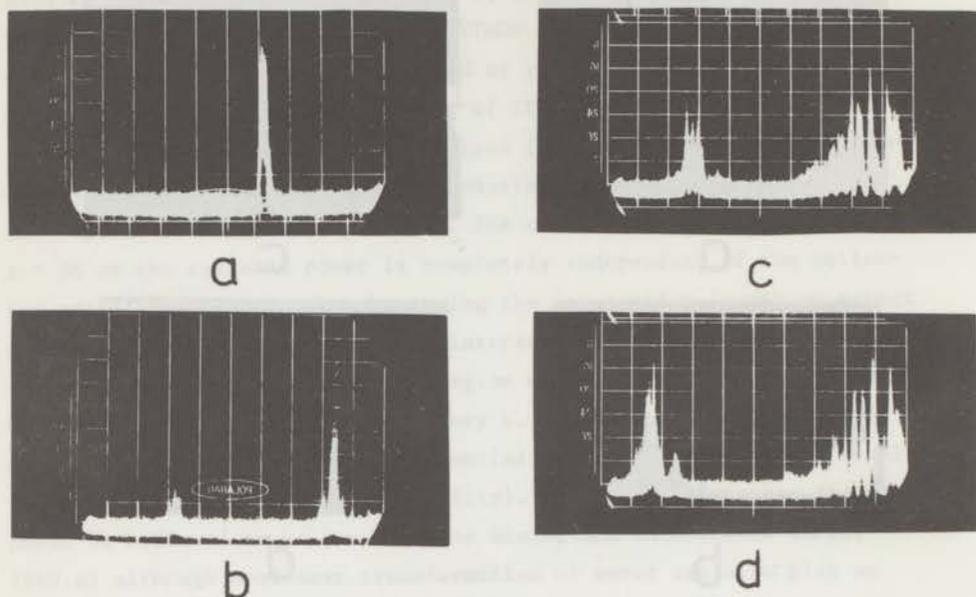


Fig. 4.8. - Some examples of typical spectra of oscillations. Horizontal scale: 200 MHz/cm. Frequency increases from right to left between 0 and 2000 MHz. Conditions: $V_b = 1500$ V; $p = 4.8 \times 10^{-4}$ Torr.

- a) $B = 0.0215$ Wb m^{-2} ; $i_b = 16$ mA; $L = 42$ cm
 b) $B = 0.0435$ Wb m^{-2} ; $i_b = 16$ mA; $L = 40$ cm
 c) $B = 0.0325$ Wb m^{-2} ; $i_b = 16$ mA; $L = 68$ cm
 d) $B = 0.0435$ Wb m^{-2} ; $i_b = 16$ mA; $L = 68$ cm

(b) - Excited spectrum - For all values of B , the cyclotron instability is the only one present for small L . Figure 4.8.a presents a typical spectrum of a first regime state with low B . This spectrum shows a large amplitude cyclotron peak. For the case of $B = 0.0215$ Wb m^{-2} we noticed, before the appearance of the plasma instability, the presence of the second harmonic cyclotron instability. For this low value of the magnetic field the plasma instability is not observed in the first regime of the plasma. The case of $B = 0.0430$ Wb m^{-2} is qualitatively similar to the one presented in figure 4.4. For the highest magnetic field ($B = 0.0650$ Wb m^{-2}) we observed, for $46 \leq L \leq 54$ cm, besides the plasma instability the presence of its second and third harmonics. These three plasma instabilities join together at $L = 58$ cm and so they constitute

a single broad peak extending from 0 to 1300 MHz.

Figure 4.8.b shows a first regime spectrum for a high value of the magnetic field. We verify that in this case the plasma instability is stronger than the cyclotron one.

Figures 4.8.c and 4.8.d represent second regime spectra. These ones, as we see, are rather similar. We notice the existence of a broad plasma peak with high amplitude and an equally strong cyclotron peak.

(c) - Radiated power - For $B < 0.0430 \text{ Wb m}^{-2}$ we verified that the power remains constant along the experimental tube. For the higher values of B we always observed an exponential increase in space, and the appearance of a radiation maximum in the neighbourhood of the coordinate z corresponding to the value of L at which the different harmonics of the plasma instability merge into a single broad peak. After reaching this maximum we did not observe a saturation of the emitted power but rather an exponential decay in space.

At a fixed point z we verified, varying the beam current, that the maximum radiated power was always associated with the 1st-2nd regime transition (APEL, 1969.b). Going deeper into a second regime results in the decrease of the plasma radiation. For the larger magnetic fields the cyclotron instability has a small amplitude and it hardly contributes to the measured power.

4.5.2. Dependence of the beam-plasma internal parameters on the beam current and on the Helium pressure

In this section we intend to analyse shortly the development of the beam-plasma interaction for a given value of the interaction length ($L = 73 \text{ cm}$) as a function of either the beam current or the neutral gas pressure, keeping the magnetic field as a parameter.

We verified that the beam-plasma system passes by the same phases if we increase the interaction strength in no matter what way. Thus, the succession of states from a weak first regime to a deep second regime can be simulated by keeping two of the following three parameters (i_b , p, L) constant and increasing the value of the other one (SHUSTIN et al., 1969).

As nothing new is obtained, we present only the results correspon-

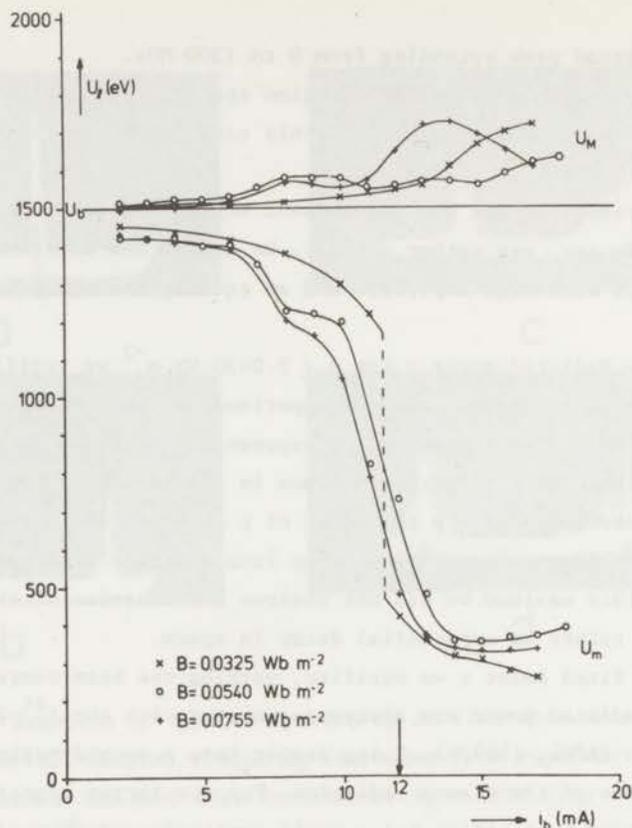


Fig. 4.9. - Variation of the beam energy spread as a function of i_b for several values of the magnetic field. U_M and U_m represent respectively the maximum and minimum energy obtained by the beam electrons according to the definitions introduced in section 4.5.1. Conditions: $V_b = 1500$ V, $p = 4.8 \times 10^{-4}$ Torr, $L = 73$ cm.

ding to the analysis of the axial velocity distribution function of both the beam and the plasma electrons. For the beam energy spread we used again the definition introduced in section 4.5.1. Figure 4.9 presents the results obtained for the beam energy spread as a function of the beam current for a given value of the Helium pressure ($p = 4.8 \times 10^{-4}$ Torr) and three values of the magnetic field. Figure 4.10 presents a similar measurement, but now as a function of the Helium pressure for a given value of the beam current ($i_b = 12$ mA). In these two figure we can

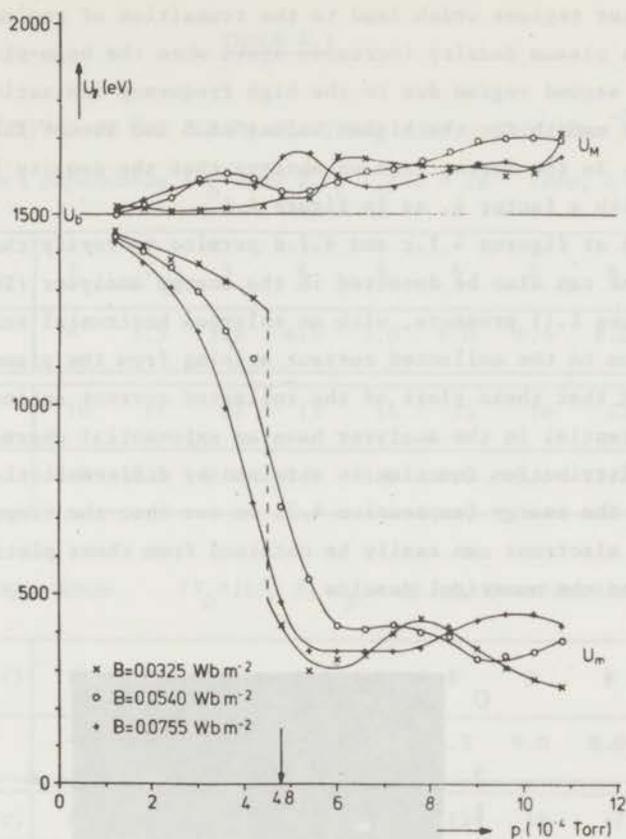


Fig. 4.10. - Variation of the beam energy spread as a function of the helium pressure for several values of the magnetic field. Conditions: $V_D = 1500$ V, $i_D = 12$ mA, $L = 73$ cm.

again verify that a low value of the magnetic field leads to an abrupt 1st-2nd regime transition and that higher values of B lead to a gradual passage from the first to the second regime. Also we can observe that the higher the magnetic field the sooner the transition of regime in the plasma is attained.

The passage from the first regime to a deep second regime is also characterized by the enlargement of the excited spectrum of oscillations. The variation in the spectral appearance is for all practical purposes identical to the one observed in the study of the development of the beam-plasma interaction as a function of L . The same happens with the radiated power which is again found to be rather peaked at

the parameter regions which lead to the transition of regime in the plasma. The plasma density increases again when the beam-plasma system enters the second regime due to the high frequency ionization, and this increase is smooth for the higher values of B and abrupt for the lower value of B . In the latter case we observe that the density increases suddenly with a factor 4, as in figure 4.4.

A look at figures 4.7.c and 4.7.d permits to verify that the plasma electrons can also be detected in the energy analyser (SHUSTIN et al. 1969). Figure 4.11 presents, with an enlarged horizontal scale, the contribution to the collected current arising from the plasma electrons. We verified that these plots of the collected current against the retarding potential in the analyser have an exponential character. As the velocity distribution function is obtained by differentiation with respect to the energy (expression 4.2) we see that the temperature of the plasma electrons can easily be obtained from these plots. Table no. 4.1 contains the numerical results.

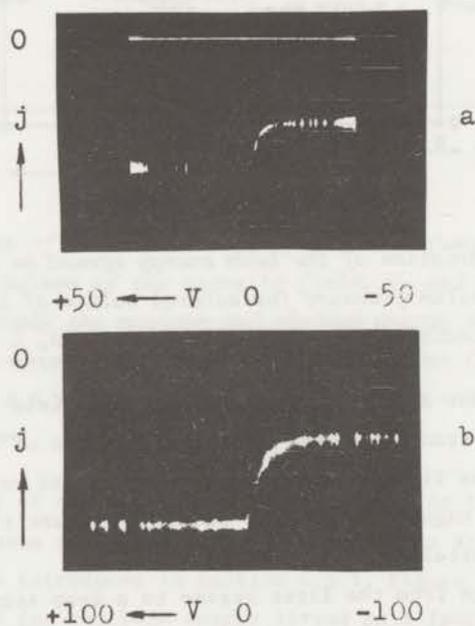


Fig. 4.11. - Determination of the plasma temperature from the energy analyser characteristics. Conditions: $V_b = 1500$ V.

a) $i_b = 0.1$ mA; $p = 2 \times 10^{-4}$ Torr; $B = 0.0810$ Wb m^{-2} ; $L = 73$ cm.

b) $i_b = 16$ mA; $p = 4.8 \times 10^{-4}$ Torr; $B = 0.0270$ Wb m^{-2} ; $L = 73$ cm.

TABLE 4.1

TEMPERATURE OF THE PLASMA ELECTRONS ($B = 0.0540 \text{ Wb m}^{-2}$)a) beam current dependence ($V_b = 1500 \text{ V}$, $p = 4.8 \times 10^{-4} \text{ Torr}$, $L = 73 \text{ cm}$)

i_b (mA)	1	2	3	4	5	6	7	8	9
T_p (eV)	-	1.5	3.5	4.5	5.0	6.0	6.5	8.0	8.0
i_b (mA)	10	11	12	13	14	15	16	17	18
T_p (eV)	8.0	8.0	8.0	6.1	6.0	6.0	5.1	5.2	5.6

b) pressure dependence ($V_b = 1500 \text{ V}$, $i_b = 12 \text{ mA}$, $L = 73 \text{ cm}$)

$p(6 \times 10^{-5} \text{ Torr})$	1	2	3	4	5	6	7	8	9
T_p (eV)	-	3.5	6.0	6.0	6.0	6.5	9.0	8.0	7.5
$p(6 \times 10^{-5} \text{ Torr})$	10	11	12	13	14	15	16	17	18
T_p (eV)	6.5	6.5	6.5	6.5	7.0	9.5	9.5	9.5	10.0

We emphasize that with an electrostatic energy analyser we can not obtain trustful results about the absolute energy of the plasma electrons. In other words, we can measure the important quantity which is their temperature but we can not have a good idea about their real energies. We only verify that there are some electrons which are able to pass potential barriers of the order of 25 eV. However, due to the presence of the sheath in front of the analyser, these electrons can have much higher energies. Thus, we only measure the tail of the electron velocity distribution function.

An estimate for the temperature of the bulk of the plasma electrons can also be obtained by other methods, namely spectroscopically or by the analysis of the Langmuir probe characteristics LEVITSKII et al., 1967). However, these two methods are not applicable in our beam-

plasma system as the first one requires a rather homogeneous plasma column and the second one can not furnish information over the distribution in the centre of the plasma column as the probes become incandescent when immersed into the energetic electron beam. So, we verified that the plasma temperature is of the order of 5 - 10 eV (LEVITSKII et al., 1966; SEIDL et al., 1967; MORSE, 1969). The analysis of its current dependence proves that the plasma temperature increases in the first regime of the plasma and has a maximum for the conditions which lead to the 1st-2nd regime transition. For the case of the pressure dependence, the former conclusions hold with the difference that for large values of p the temperature shows a second increase. Finally we verified that a temperature of about 8 eV is necessary to start high frequency ionization. The high energy tail of the electron distribution function apparently contains electrons, with energies of the order of 3 - 5 kT, as the Helium ionization energy is 24,6 eV. The plasma heating is generally believed to be related to the stochastic character of the beam-plasma instabilities (JANCARIK et al., 1969; ASTRELIN et al., 1969).

4.6. Conclusions

From the presented set of measurements we verify that the magnetic field strongly influences the beam-plasma interaction. The obtained results confirm the fact that a high value of B favours the development of the convective plasma instability while a low B value favours the growth of the absolute cyclotron instability, as predicted by linear theory (JANCARIK et al., 1969; SEIDL, 1970).

Especially for the case of high values of the magnetic field we verified that most of the effects predicted by the quasilinear theory could be observed in our experiment, in which we were able to simulate the spatial development of the beam-plasma interaction. Namely, we could observe the formation of the plateau in the velocity distribution function, the enlargement of the excited spectrum of oscillations and the growth and saturation of the power associated with these oscillations.

In section 3.8 we referred to a paper by IVANOV and RUDAKOV (1967). Following these authors, the distribution function of an ini-

tially monoenergetic beam, injected into a plasma, will have the shape of a plateau developing towards lower velocity values, during the quasilinear interaction process. We verified experimentally this prediction, as the velocity distribution functions, obtained as a function of L , had always a "plateau-like" character.

Our results are in good agreement with those published by LEVITSKII et al. (1967.b; 1969), and they constitute an extension of their work, due to the possibility of displacing axially the energy analyser.

If we assume that the group velocity of the beam-plasma instabilities is of the order of the initial beam velocity (LEVITSKII et al., 1967.b; IVANOV et al., 1967) as suggested by the dispersion diagram (figure 4.3), a good agreement between the coordinate of the region of maximum plasma radiation ($z = 52$ cm) and the value of the theoretical quasilinear relaxation length (equation 3.74) is observed (CABRAL et al., 1969). APEL (1969.b) gives an empirical expression for the relaxation length of the instabilities, which is of the order of 5 wavelengths of the most unstable wave. Applied to our experimental parameters, his expression leads to values of the relaxation length which are at least a factor 4 smaller than the ones we obtained.

It would be interesting to perform measurements in the immediate vicinity of the electron gun, but unfortunately our movable measuring devices (probe and energy analyser) could not be brought closer than 24 cm from the gun. Indeed, if the group velocity of the plasma waves is really much smaller than the beam velocity, as assumed in the theory (chapters II and III), we can expect regions of high inhomogeneity close to the entrance of the beam into the plasma.

Results which can not be explained by the formerly presented quasilinear theory, besides the increase in the plasma density, are the strong exponential decrease of the microwave power, which immediately follows its saturation (figure 4.6.a), and the acceleration of beam electrons to energies exceeding the beam initial energy.

The decay of the microwave power is presumably due to nonlinear transformation of waves.

In what concerns the fast electrons ($v > v_b$), their presence in beam-plasma systems has been theoretically explained either by considering the inhomogeneity of the plasma (RYUTOV, 1970), or by the excitation

of normal Doppler effect instabilities (SHAPIRO et al., 1962). In a completely different approximation, we shall explain their existence, in chapters V and VI, just by considering the nonlinear interaction between the beam electrons and a monochromatic wave representing a certain beam-plasma instability.

CHAPTER V

STUDY OF THE 1ST-2ND REGIME TRANSITION IN A BEAM-PLASMA EXPERIMENT

5.1. Introduction

As we have seen in chapter 5, the beam-plasma interaction is stronger for conditions which lead to the so-called 1st-2nd regime transition. Therefore, in the present chapter, we intend to study with more detail what happens at this transition of regime in the plasma.

We verified that, despite the continuous operation of the experiment, the analysis of the oscillation spectrum usually shows that more than one instability is present in the system for the same set of external parameters. These instabilities have a discontinuous character, as they appear in bursts with typical durations of the order of 100 ns. Bursts of the various instabilities alternate quickly in time (VAN WAKEREN et al., 1969) and they produce rapid changes in the internal beam-plasma parameters. Thus, if we want to perform measurements on parameters related to the presence of a single instability, we must have rather fast measuring devices and means of correlating the appearance of the bursts of this instability with a certain level of the fluctuations observed on the considered parameter.

In this chapter we present measurements that could be correlated with the existence of a single beam-plasma instability (CABRAL et al., 1970). So, the main line of investigation is now the correlation between changes in the time resolved beam-plasma parameters and the presence of a certain instability. We will present measurements of the excited frequency spectrum, plasma density and especially of the beam energy spread, taking the magnetic field as a parameter. A brief description of the correlation technique will now be made.

5.2. Correlation technique

The correlation between the variations in the internal beam-plasma parameters and the occurrence of a certain instability was obtained with intensity modulation of the oscilloscope beam. This z-modulation was made using pulses derived from the instability fields in the following manner: - A Langmuir pin probe takes from the plasma the rf sig-

nals associated with the propagation of the different beam-plasma waves. These signals are delivered to a "Polarad" Spectrum Analyser which is used as a narrow band pass filter ($\Delta f = 5$ MHz), converting any chosen frequency of the excited spectrum into 60 MHz. The rectified 60 MHz output signal contains information about the time dependence of the amplitude of the bursts appearing with the chosen frequency. This output signal consists of a series of fast pulses which, after adequate amplification, serve for the intensity modulation of the oscilloscope beam. This means that the oscilloscope screen is only illuminated by its own beam when the selected instability is excited. By this way we were able to correlate the appearance of a certain frequency of the excited spectrum with a certain level of the fluctuation on the measured signals coming from the beam-plasma experiment. These signals are of course continuously displayed in a conventional way on the oscilloscope. Due to the very small bandwidth of its active filter ("Polarad") this correlation method has the great advantage of being able to distinguish between beam-plasma states which are associated with different frequencies belonging to the same instability peak in the excited spectrum.

Because of the fast character of the plasma bursts this correlation technique was checked by using simulated bursts (rise time = 5 ns, duration down to 100 ns). In order to obtain a good autocorrelation of the test pulses it appeared necessary to use a delay cable in the circuit feeding the vertical amplifier of the oscilloscope. The delay time, mainly due to the use of amplifiers in the correlation circuit, was about 300 ns, independent of the frequency of the simulated bursts in the range 200 - 1000 MHz.

5.3. Experimental results

5.3.1. Fast analysis of the beam-plasma instabilities

One of the characteristics of beam-created plasmas is the discontinuous radiation of microwave power under the form of bursts belonging to different instabilities.

We verified that the bursts of the cyclotron instability in the first regime of the plasma are rather well defined in time. Typical durations are of the order of 100 ns. Figure 5.1.a. gives an example of the time dependence of the amplitude of the bursts of the electron

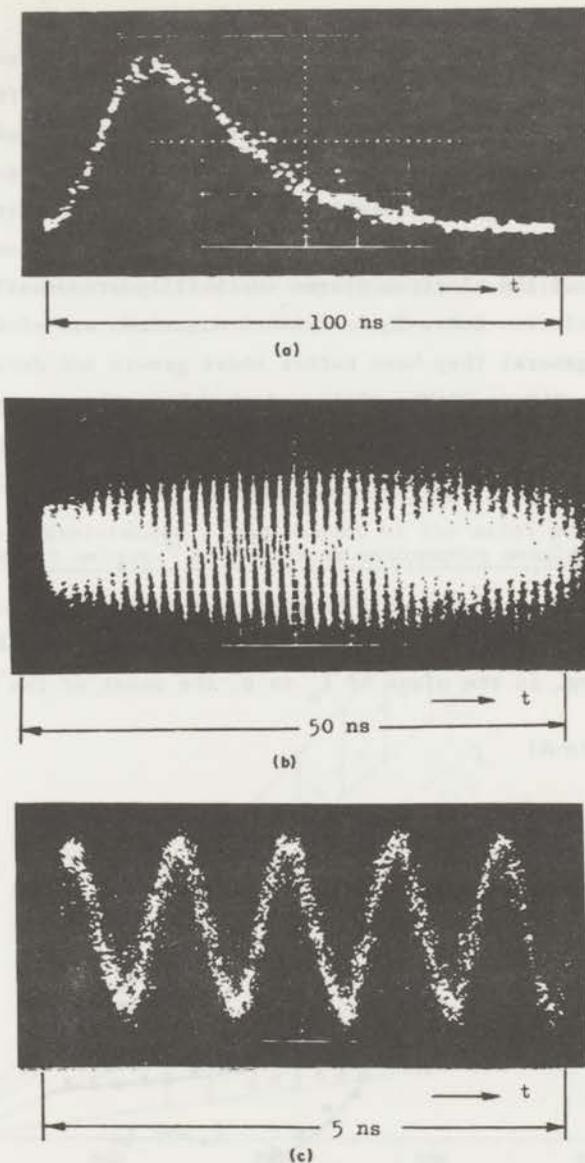


Fig. 5.1. - (a) Envelope of the electron cyclotron bursts. (b) Time dependence of the electric field of the cyclotron instability. (c) Proof that the frequency of the different consecutive bursts of the electron cyclotron instability is highly coherent. These three photographs were obtained with a sampling oscilloscope. Conditions: $V_b = 2500$ V; $i_b = 10$ mA; $p = 4.8 \times 10^{-4}$ Torr; $B = 0.0210$ Wb m $^{-2}$; $L = 73$ cm.

cyclotron instability. The three photographs belonging to figure 5.1. were obtained with the use of a sampling oscilloscope. Figures 5.1.b. and 5.1.c. show that the frequency of the different consecutive bursts of this instability is highly coherent. We also verified that the number of oscillation periods (about 80) in a cyclotron burst was almost independent of the magnetic field.

Bursts of the electron plasma instability are usually much longer than the cyclotron ones. Their typical durations are of the order of a few μ s. In general they have rather short growth and decay times (HOPMAN et al., 1968-a; FRANK, 1968) and they keep the same amplitude during a relatively long time. These bursts often show amplitude modulation related with the excitation of the ion instabilities (APEL, 1969.a).

5.3.2. Beam-plasma parameters at the 1st-2nd regime transition

As the measurements will be performed along the boundary between the two regimes of the plasma, we present in figure 5.2 a parameter diagram defining, in the plane of i_b vs B, the onset of the plasma insta-

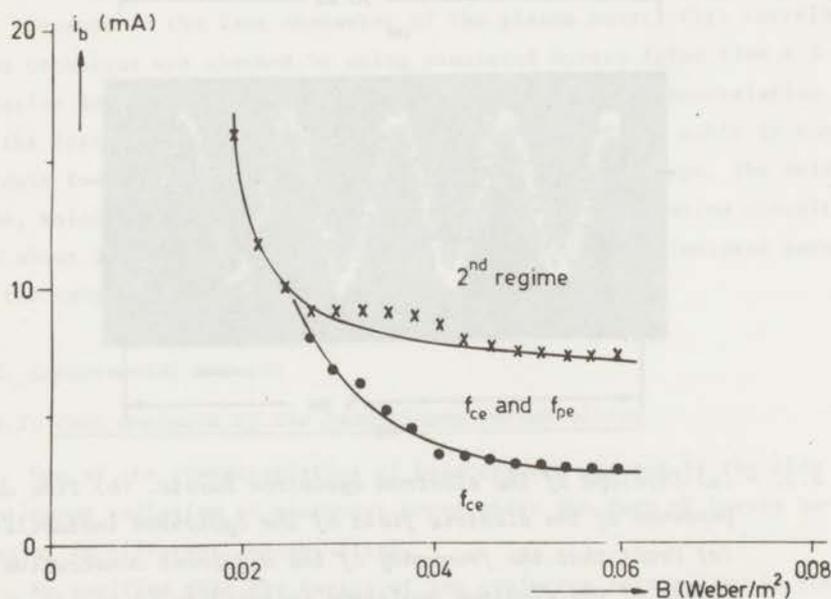


Fig. 5.2. - Parameter diagram defining the onset of the electron plasma instability and the transition 1st-2nd regime. Conditions: $V_b = 1500$ V; $p = 4.8 \times 10^{-4}$ Torr; $l = 73$ cm.

bility and the boundary between the 1st and the 2nd regimes in the plasma, for a certain value of the Helium pressure. In this diagram we can see that the cyclotron instability is always observed in the first regime of the plasma, even with very weak currents. On the contrary, the plasma instability is only observed for relatively large beam currents and can not be excited in the first regime of the plasma for $B \leq 0.0250 \text{ Wb m}^{-2}$. Unless otherwise specified the experimental conditions in all further measurements are those presented in figure 5.2.

5.3.3. The frequency spectrum

The frequency spectra were, as before, obtained with the "Polarad" Spectrum Analyser. We observed that the frequency spectrum at the transition of regime was qualitatively independent of the axial position of

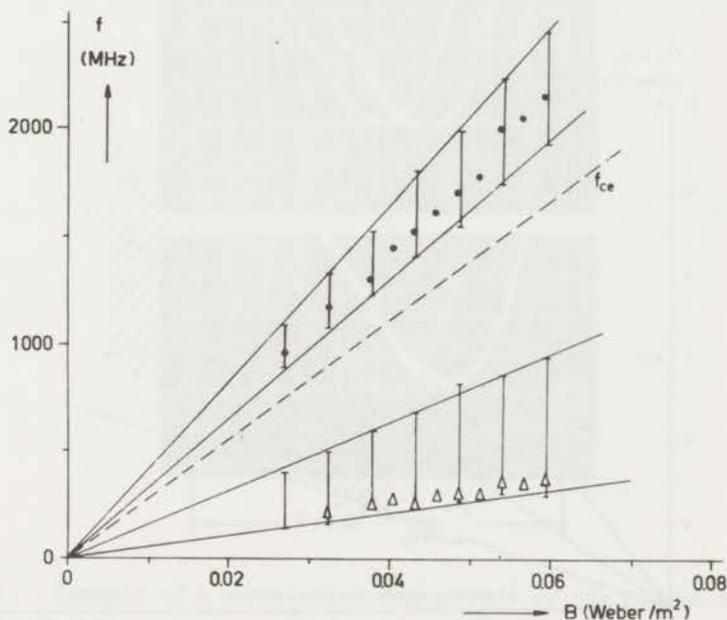


Fig. 5.3. - Excited spectrum of the beam-plasma instabilities at the regime transition. The higher frequency peak belongs to the cyclotron instability. The lower frequency one to the plasma instability. Dots and triangles represent the frequencies utilized for correlation purposes. The line separating the two peaks corresponds to the theoretical cyclotron frequency. Conditions presented in figure 5.2.

the probe. In a typical spectrum we notice a series of small peaks in the range from 10 to a few hundred MHz and two large amplitude peaks identified with the electron plasma and electron cyclotron instabilities.

Figure 5.3 shows the excited bandwidths associated with these two instabilities and the values of the frequencies used in the measurements for correlation purposes. Both instabilities occur at frequencies that show a linear dependence on the magnetic field. Due to the finite transverse dimensions of the beam-plasma system the plasma instability appears with frequencies below f_{pe} (NEZLIN et al., 1966).

5.3.4. The plasma density

Plasma densities were again measured with the electromagnetic resonant cavity. In figure 5.4 we plotted the square root of the plasma density, at the transition of regime, as a function of B . We see that the density exhibits large fluctuations (shaded area) between well defined

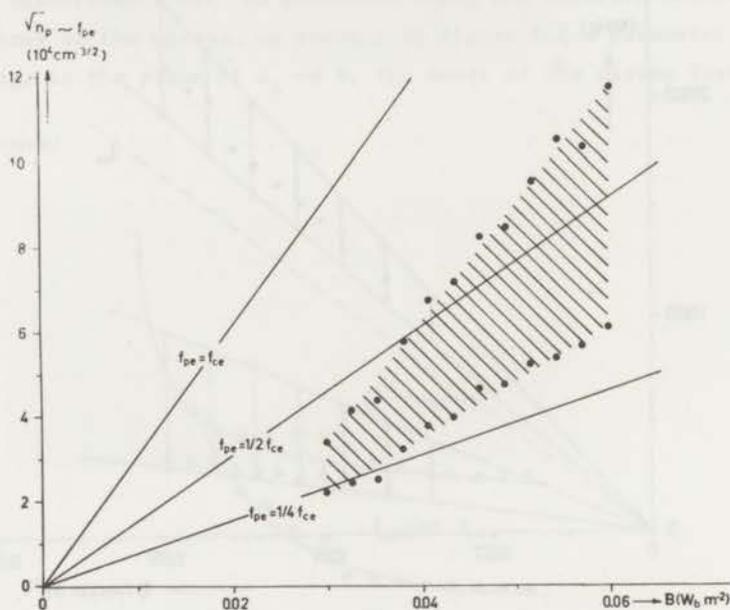


Fig. 5.4. - Square root of the plasma density as a function of the magnetic field. Dots represent the maximum and minimum values observed. Straight lines indicate the values of $\sqrt{n_p}$ corresponding to plasma frequencies equal to $\frac{1}{4}$, $\frac{1}{2}$ and 1 times the cyclotron frequency. Conditions are presented in fig. 5.2.

limits. These fluctuations were found to occur with a repetition frequency of about 30 kHz which was independent of the magnetic field. All the other beam-plasma internal parameters showed fluctuations with this same repetition frequency, which presumably results from the excitation of a low frequency ion instability (VERMEER et al., 1967; FEDORCHENKO, 1967;

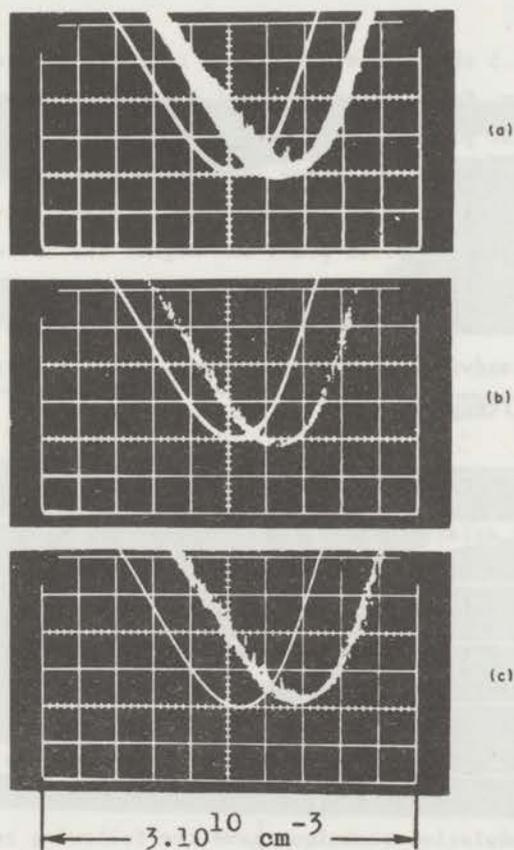


Fig. 5.5. - Example of a correlation measurement of the plasma density with an electromagnetic resonant cavity. The curve at the left side is the resonance of the cavity in the absence of plasma. The displacement of the resonance curve to the right is proportional to the plasma density. The densities were measured: (a) uncorrelated, (b) during the bursts of the plasma instability, (c) during the bursts of the cyclotron instability. Conditions: $V_b = 1500 \text{ V}$; $i_b = 12 \text{ mA}$; $p = 5 \times 10^{-4} \text{ Torr}$; $B = 0.0380 \text{ Wb m}^{-2}$.

LEVITSKII et al., 1969). A relaxation regime with the same repetition frequency is referred to by FRANK (1968).

The measurements presented in figure 5.4 permit us to conclude that, at the regime transition, the plasma frequency lies in the range 0.25 - 0.65 times the cyclotron frequency. In order of magnitude these values agree with those published by BOTTIGLIONI (1969) and JANCARIC et al. (1969).

Figure 5.5 shows an example of a correlation measurement of the plasma density. For a given value of B these measurements permit us to conclude: - The plasma instability is observed when the density is minimum; - During the cyclotron instability the plasma density always exceeds this minimum value (HOPMAN et al., 1968-b); - The higher the frequency in the cyclotron peak, the higher the corresponding value of the plasma density. Though the magnetic field is kept constant in each measurement, this last result agrees with dispersion theory because the excited bandwidth of the cyclotron instability appears near the upper hybrid frequency.

5.3.5. Axial energy spread in the beam centre

The beam axial energy spread was obtained with the electrostatic energy analyser in the manner described in section 4.2.3. We remember that the beam axial velocity distribution function is determined from the so-called energy analyser characteristic $j = j(V, r)$, by differentiation with respect to the energy (equation 4.2).

Figure 5.6.a shows an example of an uncorrelated energy analyser characteristic and figure 5.6.b another one, but now correlated with the cyclotron instability.

The z-modulation technique gave the following results:

(1) During the electron plasma bursts the beam has a narrow energy spread almost symmetric around its initial energy. The energy spread depends little on B (fig. 5.7).

(2) For the cyclotron instability the energy spread depends on the frequency selected in the associated peak. The higher the frequency the larger the energy spread. The largest energy spread is also plotted in fig. 5.7.

(3) The shape of the energy analyser characteristic resembles in every case a trapezium (fig. 5.6.b), showing that the beam distribution

function, at the transition of the regime, has always a plateau.

A set of measurements made as a function of the magnetic field leads to the results presented in figure 5.7. In this figure we can see that, in the centre of the beam: - The maximum energy gain is independent of B ; - The maximum energy loss varies with B and shows, for the case of the cyclotron instability, a clear decrease with increasing magnetic field.

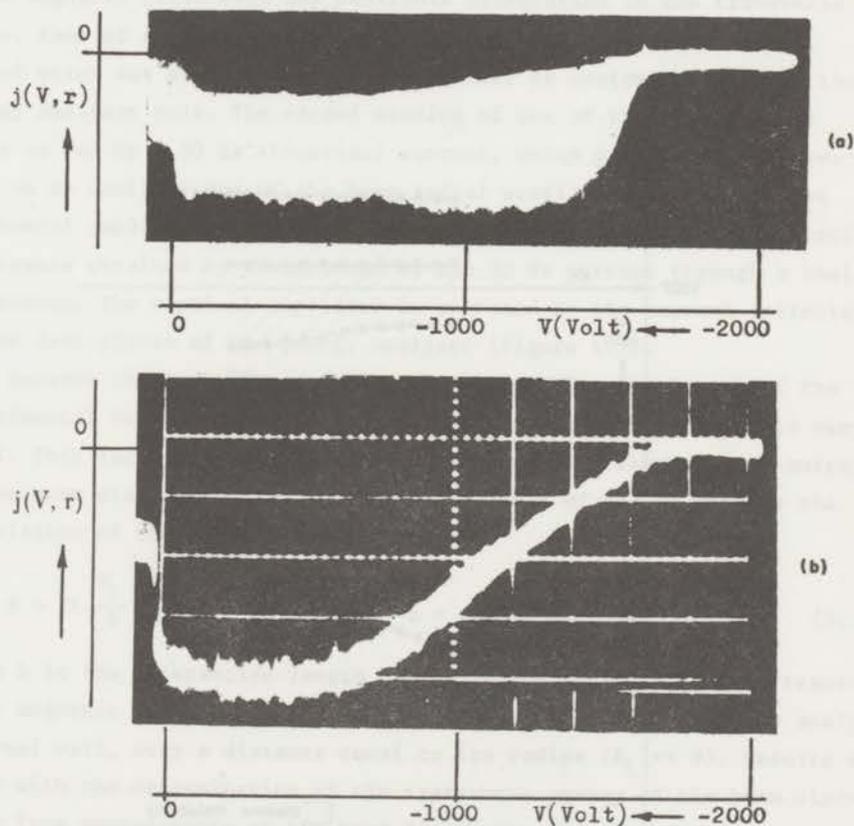


Fig. 5.6. - (a) Example of an uncorrelated energy analyser characteristic at the beam centre. Conditions: $V_b = 1500$ V; $i_b = 8$ mA; $p = 4.8 \times 10^{-4}$ Torr, $B = 0.0485$ Wb m^{-2} . (b) A trapezoidal energy analyser characteristic, correlated with the electron cyclotron instability. Conditions: $V_b = 1500$ V; $i_b = 9$ mA; $p = 4.8 \times 10^{-4}$ Torr; $B = 0.0325$ Wb m^{-2} .

At the transition of the regime in the plasma the relaxation of the electron beam is not yet complete. Plateaus extending to energies of the order of the thermal energy of the plasma electrons are only found in the second regime of the plasma as we verified in chapter IV. Such a complete relaxation of the beam requires an increase of either the beam current or the neutral gas pressure of about 50% of the values corresponding to the 1st-2nd regime transition (figures 4.9 and 4.10).

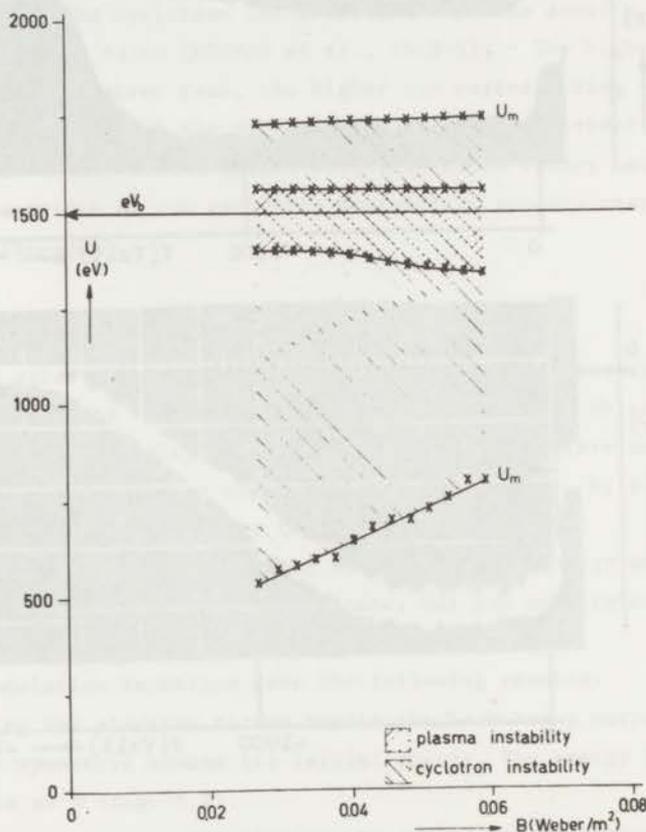


Fig. 5.7. - Extension of the axial energy spread in the beam centre as a function of the magnetic field. The smaller energy spread is correlated with the plasma instability and the larger one is the maximum that can be observed in correlation with the cyclotron instability. Conditions presented in figure 2.

5.3.6. Radial dependence on the axial energy spread in the beam

For these measurements we have to analyse the radial profiles of the beam. This was realized by deflecting the electron beam to both sides of the energy analyser entrance hole. This deflection was performed by using two long rectangular shaped coils (200×50 cm) disposed along the experimental tube and making an angle of 90° in relation to each other. In this way they can create, in combination, a homogeneous transverse magnetic field with any desirable orientation in the transverse plane. Each of these two coils is made of two independent windings, one of which was always DC operated in order to centre the beam in the energy analyser hole. The second winding of one of these transverse coils is fed by a 50 Hz sinusoidal current, which permits the observation on an oscilloscope of the beam radial profile (figure 7.2). The horizontal amplifier of the oscilloscope was operated with the potential difference obtained by the passage of the 50 Hz current through a small resistance. The vertical amplifier is operated by the current collected on the last plates of the energy analyser (figure 4.2).

Because the beam diameter is much smaller than the length of the experimental tube, the angle α over which the beam is deflected is very small. This fact, together with the assumption that the guiding centres of the beam electrons follow the magnetic lines of force, permits the calculation of the beam diameter d from

$$d = 2L \frac{B_1}{B} \quad \text{as} \quad \alpha = \text{tg } \alpha = \frac{d}{2L} = \frac{B_1}{B} \quad (5.1)$$

where L is the interaction length and B_1 is the variation on the transverse magnetic field necessary to deflect the beam, on the energy analyser external wall, over a distance equal to its radius ($B_1 \ll B$). Results related with the determination of the transverse energy of the beam electrons from measurements of the beam diameters are presented in chapter VII.

Using the deflection technique described above, we determined the radial dependence of the beam axial energy spread, during the bursts of the cyclotron instability. It is assumed that our beam-plasma system is rotationally symmetric so that the analysis along one beam diameter is sufficient. Deviations from the assumed symmetry were negligible. The results presented are obtained by averaging over two beam radii.

We verified that the energy analyser characteristics, current densi-

ty versus retarding potential for a given radius r , $j = j(V, r)$, remain approximately trapezoidal as in the centre of the beam (fig. 5.6.b) for all values of the radius. Measurements for $B < 0.04 \text{ Wb m}^{-2}$ appeared to be rather difficult and did not reproduce well.

Results are presented in figure 5.8, where a plot of the extension

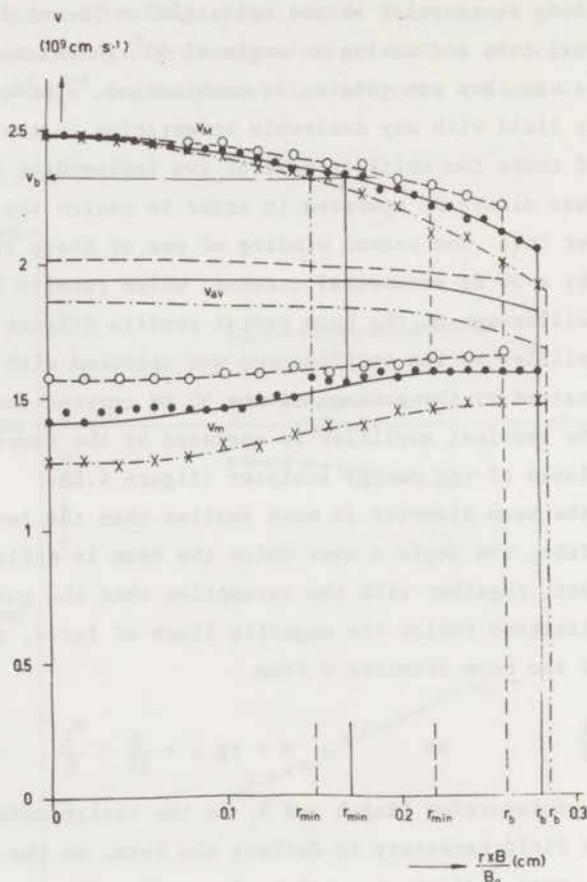


Fig. 5.8. - Radial dependence of the extension of the velocity plateau obtained in correlation with the cyclotron instability for different values of the magnetic field. r_{\min} is the radius of the beam in the absence of instabilities. Crosses represent $B = 0.0405 \text{ Wb m}^{-2}$. Filled dots, $B = 0.0485 \text{ Wb m}^{-2}$. Circles, $B = 0.0675 \text{ Wb m}^{-2}$. $B_0 = 0.0640 \text{ Wb m}^{-2}$. Conditions: $V_b = 1500 \text{ V}$; $i_b = 12 \text{ mA}$; $3.4 \times 10^{-4} \leq p \leq 4.6 \times 10^{-4} \text{ Torr}$. The pressure was adjusted in order to lead to the 1st-2nd regime transition.

of the plateau in a velocity scale is made as a function of the product $r.B/B_0$, a kind of normalized radius. The beam axial velocity distribution function, is for every radius, a plateau extending from $v_m(r)$ to $v_M(r)$ (figure 5.8) with an amplitude proportional to $j(0,r)/(U_M - U_m)$, where $U = \frac{1}{2}mv^2$ (equation 5.8). In figure 5.8 we see:

- The beam electrons are only accelerated to velocities greater than the initial beam velocity if they are inside a cylinder with a diameter of the order of the minimum beam diameter (diameter in the absence of instabilities).
- The electrons collected outside this cylinder always experienced an axial deceleration.
- The curves for the minimum velocity $v_m = v_m(r)$ are found at lower

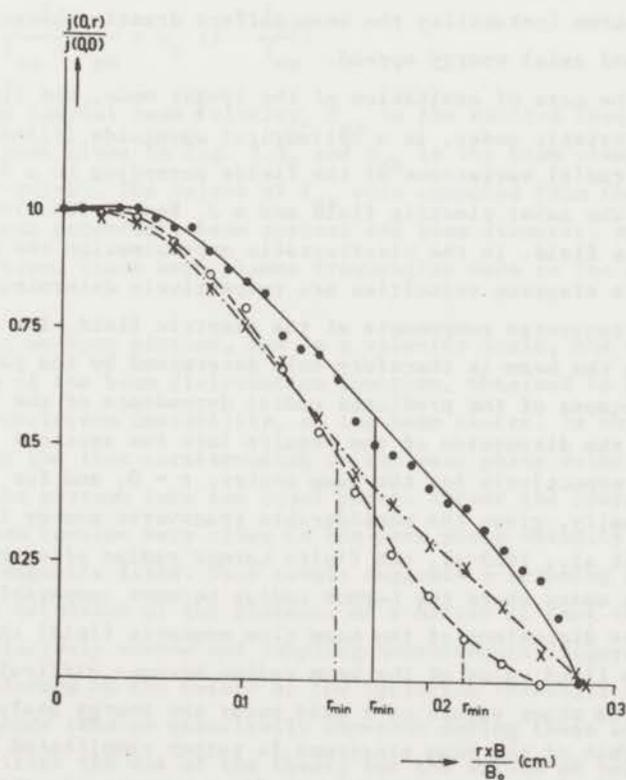


Fig. 5.9. - Normalized beam radial profiles. Conditions are the same as in figure 5.8.

values of v for lower values of the magnetic field.

- The average velocity $v_{av} = \frac{1}{2} (v_M + v_m)$ remains practically constant over the beam cross section. This average velocity is an increasing function of B in the entire beam cross section.

In fig. 5.9 we plotted the normalized beam current density, $j(0,r)/j(0,0)$, also as a function of the normalized beam radius. These plots define the beam radial profiles. We notice that these three normalized profiles are rather similar. The differences between them are more accentuated for values of r corresponding to regions outside the beam minimum diameter.

5.4. Interpretation of the results

We have thus seen that during the bursts of both the plasma and the cyclotron instability the beam suffers drastic changes in its radial profile and axial energy spread.

In the case of excitation of the lowest mode, the linearized theory of electrostatic modes, in a cylindrical waveguide filled with plasma, predicts radial variations of the fields according to a J_0 Bessel function for the axial electric field and a J_1 Bessel function for the transverse field. In the electrostatic approximation the parallel and transverse electron velocities are respectively determined by the parallel and transverse components of the electric field. The axial velocity spread in the beam is therefore only determined by the parallel electric field. Because of the predicted radial dependence of the electric field we split the discussion of the results into two sections (4.5.1 and 4.5.2), respectively for the beam centre, $r = 0$, and for $r \neq 0$.

Actually, given the considerable transverse energy in the beam (CABRAL et al.; 1969-a), the finite Larmor radius effects cannot be ignored. In cases where the Larmor radius becomes comparable with the transverse dimensions of the beam (low magnetic field) the analysis realized at a fixed value of the beam radius becomes difficult, as particles coming from other values of r also enter the energy analyser hole. The Larmor orbit of the beam electrons is rather complicated due to the radial variation of the electric field components. In this sense the measurements presented can only be considered as averages valid for the immediate neighbourhood of the measuring coordinate r .

5.4.1. Analysis of the results obtained at the beam centre

According to the last considerations we expect the electric field at the beam centre to be parallel to the axial magnetic field. Thus in the beam centre the transverse field is assumed null.

Let us first consider the case of the cyclotron instability. We found that during the bursts of this instability the beam attains its maximum energy spread. In order to explain these results we begin with the determination of an approximate value for the phase velocity of the cyclotron wave, under the referred experimental conditions. We know, from wavelength measurements, that in our beam-plasma experiment the cyclotron instability is excited by the slow beam space-charge wave. Then it is possible to compute theoretically an approximate value for the wave phase velocity. This value is given by (fig. 5.10)

$$v_{ph} = v_b \frac{f_{ex}}{f_{ex} + f_{pb}} \approx v_b \left(1 - \frac{f_{pb}}{f_{ex}}\right) \quad (5.2)$$

where v_b is the initial beam velocity, f_{ex} is the excited frequency in the cyclotron peak given in fig. 5.3, and f_{pb} is the beam plasma frequency (APEL, 1969-b). The values of f_{pb} were computed from the knowledge of the beam potential, beam current and beam diameter, assuming a homogeneous beam. These beam plasma frequencies were in the range 135 - 165 MHz.

In fig. 11 we have plotted, now in a velocity scale, the extension of the plateau of the beam distribution function, obtained in correlation with the cyclotron instability, at the beam centre. In this figure we can see that the line corresponding to the wave phase velocity almost divides the plateau into two equal parts. Indeed the average velocity of the beam remains very close to the wave phase velocity for all values of the magnetic field. This result suggests a trapping mechanism to explain the extension of the plateau. As a matter of fact the excited spectrum is relatively narrow and sampling measurements (figures 5.1-b and 5.1-c) performed on the bursts of the cyclotron instability proved that the frequency remains practically constant during these bursts. This fact justifies the use of the theory for the motion of beam electrons in the field of a monochromatic large amplitude wave (O'NEIL, 1965; DAWSON et al., 1968).

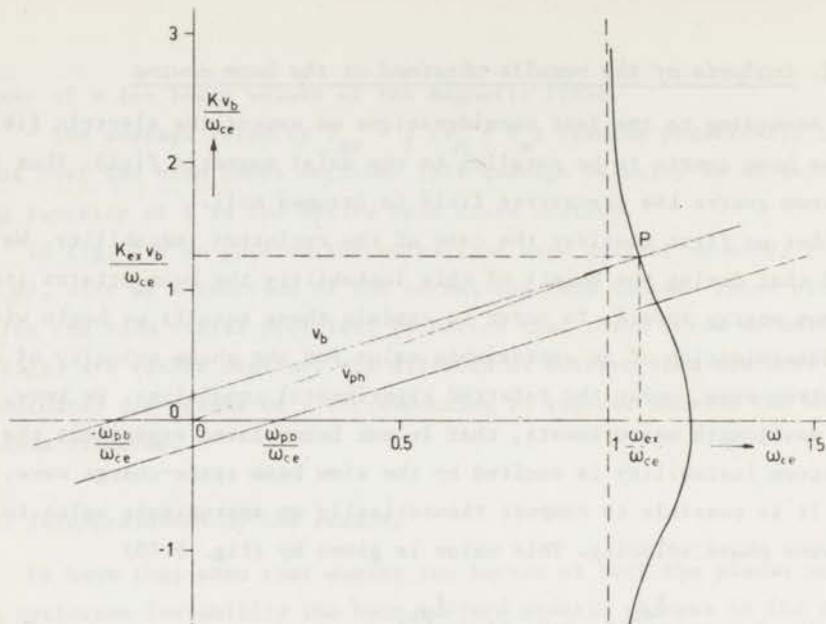


Fig. 5.10. - Simplified dispersion diagram for the cyclotron instability.

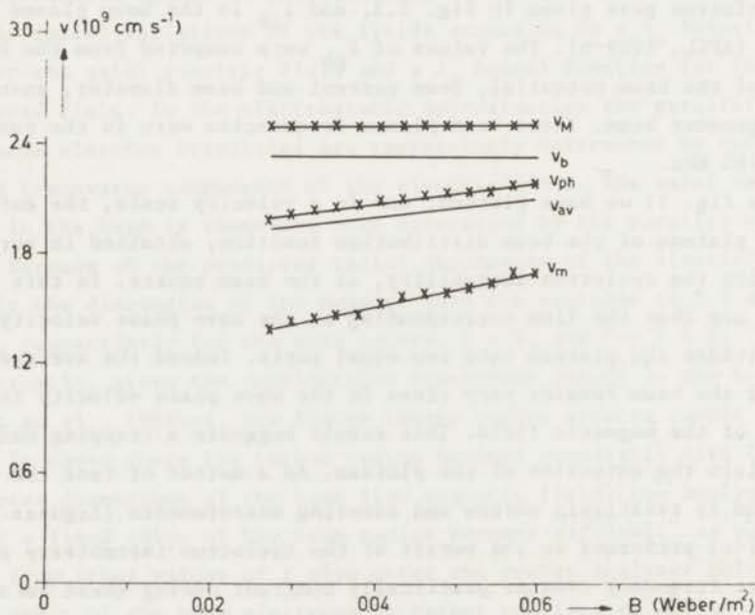


Fig. 5.11. - Some important velocities in the plateau obtained in correlation with the cyclotron instability. Conditions are presented in figure 2.

The condition for trapping is

$$E > E_c = -\frac{mk}{4e} (v_{ph} - v)^2 \quad (5.3)$$

where $v_{ph} = \omega/k$ is the wave phase velocity. E_c is the minimum electric field which is required to trap an electron with an axial velocity equal to v . The amplitude of the E field necessary for trapping depends on the phase difference between the wave and the electron movement (CABRAL et al., 1969-b). Then, if almost all the beam electrons are trapped in the potential well of the cyclotron wave, due to phase mixing in their relative motion, they will have a tendency to form a distribution function which is symmetric around the wave phase velocity. Condition 5.3 alone is not enough to assure the symmetry of the distribution function. Another condition requires that during its short travelling time ($t = 3.10^{-8}$ sec) the beam electrons perform several oscillations in the wave potential well in order to attain phase mixing in their relative motion. This means that the period of this oscillation must be considerably smaller than the transit time of the beam electrons. An approximate expression for the oscillation period is given by (STIX, 1962; WHARTON et al., 1968):

$$\tau = 2\pi (-m/eEk)^{\frac{1}{2}} \quad (5.4)$$

If we substitute into (5.4) the values of the axial electric field deduced from equation (5.3), considering $v_{ph} = v_{av}$ and v equal to either v_M or v_m ,

$$E_{||} = -\frac{mk}{4e} \left\{ \frac{v_M - v_m}{2} \right\}^2 \quad (5.3a)$$

we obtain for the period τ of these oscillations

$$\tau = \frac{4\lambda}{(v_M - v_m)} \quad (5.5)$$

where λ is the cyclotron wavelength. Typical values for this period are of the order of 5 - 7 nsec which is considerably smaller than the electron transit time.

In chapter 6 we will make a rigorous numerical study of the nonlinear equation of motion of the beam electrons under the presence of a large amplitude monochromatic traveling wave in the plasma. In that chap-

ter we will see that all the considerations just presented seem to sustain the conclusion that, in the case of excitation of the cyclotron instability, the velocity plateau results from the trapping of the beam electrons by the potential barrier of the parallel electric field.

The same type of considerations can be made for the case of the plasma instability. But now the energy spread (fig. 5.7) is rather small. Apparently in the plasma instability the wave phase velocity is much smaller than any velocity attained by the beam electrons during the bursts of this instability and so trapping does not occur. The corresponding measurements are better explained on basis of the nonlinear interaction between the beam and the plasma wave as it was done by CABRAL et al. (1969.b). In that paper we obtained, numerically, plateaus developing around the beam initial velocity just by considering the spatial evolution of the beam distribution function under the action of a pure longitudinal travelling wave.

5.4.2. Analysis of the radial dependence of the axial energy spread in the beam

We have seen that, at the beam centre, the measurements obtained in correlation with the cyclotron instability can be explained on basis of the trapping of beam electrons by the parallel electric field of this instability. If this trapping mechanism applied to all values of the beam radius, the velocity plateau would remain symmetric around the wave phase velocity. In fig. 5.8 we see that this happens only in regions of the beam near its centre. For larger values of r we notice that the beam average velocity begins to decrease with r . A possible explanation for this effect can be based on the inhomogeneity of the axial electric field which, as we admitted, varies over the Larmor orbit of the beam electrons. It is possible that, in their Larmor gyrations, the beam electrons can be retarded by an axial field which is stronger than the one that accelerates them half a cyclotron period later in their outermost position. In this way the velocity plateaus for large radius would be found to develop asymmetrically around v_{ph} and with a preponderance for the lower values of the velocity, in agreement with the measurements of fig. 5.8. However the variation of v_{av} with r is relatively small and so we will assume that the trapping mechanism proposed for the beam centre can be applied to all values of r .

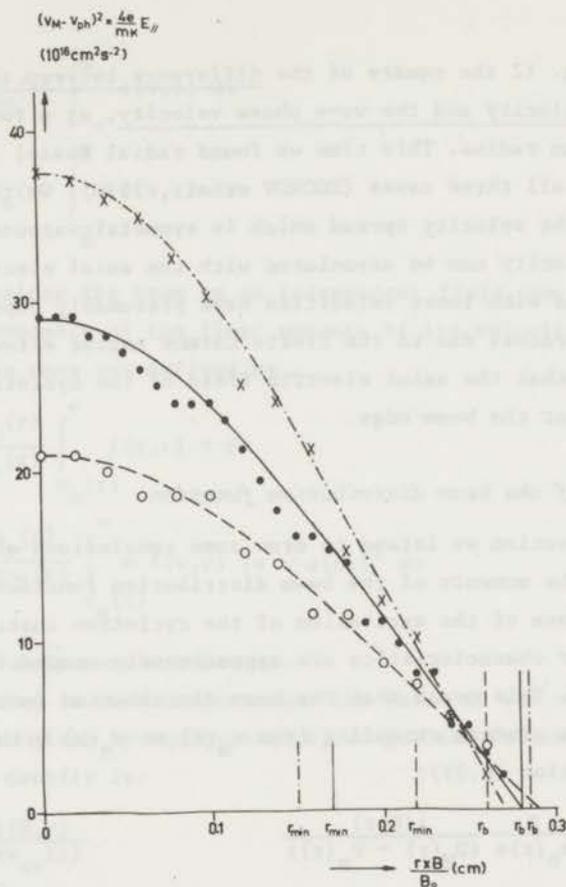


Fig. 5.12. - Radial dependence of the axial electric field of the cyclotron instability $E_{\parallel} = (mk/4e)(v_M - v_{ph})^2$. The lines passing by the experimental points are J_0 Bessel function dependences. Conditions are the same as in fig. 5.8.

According to our interpretation, the axial electric field is proportional (equation (5.3.a)) to the square of the total velocity spread in the beam. The linear theory of electrostatic modes propagating in a plasma filled waveguide predicts a J_0 Bessel function dependence on the radius for the axial electric field. So, an attempt was made to fit a J_0 Bessel function curve through the experimental points, obtained by plotting the square of the velocity spread as a function of the radius. The agreement was far from being acceptable. On the basis of the proposed deceleration mechanism, mentioned above, we

plotted in fig. 12 the square of the difference between the maximum attained beam velocity and the wave phase velocity, as a function of the normalized beam radius. This time we found radial Bessel function dependences for all three cases (EGOROV et al., 1970). We think that only that part of the velocity spread which is symmetric around the instability phase velocity can be associated with the axial electric field. Electrons found with lower velocities have presumably experienced a deceleration process due to the finite Larmor radius effect. From fig. 5.12 it seems that the axial electric field of the cyclotron instability has a null at the beam edge.

5.5. Moments of the beam distribution function

In this section we intend to draw some conclusions about the radial variation of the moments of the beam distribution function. As we have seen, in the case of the excitation of the cyclotron instability, the energy analyser characteristics are approximately trapezoidal in energy (figure 5.6.b). This means that the beam distribution function is approximately a plateau extending from $v_m(r)$ to $v_M(r)$ with an amplitude equal to (equation (4.2)):

$$f(v,r) = \frac{m}{n_o(r)e} \frac{j(0,r)}{(U_M(r) - U_m(r))} \quad (5.6)$$

We remember that we normalized the electron velocity distribution function to unity (equations (2.2) and (4.1)). This means that

$$\int_{-\infty}^{\infty} f(v,r) dv = 1 \quad (5.7)$$

We must now distinguish between the beam and the plasma electrons. As we have verified in the last sections the relaxation of the beam distribution function is not complete at the 1st-2nd regime transition. As the minimum energies possessed by the beam electrons are of the order of 500 eV we expect to have the two electron distributions (beam and plasma) separated in velocity space. Indeed the plasma temperature is rather low (section 4.5.3 and Table 4.1) and there was no evidence for the presence in our system of electrons with more than 25 eV above the energy corresponding to the plasma potential. So we can write:

$$n_p(r) = n_o(r) \int_{-\infty}^{v_m(r)} f(v,r) dv \quad (5.8)$$

$$n_b(r) = n_o(r) \int_{v_m(r)}^{\infty} f(v,r) dv \quad (5.9)$$

If we consider the beam as an independent fluid, we can then study the radial dependence of the first moments of its velocity distribution function. These ones are defined by

$$u(r) = \frac{n_o(r)}{n_b(r)} \int_{v_m(r)}^{\infty} f(v,r) v dv \quad (5.10)$$

$$T_{\parallel}(r) = \frac{n_o(r)}{\kappa n_b(r)} \int_{v_m(r)}^{\infty} m f(v,r) [v - u(r)]^2 dv \quad (5.11)$$

where κ is the Boltzmann's constant.

Substituting in these expressions the value of the velocity distribution function given by equation (5.6) we get the following results:

The beam density is:

$$n_b(r) = \frac{j(0,r)}{ev_{av}(r)} \quad (5.9.a)$$

Because we have seen (fig. 5.8) that the average velocity in the plateau does not depend significantly on the beam radius, the beam density has approximately the same radial variation as the beam profile (fig. 5.9).

The beam directed velocity $u(r)$ coincides with the average velocity in the plateau

$$u(r) = v_{av}(r) . \quad (5.10.a)$$

The axial beam temperature $T_{\parallel}(r)$ is:

$$T_{\parallel}(r) = \frac{m}{12\kappa} (v_M - v_m)^2 . \quad (5.11.a)$$

In fig. 13 we have plotted the radial dependence of the axial velocity spread on the beam. We verify that this velocity spread also shows a J_0 Bessel function variation with r . Thus the beam temperature shows a J_0^2 dependence on r . Typical values of the axial beam temperature, at

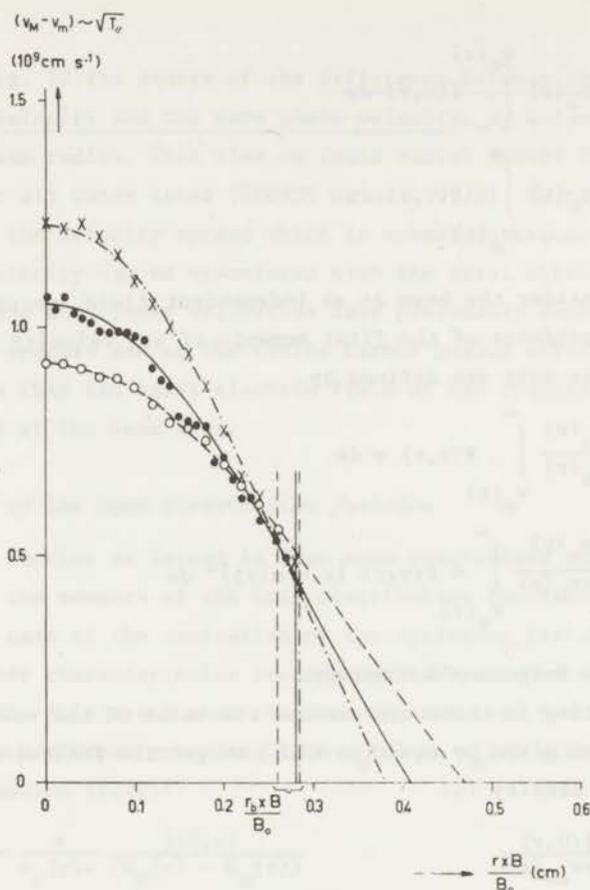


Fig. 5.13. - Radial dependence of the axial velocity spread in the beam. The velocity spread is proportional to the square root of the beam axial temperature. Conditions are the same as in figure 5.8.

the beam centre, are of the order of 35 - 70 eV, at the 1st-2nd regime transition.

5.6. Energy considerations

The axial power density is given by

$$P_{\parallel}(r) = n_0(r) \int_0^{\infty} f(v, r) \frac{1}{2} m v^3 dv \quad (5.14)$$

where, for simplicity, f is here identified with the beam distribution

function alone. Using equation (4.2) we obtain

$$\begin{aligned}
 p_{\parallel}(r) &= -\frac{m}{e} \int_0^{\infty} \frac{dj(U,r)}{dU} U \frac{dU}{m} = -\frac{1}{e} \int_{-\infty}^0 U(j,r) dj \\
 &= -\int_{-\infty}^0 V(j,r) dj = \int_0^{-\infty} j(V,r) dV \quad (5.15)
 \end{aligned}$$

The last translation is possible because $j(V,r)$ is a monotonically increasing function of eV , by definition tending to zero when eV tends to ∞ . We see that the areas under the energy analyser characteristics $j=j(V,r)$ represent directly the power density in the beam, at radius r (SHUSTIN et al., 1969). To get the total power in the beam, in the axial direction, we must integrate the power density $p_{\parallel}(r)$ over the entire beam cross section

$$P_{\parallel} = \int_0^{\infty} \int_0^{-\infty} j(V,r) dV \, 2\pi r \, dr = \int_0^{\infty} p_{\parallel}(r) \, 2\pi r \, dr \quad (5.16)$$

The initially injected power is given by the product of the beam potential V_b and the beam current, and so can be determined from

$$P_{in} = V_b i_b = V_b \int_0^{\infty} j(0,r) \, 2\pi r \, dr \quad (5.17)$$

Applying these relations to our measurements of the radial dependence of the axial beam distribution function, we can determine the axial power losses during the electron instability. In percentage these are given by

$$\eta = \left\{ 1 - \frac{P_{\parallel}}{P_{in}} \right\} \times 100\% \quad (5.18)$$

The numerical results are presented in fig. 5.14, as a function of the magnetic field. We find that the beam losses decrease with the magnetic field.

This decrease of the beam losses with B can be easily understood. Indeed the energy analyser characteristics are approximately trapezoidal and so we can write

$$P_{\parallel}(r) = \int_0^{\infty} j(V,r) dV = j(0,r) V_{av} \quad (5.19)$$

with $V_{av} = (\frac{1}{2e})(U_M + U_m)$. But, from fig. 5.8, we can easily verify that the average potential does not vary significantly with r . Under these conditions the total power is approximately given by

$$P_{\parallel} \approx V_{av} \int_0^{\infty} j(0,r) 2\pi r dr \approx V_{av} i_b \quad (5.20)$$

and the power losses are then obtained by

$$\eta = \left(1 - \frac{P_{\parallel}}{P_{in}}\right) \times 100 \% \approx \left(1 - \frac{V_{av}}{V_b}\right) \times 100 \% \approx \left(1 - \frac{v_{ph}^2}{v_b^2}\right) \times 100 \% \quad (5.21)$$

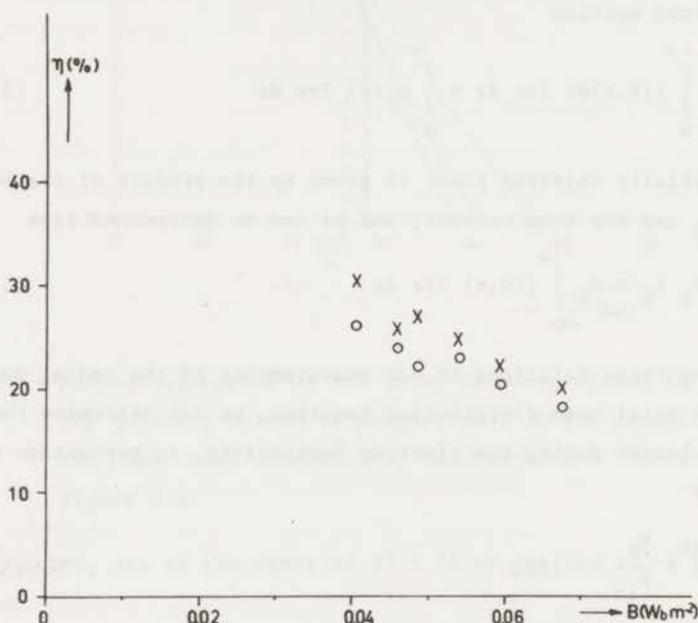


Fig. 5.14. - Axial power losses, in percentage, verified during the cyclotron instability. Crosses represent the calculated losses obtained with equations (5.16-5.18). Circles represent the approximate value for these losses obtained from the measurements made at the beam centre (equation (5.21)). Conditions are the same as in figure 5.8.

The last equality in equation (5.21) is only qualitatively correct as the velocity corresponding to the average potential is larger than v_{ph} , which is assumed to be the average velocity in the plateau (equation (5.26)).

Using equation (5.2) for the cyclotron wave phase velocity we can write (5.21) under the form

$$\eta = 2 \frac{f_{pb}}{f_{ex}} \approx 2 \frac{f_{pb}}{f_{ce}} \quad (5.21.a)$$

and so we verify that the beam power losses are then directly determined by the magnetic field and by the beam density (beam plasma frequency). As at the 1st-2nd regime transition f_{pb} does not vary significantly with B, we see that the beam losses decrease indeed with B.

A test on the accuracy of the power calculations was always done, computing with equation (5.17) the value of the beam current used. We found experimental errors of the order of 5 per cent. A test of the effectiveness of the beam injection was also done and we found that, in the absence of instabilities, the beam transverse energy was very small (of the order of 0.5 per cent of the axial energy).

We finally want to stress that the power density at the beam centre during the cyclotron instability is only 30 per cent of the power density in the beam in the absence of instabilities. This is partly caused by the increase in the beam diameter. This value would indicate an apparent power loss of 70 per cent if the radial analysis was not done. The more reasonable value of 20-30 per cent is recovered with the integration over the beam cross section. Because of the unknown value of the power flowing into the radial direction the values given in figure 14 cannot be identified with the total loss of kinetic energy of the beam.

5.7. Conclusions

From the results presented in the last sections, related with the electron cyclotron instability at the transition of plasma regime, we can conclude:

(a) A certain percentage of the beam initial power (30.7 per cent for $B = 0.0405 \text{ Wb m}^{-2}$ and 20.3 per cent for $B = 0.0675 \text{ Wb m}^{-2}$) is not found in the axial direction This power must have been delivered partly

to the plasma for building up the oscillations and partly converted into a transverse energy flow.

(b) From the beam initial power only 41.3 per cent, for $B = 0.0405 \text{ Wb m}^{-2}$, and 75.7 per cent, for $B = 0.675 \text{ Wb m}^{-2}$, remains in the axial direction, inside the cylinder occupied by the beam in the absence of oscillations.

(c) The remaining axial power percentage (28 per cent for $B = 0.0405 \text{ Wb m}^{-2}$ and 4 per cent for $B = 0.0675 \text{ Wb m}^{-2}$) is found outside that cylinder.

Thus, due to the interaction of the beam particles with the cyclotron wave, a reasonable part of their energy is converted from parallel into transverse energy.

It is important to stress that an analysis of the power density at the beam centre is not enough. An integration over the beam cross section is necessary to obtain trustworthy results.

If we substitute in equation (5.3.a) the experimental values for the maximum and minimum velocities in the plateau (figure 5.11) and the values of k determined from the knowledge of the excited frequency (figure 5.3) and of the wave phase velocity ($v_{\text{ph}} = \frac{1}{2}(v_M + v_m)$), we obtain the interesting result that the electric field of the cyclotron instability at the 1st-2nd regime transition is, at the beam centre, independent of the magnetic field. Indeed we find for all the cases values of E equal to $150 \pm 5 \text{ V cm}^{-1}$ (SEIDL et al., 1967).

If our interpretation of the results in terms of trapping of the beam electrons in the potential well of the cyclotron wave is correct, there is reason to believe that it is this trapping mechanism that is responsible for the saturation of the cyclotron bursts (fig. 5.1.a). Indeed, after the trapping of the beam electrons, there cannot exist any further net energy transfer from the beam to the wave. The beam electrons will only interchange their positions in velocity space without any further loss of kinetic energy.

A last result in favour of our interpretation of the velocity spread in the beam is the agreement, in order of magnitude, between the energy density associated with the propagation of the electrostatic wave ($2 \times \frac{1}{2} \epsilon_0 E^2$) and the energy density which would be obtained if the total energy lost by the beam, during the growth of the wave, were equally distributed inside the cylinder occupied by the beam. The ener-

gy density associated with the wave is about $2 \times 10^{-3} \text{ J m}^{-3}$. The density of the energy lost by the beam under the above conditions is $3.3 \times 10^{-3} \text{ J m}^{-3}$. This last value was obtained assuming a beam of 1500 V, 10 mA, 20 per cent energy loss, diameter of 0.55 cm and taking L, the interaction length, to be 75 cm. The growth time for the cyclotron wave was assumed 20 nsec (fig. 5.1.a).

Finally we can verify that the electrostatic energy density in the cyclotron wave (which is the highest attained during the 1st-2nd regime transition) is anyhow smaller than the plasma thermal energy density, as required by the condition of weak turbulence (equation 3.4). Indeed, for the case of $B = 0.0540 \text{ Wb m}^{-2}$, we determined the plasma temperature at the transition of regime in the plasma ($T_p = 8 \text{ eV}$). The plasma density, attained during the bursts of the cyclotron instability, was for this value of B (figure 5.4) $n_p = 1.1 \times 10^{10} \text{ cm}^{-3}$. So the plasma thermal energy density ($w_T = 14.1 \times 10^{-3} \text{ J m}^{-3}$) is an order of magnitude larger than the wave energy density ($Q_W = 10^{-3} \text{ J m}^{-3}$). The assumption of monochromaticity of the cyclotron wave (absence of turbulence in the plasma) would be subjected to a serious criticism if the electrostatic energy density of the cyclotron wave would be found to be larger (or of the same order) than the plasma thermal energy density.

For the case of the plasma instability, apparently the electric field is weaker than the critical field necessary for trapping to occur. Linearizing the exact equation of motion for the beam electrons acted by a monochromatic wave (equation 6.11) for the case in which the electric field is much smaller than the critical field necessary for trapping, we obtain

$$v_M = v_b + \frac{2eE}{m(\omega - kv_b)} \quad (5.22)$$

$$v_m = v_b - \frac{2eE}{m(\omega - kv_b)} \quad (5.23)$$

We see that in this case the velocity spread increases linearly with E. From the last equations we can determine the value of the electric field

$$E = \frac{mk}{4e} (v_{ph} - v_b)(v_M - v_m) \quad (5.24)$$

If we compute the phase velocity of the plasma waves still with equation (5.2) we can determine the values of the electric field of

these waves at the transition of regime in the plasma. We stress that in this case the approximation for the wave phase velocity is less accurate. Anyhow our intention is only to determine the order of magnitude of the electric field. Using equation (5.24) we obtained for E the value of $40 \pm 2.5 \text{ V cm}^{-1}$. Typical values for the minimum field necessary to trap electrons with an initial velocity equal to v_b were, for the considered values of the wave phase velocity, in the range $90 - 150 \text{ V cm}^{-1}$.

Therefore it seems that the two instabilities (electron plasma and electron cyclotron) which appear at the 1st-2nd regime transition in the plasma, have electric fields which are independent of the value of the external magnetic field and so independent of the value of their frequency (figure 5.3).

We can now explain qualitatively why is the electric field of the cyclotron instability almost independent of B at the 1st-2nd regime transition. We verified that the beam velocity distribution function is a plateau extending from v_m to v_M . We also verified that this plateau develops symmetrically around the wave phase velocity. To this distribution function corresponds an energy analyser characteristic which is a trapezium (like the one in figure 5.6.b). We have seen (equation 5.15) that the areas under the energy analyser characteristics represent directly the power density in the beam. Therefore a beam with a plateau in the velocity distribution will have no more power losses if the average energy in the analyser characteristic $U_{av} = \frac{1}{2}(U_M + U_m)$ will coincide with the beam initial energy U_b .

The average energy is

$$U_{av} = \frac{1}{2} m (v_m^2 + v_M^2) \quad (5.25)$$

If the average velocity in the plateau is equal to the wave phase velocity we can write the average energy as

$$U_{av} = U_{ph} + \frac{1}{2} m \left(\frac{v_M - v_m}{2} \right)^2 \quad (5.26)$$

with $U_{ph} = \frac{1}{2} m v_{ph}^2$.

The maximum attainable velocity spread will then be, according to the considerations presented in section 6.5.3, the one which leads to the equality between the average energy and the beam initial energy.

Therefore we have:

$$(v_M - v_m)_{\text{Max}}^2 = \frac{8}{m} (U_b - U_{\text{ph}}) \quad (5.27)$$

Using now equation (5.3.a) for the electric field associated with this value of the velocity spread, we get for the maximum value of E

$$E_{\text{Max}} = \frac{k}{2e} (U_b - U_{\text{ph}}) \quad (5.28)$$

If we recall equation (5.2) for the phase velocity of the cyclotron wave we can write:

$$k = \frac{2\pi f_{\text{ce}}}{v_b \left(1 - \frac{f_{\text{pb}}}{f_{\text{ce}}}\right)} \quad (5.29)$$

and

$$U_{\text{ph}} = \frac{1}{2} m v_b^2 \left(1 - \frac{2 f_{\text{pb}}}{f_{\text{ce}}}\right) \quad (5.30)$$

assuming that $(f_{\text{pb}}/f_{\text{ce}}) \ll 1$ and that the excited frequency is close to the electron cyclotron frequency.

Substitution of these results into equation (5.28) leads to

$$E_{\text{Max}} = \frac{2\pi V_b}{v_b} f_{\text{pb}} \left(1 + \frac{f_{\text{pb}}}{f_{\text{ce}}}\right) \quad (5.31)$$

which is the equation we intended to derive.

We can see that the maximum electric field attainable during the development of the cyclotron instability, under the referred conditions is practically independent of the cyclotron frequency and so of the magnetic field.

On the other hand we see that the maximum value of E varies linearly with the beam velocity and with the plasma frequency of the beam. Therefore the beam seems to determine completely the final amplitude of the electron cyclotron instability. We can then expect that beams of high energy and with a high density will lead to strong cyclotron interactions.

Substitution into (5.31) of our experimental parameters leads to values of the maximum attainable electric field of the order of 550 V cm^{-1} . However, because the beam must lose 20 to 30% of its power to

build up the instabilities, we see that the electric field must therefore be smaller than this limit value, as it was experimentally verified.

CHAPTER VI

NUMERICAL STUDY OF THE NONLINEAR INTERACTION BETWEEN A MONOENERGETIC ELECTRON BEAM AND A PLASMA WAVE IN A BEAM-PLASMA SYSTEM OF FINITE LENGTH

6.1. Introduction

In the last chapter we assumed that, in the 1st-2nd regime transition, the velocity spread obtained in correlation with the cyclotron instability could be explained by the consideration of the trapping of beam electrons in the wave potential well. We thus expect that the nonlinear interaction between an initially monoenergetic beam and a large amplitude monochromatic wave propagating along the plasma column, as studied in this chapter, will be a reasonable approximation for the real beam-plasma interaction occurring under similar conditions. Therefore the purpose of this chapter is to study, numerically, the nonlinear response of the beam electrons to the electric field of a beam-plasma instability under conditions obtained from the experimental results presented in the last chapter.

We will see that the formerly obtained results (concerning the beam axial velocity spread and its power losses), can be qualitatively explained, just by considering the nonlinear Lorentz force equation, with a simple model for the wave-beam interaction.

6.2. Numerical determination of the axial velocity distribution function and of the power losses of the beam at the end of the interaction chamber.

We suppose that an electrostatic wave has been set-up in the plasma as a result of the development of a beam-plasma instability. As in a collisionless plasma a single particle only feels the electric field of the wave, we replace the complete beam-plasma system by the wave alone. We then want to study the nonlinear behaviour of a single beam electron moving along the interaction chamber in the presence of this wave. We also assume that the passage of the beam electron does not perturb the wave. By separating the collective from the individual res-

ponse of the particles, the back coupling of these ones to the plasma wave is lost. The treatment is therefore nonadiabatic.

Restricting ourselves to a one-dimensional calculation, we start with the assumption that the plasma wave propagates along the z -direction with a phase velocity $v_{ph} = \omega/k$. Thus we write: $E(z,t) = E \cos(\omega t - kz)$. In cases when the growth time of the wave, as seen by the test electron, is longer than the time needed by this electron to cover distances of interest, the wave amplitude E may be assumed constant. This is certainly the situation when the bursts of the beam-plasma instabilities attain their maximum amplitude.

The test electron is injected into the wave at $z=0$ and $t=0$, when the wave has a phase ϕ . The behaviour of this electron, under the referred conditions, is completely described by the Lorentz force equation (6.1), with the following boundary conditions: $z(t=0) = 0$
 $\dot{z}(t=0) = v_b$.

$$\ddot{z} = eE \cos(\omega t - kz + \phi)/m \quad (6.1)$$

Our fundamental problem is to determine the electron velocity at a certain distance L as a function of the initial phase ϕ . Varying ϕ in steps of one half degree from 0 to 359.5° , we simulate a continuous electron stream. It is then possible to compute, from the knowledge of the 720 final velocities (at $z=L$), the beam velocity distribution function, averaged over one oscillation period, at that distance from the injection plane ($z=0$). This is simply done by counting the number of values of ϕ which lead to a final velocity comprised between $v - \frac{1}{2}\Delta v$ and $v + \frac{1}{2}\Delta v$, with $\Delta v \ll v$.

The power losses, in percentage, are then given by

$$\eta = \left(1 - \frac{\sum_{\phi} v^3(\phi)}{720 v_b^3}\right) \times 100 \% \quad (6.2)$$

Equation (6.1) is exactly soluble in terms of elliptic integrals (O'NEIL, 1965; BAILEY et al., 1970). To solve it we make the substitution:

$$\emptyset = \omega t - kz \quad (6.3)$$

where z , the coordinate of the electron, is a function of time. \emptyset is the phase variation (relative to $t=0$) in the electric field felt by the

electron during its movement along z . With this substitution we have:

$$\ddot{\theta} = -eEk \cos(\theta + \phi) / m \quad (6.4)$$

Multiplying both sides of this equation by $2\dot{\theta}$ and integrating we get

$$\dot{\theta}^2 = \gamma - 2eEk \sin(\theta + \phi) / m \quad (6.5)$$

The integration constant γ is determined by the initial values $\dot{\theta}(0) = \omega - kv_b$ and $\theta(0) = 0$:

$$\gamma = (\omega - kv_b)^2 + 2eEk \sin \phi / m \quad (6.6)$$

Then equation (6.5) is written as

$$\dot{\theta}^2 = (\omega - kv_b)^2 - \frac{2eEk}{m} [\sin(\theta + \phi) - \sin \phi] \quad (6.7)$$

Separating variables in equation (6.7) and integrating again we obtain:

$$\int_0^t dt = \int_0^{\theta} \frac{d\theta}{\pm \sqrt{(\omega - kv_b)^2 - \frac{2eEk}{m} [\sin(\theta + \phi) - \sin \phi]}} \quad (6.8)$$

This is the integral equation which is to be solved numerically. Because v_b exceeds v_{ph} , the relative phase θ is, in the beginning of the interaction process, a decreasing function of time. In other words, the electron always begins to overtake the wave. For simplicity let us first consider the case in which trapping of beam electrons in the wave potential well does not occur.

6.3. Solution in the absence of trapping

Inspecting equation (6.8) we verify that, if the electric field obeys the following condition

$$E < \frac{-m(\omega - kv_b)^2}{4ek} \leq \frac{-m(\omega - kv_b)^2}{2ek [|\sin(\theta + \phi) - \sin \phi|]} = E_c(\phi) \quad (6.9)$$

the integrand in θ remains finite. This means also that $\dot{\theta}$ (equation 6.7) keeps its initial negative sign and so θ is a monotonically decreasing function of time. The electron continuously overtakes the wave and its

velocity is therefore always greater than the wave phase velocity. In this case, from the two mathematically valid solutions of our equation, we must choose the one with the negative sign in the denominator of (6.8). By convention, from now on, all radicals are taken to be positive.

If we call θ^* the value of θ at the time τ of arrival at the distance $z=L$, then θ^* is simply related to τ by: $\theta^* = \omega\tau - kL$. Equation (6.8), written for $t=\tau$, takes the form of an integral equation in θ^* .

$$\frac{\theta^* + kL}{\omega} = - \int_0^{\theta^*} \frac{d\theta}{\sqrt{(\omega - kv_b)^2 - \frac{2eEk}{m} [\sin(\theta + \phi) - \sin \phi]}} \quad (6.10)$$

This equation can be numerically solved and so, for each value of E , we can determine the phase θ^* as a function of ϕ . Knowing θ^* we can compute $\dot{\theta}^*(\tau)$ given by (6.7), and finally the electron velocity is calculated from $v = \dot{z} = (\omega - \dot{\theta})/k$.

$$v(\tau) = \frac{\omega}{k} + \frac{1}{k} \sqrt{(\omega - kv_b)^2 - \frac{2eEk}{m} [\sin(\theta^* + \phi) - \sin \phi]} \quad (6.11)$$

With the knowledge of the final velocities as a function of ϕ the problem is formally solved (CABRAL et al., 1969).

6.4. Solution in the presence of trapping

Let us now consider the case in which the electric field is so large that condition (6.9) is not fulfilled for a great percentage of the values of ϕ . In this case the first thing we ought to do is to verify if, for a certain value of ϕ , trapping occurs or not. Trapping occurs of course when a beam electron is seen to stop in the wave referential. At that particular instant of time $\dot{\theta}$ must then be zero. So in conclusion, trapping will occur if we can find real roots for the following equation:

$$(\omega - kv_b)^2 - \frac{2eEk}{m} [\sin(\theta + \phi) - \sin \phi] = 0 \quad (6.12)$$

Let us assume that we are dealing with a case in which trapping does really occur. Then, among the infinity of solutions of the last equation

$$\theta = \arcsin \left[\sin \phi + \frac{m}{2eEk} (\omega - kv_b)^2 \right] - \phi \quad (6.13)$$

only two of them are physically interesting. These ones are respectively the first positive and the first negative solution of (6.12). Indeed, in our case $\phi(t=0)=0$ and, because v_b exceeds v_{ph} , the relative phase ϕ begins to become negative with the passage of time. ϕ continues to decrease until $\dot{\phi}$ becomes zero. This happens when ϕ attains the value of the first negative root of (6.12), which we call ϕ_m . At that moment the electron velocity is equal to the wave phase velocity (equation 6.11). The action of the wave electric field then inverts the electron movement in the wave referential, so that $\dot{\phi}$ is now positive; ϕ will then increase from its minimum value ϕ_m to higher values; in the course of time ϕ will pass again through zero and becomes positive. In the wave referential the electron will again stop when ϕ attains the value of the first positive root of (6.12) which we call ϕ_M . Afterwards ϕ will again decrease due to the action of the electric field of the wave and so we see that the relative phase ϕ will be forever comprised between ϕ_m and ϕ_M .

We can now analyse the behaviour of the integrand of the integral in ϕ in equation (6.8). For $\phi=0$ this integrand is $|(\omega - kv_b)|^{-1}$ and it approaches infinity when ϕ tends towards ϕ_m or ϕ_M . However, except when $\phi_M - \phi_m = 2\pi$, the improper integral

$$\int_{\phi_m}^{\phi_M} \frac{d\phi}{\sqrt{(\omega - kv_b)^2 - \frac{2eEk}{m} [\sin(\phi + \phi) - \sin \phi]}} \quad (6.14)$$

is convergent. When $\phi_M - \phi_m = 2\pi$ (limit that separates the trapping regime from the free running one) this integral diverges.

To solve the integral equation (6.8) when trapping occurs, we can look at figure 6.1, which helps to understand our numerical method of integration. In the lower part of this figure we represented by $eV_w = eV_w(\phi)$ the potential of the plasma wave. The electron is injected into the wave at the point A with a velocity $v_b > v_{ph}$. As it becomes trapped in the wave potential well, it therefore oscillates in the wave between points B and C.

To solve our equation we begin to remember that the integral in ϕ represents time, as stated in (6.8), and so it must be a monotonically increasing function of the periodical variable ϕ . In this way we define

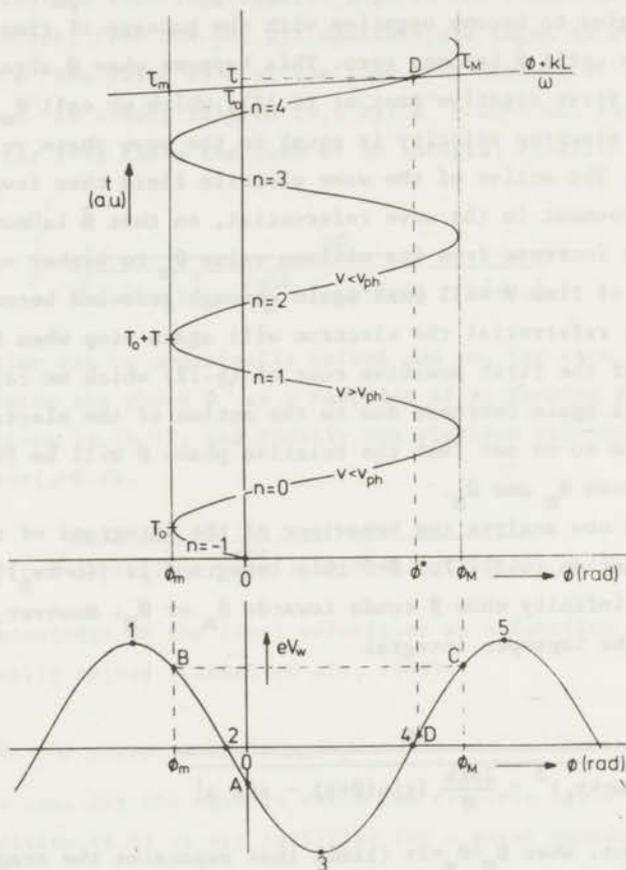


Fig. 6.1. - Schematic drawing helping to understand the numerical way of solving equation (6.8) when trapping occurs. The electron is injected at point A and then oscillates between points B and C. It arrives to $z=L$ at point D. Points 2, 3, 4 and 5 represent the position of the electron injection respectively for $\phi = 0, \pi/2, \pi$ and $3\pi/2$.

$$T_0 = - \int_0^{\theta} \frac{d\theta}{\sqrt{(\omega - kv_b)^2 - \frac{2eEk}{m} [\sin(\theta + \phi) - \sin \phi]}} \quad (6.15)$$

to be the time elapsed since the injection of the electron into the wave until its first stop in the wave referential. The minus sign is again due to the fact that $v_b > v_{ph}$. We also define the oscillation period in the wave potential well by

$$T = 2 \int_{\theta_m}^{\theta_M} \frac{d\theta}{\sqrt{(\omega - kv_b)^2 - \frac{2eEk}{m} [\sin(\theta + \phi) - \sin \phi]}} \quad (6.16)$$

In figure 6.1 the almost horizontal straight line represents $(\theta^* + kL)/\omega$, the l.h.s. of equation (6.10), which as we know (section 6.3) represents the total travelling time τ of an electron arriving at $z=L$, as a function of its relative phase θ^* . $\tau_0 = kL/\omega$ is the time needed for the wave to travel from $z=0$ to $z=L$. The straight line $(\theta^* + kL)/\omega$ simply states that if an electron has overtaken the wave ($\theta^* < 0$) its travelling time must be smaller than kL/ω and vice-versa. For a trapped electron the minimum and the maximum time of flight are respectively given by

$$\tau_m = \frac{kL + \theta_m}{\omega} \quad \tau_M = \frac{kL + \theta_M}{\omega} \quad (6.17)$$

Looking again at figure 6.1 we can see that the integral equation can be written as

$$\frac{\theta^* + kL}{\omega} = 2 T_0 + n \frac{T}{2} + \int_0^{\theta^*} \frac{d\theta}{\sqrt{(\omega - kv_b)^2 - \frac{2eEk}{m} [\sin(\theta + \phi) - \sin \phi]}} \quad (6.18)$$

for the even values of n and as

$$\frac{\theta^* + kL}{\omega} = (n+1) \frac{T}{2} - \int_0^{\theta^*} \frac{d\theta}{\sqrt{(\omega - kv_b)^2 - \frac{2eEk}{m} [\sin(\theta + \phi) - \sin \phi]}} \quad (6.19)$$

when n is odd; n is a parameter, to be determined for every value of ϕ , which approximately represents the number of half oscillations in the wave potential well. This number n must satisfy the following simultaneous conditions:

$$\left\{ \begin{array}{l} T_0 + n \frac{T}{2} \leq \tau_m \\ T_0 + (n+1) \frac{T}{2} > \tau_M \end{array} \right. \quad \text{with } n = \text{even} \quad (6.20)$$

or:

$$\left\{ \begin{array}{l} T_0 + n \frac{T}{2} \leq \tau_M \\ T_0 + (n+1) \frac{T}{2} > \tau_m \end{array} \right. \quad \text{with } n = \text{odd} \quad (6.21)$$

We thus see that ascertaining a value to n is equivalent to saying that the solution of the integral equation will be found, starting from $t=T_0$, after the passage of n half periods of oscillation and before the passage of $n+1$ of these periods. It is also easy to verify that when n is odd the final electron velocity will be greater than the phase velocity of the wave. Conversely when n is even the arrival velocity will be smaller than v_{ph} . Thus the final electron velocities are easily determined if we can solve equations (6.18) and (6.19) and obtain, for every ϕ , the corresponding value of θ^* , the relative phase of the electrons at the arrival at $z=L$.

The arrival velocity is then computed from

$$v = \frac{\omega}{k} - \frac{1}{k} \sqrt{(\omega - kv_b)^2 - \frac{2eEk}{m} [\sin(\theta^* + \phi) - \sin \phi]} \quad (6.22)$$

when n is even, and from

$$v = \frac{\omega}{k} + \frac{1}{k} \sqrt{(\omega - kv_b)^2 - \frac{2eEk}{m} [\sin(\theta^* + \phi) - \sin \phi]} \quad (6.23)$$

when n is odd.

From figure 6.1 it is also easy to verify that, when trapping does not occur for a certain value of ϕ , this fact is simply characterized by giving to n the value $n = -1$. With this value of n (odd) equation (6.19) indeed becomes equal to equation (6.10). We have also verified that equation (6.10) can be used either in the case of the free running regime (no existence of real solutions for equation (6.12)) or in the case when the stopping time T_0 exceeds the minimum value of the flight time τ_m (condition 6.21).

In short, we developed a computer program which was able to determine, for every value of ϕ , the following quantities:

- a) The values of ϕ_M and ϕ_m (equation 6.13), or the information that trapping does not occur. In this last case it gives to n the value $n = -1$.
- b) The period T_0 and the oscillation period T (equations 6.15 and 6.16).
- c) The maximum and minimum values of the electron traveling time, τ_M and τ_m (equations 6.17).
- d) The value of n (conditions 6.20 and 6.21).
- e) The solution of equation (6.18) if n is even or the solution of (6.19) if n is odd. These solutions are represented by the value ϕ^* of the relative phase ϕ at the time of the arrival of the electron at $z=L$.
- f) The value of the electron final velocity (equation 6.22 if n is even or 6.23 if n is odd).

So, we can obtain numerically the value of the final electron velocity for every value of ϕ . The computation of the final velocity distribution function and of the percentual power losses (equation 6.2) follows in precisely the same way as in the case in which trapping does not occur.

6.5. Numerical results

6.5.1. Results obtained without trapping

We used the following parameters: $\omega = 5 \times 10^9 \text{ rad s}^{-1}$, $v_b = 2.30 \times 10^9 \text{ cm s}^{-1}$, $v_{ph} = 0.9 \times v_b$, $\Delta v = 0.01 \times 10^9 \text{ cm s}^{-1}$. With these conditions the critical field E_c is always greater than 18.1 V cm^{-1} (equation 6.9).

In a first study we analyzed the influence of the amplitude of the electric field on the beam distribution function at $z = 75 \text{ cm}$ (length of our experimental tube). We found that the width of the distribution function in velocity space increases monotonically with E , as expected. Remarkable is the result that the distribution function becomes almost a plateau for the higher values of E in agreement with our former measurements (chapter 4). This result was predicted in a completely different approach by the quasilinear theory (IVANOV et al., 1967). We stress that these results are obtained in cases in which there is no resonant interaction (the beam electrons are always faster than the wave).

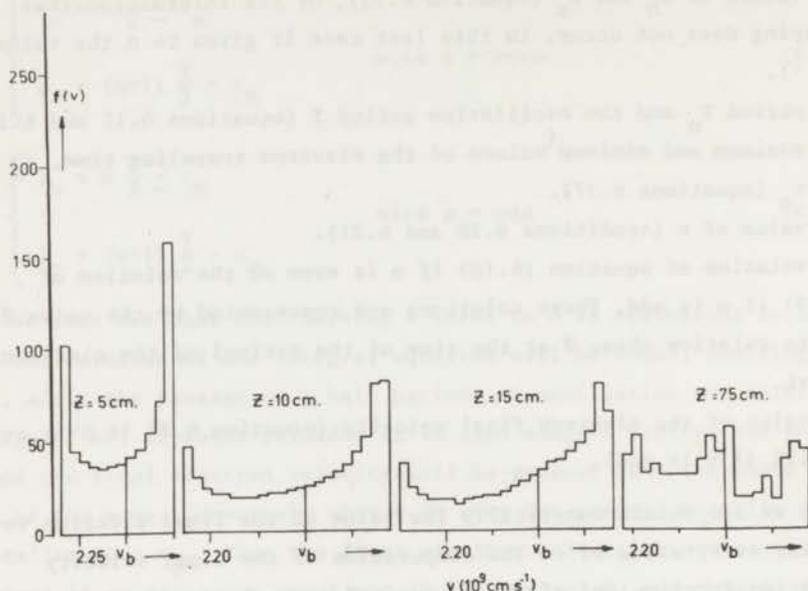


Fig. 6.2. - Spatial evolution of the beam distribution function for $E = 16 \text{ V cm}^{-1}$, $\omega = 5 \times 10^9 \text{ rad s}^{-1}$, $v_b = 2.30 \times 10^9 \text{ cm s}^{-1}$, $v_{ph} = 2.07 \times 10^9 \text{ cm s}^{-1}$.

Figure 6.2 presents the distribution functions obtained at $z = 5, 10, 15$ and 75 cm for the case of $E = 16 \text{ V cm}^{-1}$. We notice that for small z the shape of the distribution function resembles the theoretical one, calculated on basis of a linearized theory. For large z the distribution has a "plateau-like" character.

Analysis of the z dependence of the width of the beam distribution function showed (figure 6.3) that the maximum and minimum velocities are periodic in space but with different periodicity, as a result of both the nonlinearity of the equation of motion and of the spread in the average energy of the beam electrons. For $z < 5 \text{ cm}$ the linearized theory holds and we notice that the beam velocity spread increases linearly in space (or time) and proportional to E .

Figure 6.4 shows the beam energy losses after the passage through the plasmas as a function of z for the same parameters.

The beam energy losses were computed from

$$\rho = \left(1 - \int_{\phi} \frac{v^2(\phi)}{720 v_b^2} \right) \times 100\% \quad (6.24)$$

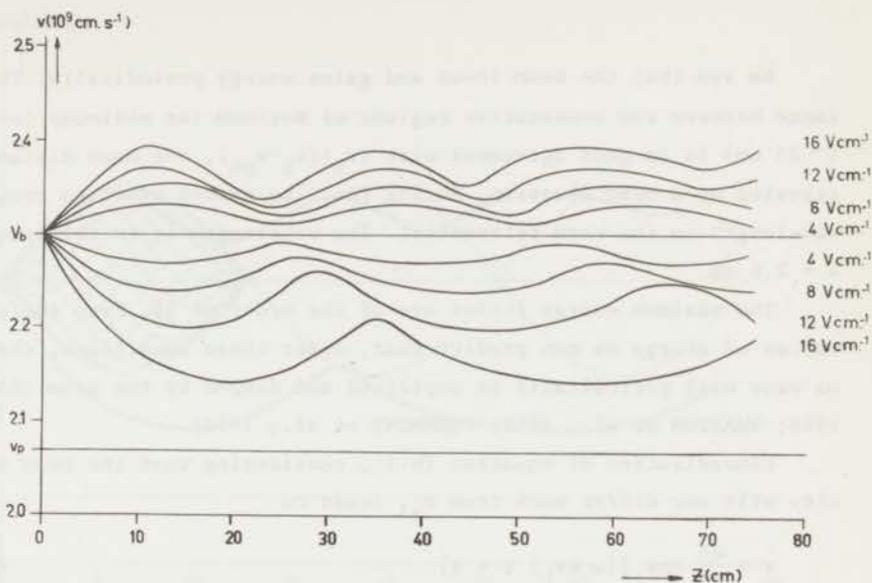


Fig. 6.3. - Beam velocity spread as a function of z for several values of the electric field. $\omega = 5 \times 10^9 \text{ rad s}^{-1}$; $v_b = 2.30 \times 10^9 \text{ cm s}^{-1}$; $v_{ph} = 2.07 \times 10^9 \text{ cm s}^{-1}$.

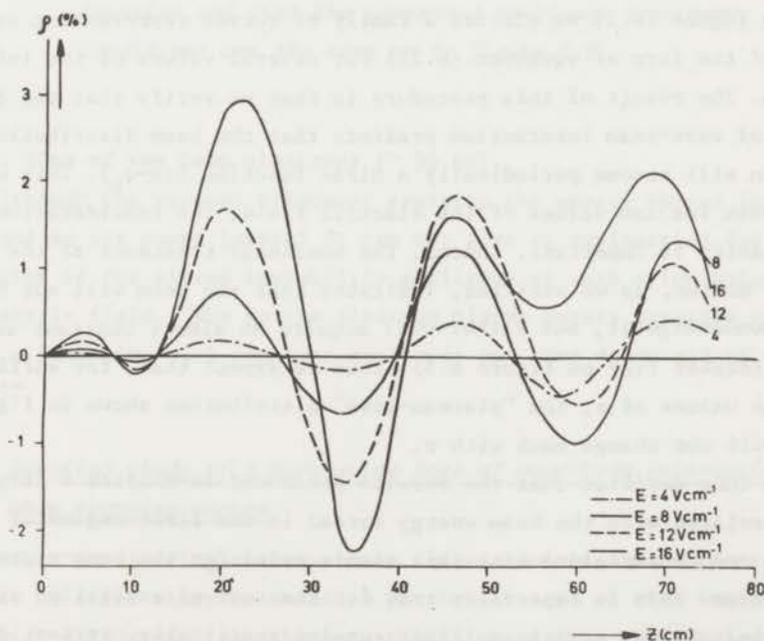


Fig. 6.4. - Beam energy losses as a function of z for several values of E . $\omega = 5 \times 10^9 \text{ rad s}^{-1}$; $v_b = 2.30 \times 10^9 \text{ cm s}^{-1}$; $v_{ph} = 2.07 \times 10^9 \text{ cm s}^{-1}$.

We see that the beam loses and gains energy periodically. The distance between two consecutive regions of maximum (or minimum) losses (~ 25 cm) is in good agreement with $\lambda v_b / (v_b - v_{ph})$, the mean distance traveled by a beam electron, during the time needed by it to cross one wavelength in the wave referential. The wavelength is in this case $\lambda = 2.6$ cm.

The maximum energy losses are of the order of 3%. From the conservation of energy we can predict that, under these conditions, the plasma wave will periodically be amplified and damped by the beam (BARTLETT, 1968; WHARTON et al., 1968; DRUMMOND et al., 1970).

Linearization of equation (6.1), considering that the beam velocity will not differ much from v_b , leads to

$$\dot{v} = \frac{eE}{m} \cos [(\omega - kv_b) t + \phi] \quad (6.25)$$

By integration we obtain

$$v = v_b + \frac{eE}{m} \frac{\sin [(\omega - kv_b) t + \phi]}{(\omega - kv_b)} \quad (6.26)$$

In figure (6.5) we plotted a family of curves representing solutions of the form of equation (6.26) for several values of the initial phase ϕ . The result of this procedure is that we verify that the linear theory of wave-beam interaction predicts that the beam distribution function will become periodically a Dirac function $\delta(v - v_b)$. This means that, even for low values of the electric field, the consideration of nonlinearity is important. Indeed, the nonlinear treatment of the equation of motion, as we verified, indicates that the beam will not become again monoenergetic, but rather will acquire an almost constant velocity spread (darker line on figure 6.5). Thus we expect that, for sufficiently large values of z , the "plateau-like" distribution shown in figure (6.2) will not change much with z .

We thus verified that the results presented in chapter 4 (figure 4.7a), related with the beam energy spread in the first regime of the plasma, can be explained with this simple model for the beam-plasma interaction. This is especially true for the case of excitation of the plasma instability as its amplitude remains practically constant during a great part of the burst duration. This one is of the order of 1000 oscillation periods (a few μs) which is extremely long compared with the

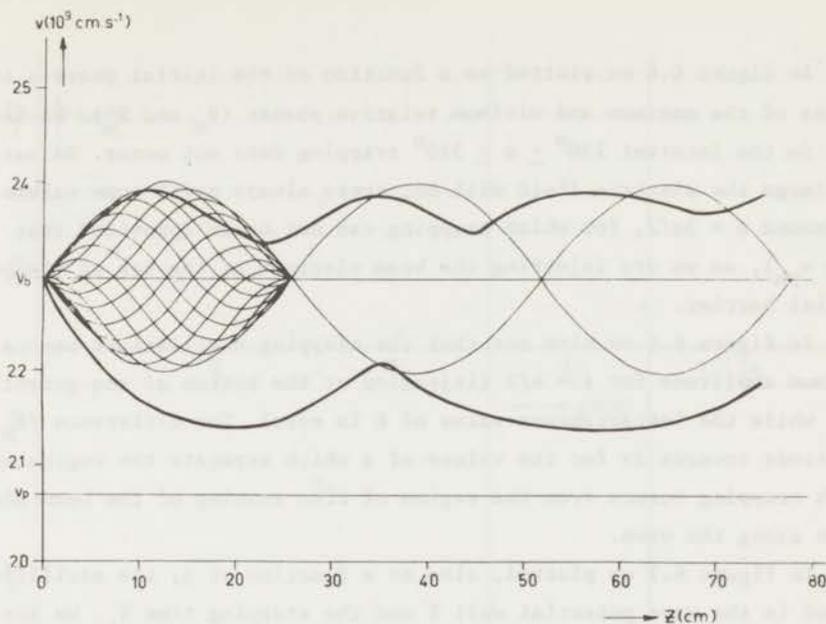


Fig. 6.5. - Comparison between the velocity spread in the beam as a function of z , obtained respectively with a linearized equation and with the presented nonlinear treatment. Conditions are the same as in figure 6.2.

transit time of the beam electrons (~ 30 ns).

Although the present treatment explains the energy spread in the beam (and so its power losses) it can not give an explanation for the saturation of the plasma instability amplitude at such a low value of the electric field. "Why do the electron plasma bursts saturate quickly, remain a long time with constant amplitude and then decay all of a sudden?"

6.5.2. Detailed study of a particular case of wave-beam interaction when trapping occurs

Before considering the wave-beam interaction in a more general way, let us first study in detail a particular case of this interaction, which will reveal all the potentialities of this numerical analysis. We choose for parameters: $\omega = 5 \times 10^9$ rad s⁻¹, $v_b = 2.30 \times 10^9$ cm s⁻¹, $v_{ph} = 0.9 \times v_b$, $\Delta v = 0.05 \times 10^9$ cm s⁻¹, $L = 75$ cm, $E = 150$ V cm⁻¹.

In figure 6.6 we plotted as a function of the initial phase ϕ the values of the maximum and minimum relative phases (ϕ_M and ϕ_m). We see that in the interval $230^\circ \leq \phi \leq 310^\circ$ trapping does not occur. No matter how large the electric field will be, there always exist some values of ϕ , around $\phi = 3\pi/2$, for which trapping can not occur (provided that $v_b \neq v_{ph}$), as we are injecting the beam electron at the top of the potential barrier.

In figure 6.6 we also see that the trapping oscillations have a minimum amplitude for $\phi = \pi/2$ (injection at the bottom of the potential well while the instantaneous value of E is zero). The difference ($\phi_M - \phi_m$) tends towards 2π for the values of ϕ which separate the region in which trapping occurs from the region of free running of the beam electrons along the wave.

In figure 6.7 we plotted, also as a function of ϕ , the oscillation period in the wave potential well T and the stopping time T_o . We see that the oscillation period depends on ϕ and so (figure 6.6) on the amplitude of the trapping oscillation ($\phi_M - \phi_m$) as is wellknown. In this case it varies from the minimum value $T=8.12$ ns (for $\phi = \pi/2$) to ∞ for the values of ϕ corresponding to the so-called separatrix (line separating in phase space the trapping from the free running regimes) (BEST, 1968). T_o has a minimum for $\phi = 90^\circ$, and becomes also ∞ at the separatrix.

Linearizing equation (6.4) for small amplitude oscillations, in the case of $\phi = \pi/2$, we obtain

$$\ddot{\phi} - \frac{eEk}{m} \phi = 0 \quad (6.27)$$

the wellknown linear harmonic oscillator equation. The period of these oscillations then is

$$T_m = 2\pi(-m/eEk)^{-1/2} \quad (6.28)$$

Substituting in this equation our parameters, we get

$$T_m = 7.87 \text{ ns.}$$

We verified that, in the neighbourhood of $\phi = \pi/2$, the oscillation period is only some 3% higher than this limit value.

The approximate number of half oscillations n made by the beam elec-

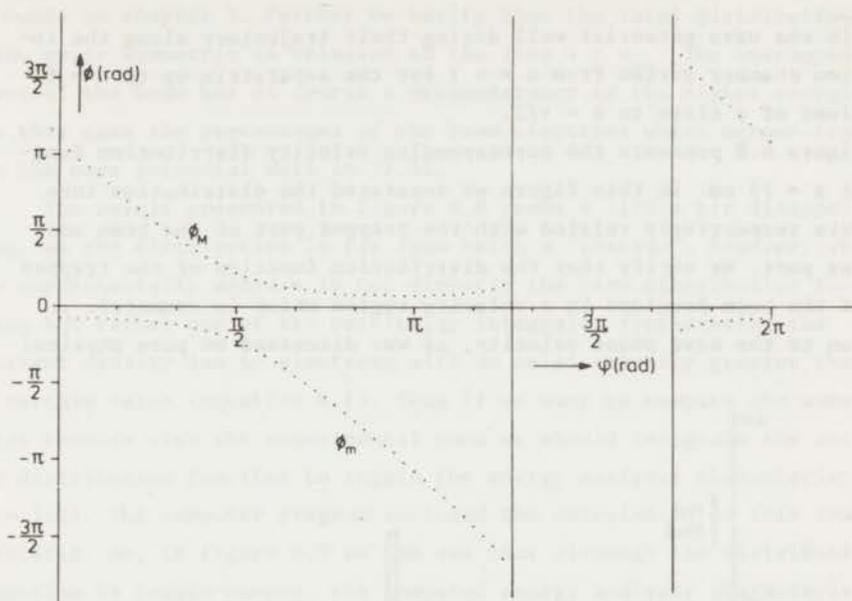


Fig. 6.6. - Maximum and minimum values of ϕ as a function of ϕ . Conditions: $\omega = 5 \times 10^9 \text{ rad s}^{-1}$; $v_b = 2.30 \times 10^9 \text{ cm s}^{-1}$; $v_{ph} = 2.07 \times 10^9 \text{ cm s}^{-1}$; $L = 75 \text{ cm}$; $E = 150 \text{ V cm}^{-1}$.

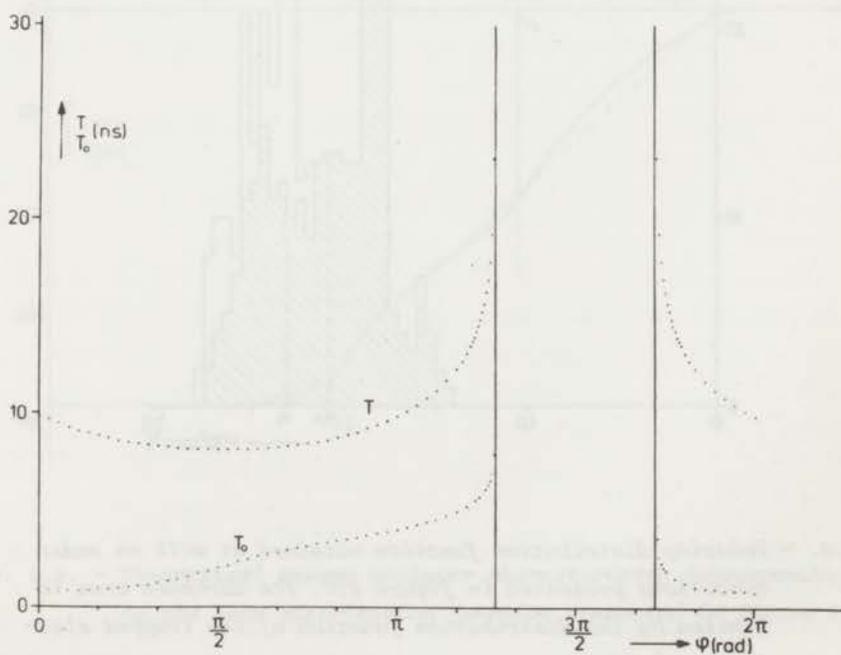


Fig. 6.7. - Oscillation period T and stopping time T_0 as a function of ϕ . Conditions are the same as in figure 6.6.

trons in the wave potential well during their trajectory along the interaction chamber varies from $n = -1$ for the separatrix up to $n = 8$ for values of ϕ close to $\phi = \pi/2$.

Figure 6.8 presents the corresponding velocity distribution function at $z = 75$ cm. In this figure we separated the distribution into two parts respectively related with the trapped part of the beam and its free part. We verify that the distribution function of the trapped part of the beam develops in a velocity region which is symmetric in relation to the wave phase velocity, as was discussed on pure physical

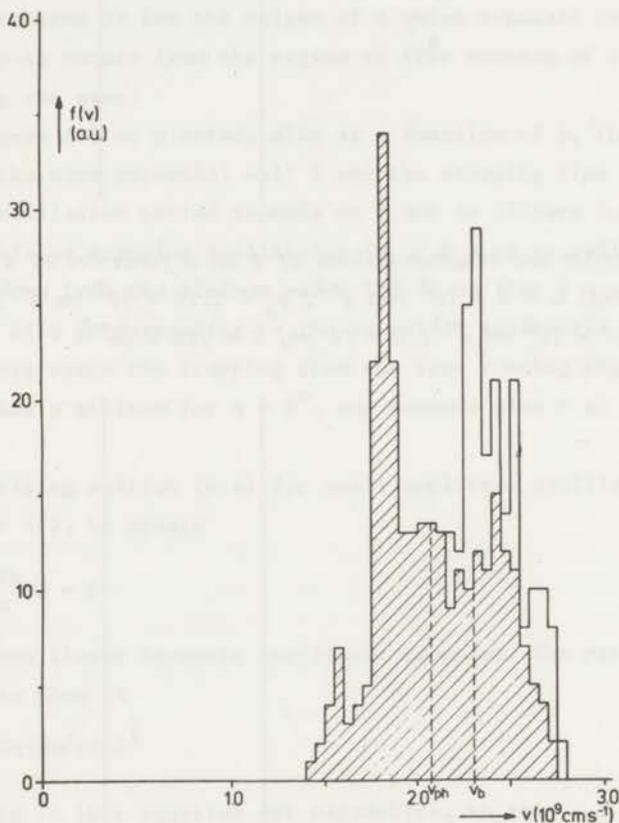


Fig. 6.8. - Velocity distribution function obtained at $z=75$ cm under conditions presented in figure 6.6. The darkened area is limited by the distribution function of the trapped electrons.

grounds in chapter 5. Further we verify that the total distribution is also quite symmetric in relation to the line $v = v_{ph}$. The untrapped part of the beam has of course a preponderancy to the higher energies. In this case the percentages of the beam electrons which become trapped in the wave potential well is 77.5%.

The result presented in figure 6.8 seems a little bit disappointing, as the distribution is far from being a "plateau". However, what we experimentally measure is not directly the beam distribution function but rather one of its particular integrals, representing the current density due to electrons with an axial velocity greater than a certain value (equation 4.1). Thus if we want to compare the numerical results with the experimental ones we should integrate the obtained distribution function to regain the energy analyser characteristics $j = j(V)$. The computer program included the calculation of this characteristic. So, in figure 6.9 we can see that although the distribution function is double-humped, the computed energy analyser characteristic is not far from having a trapezoidal shape, in agreement with our for-

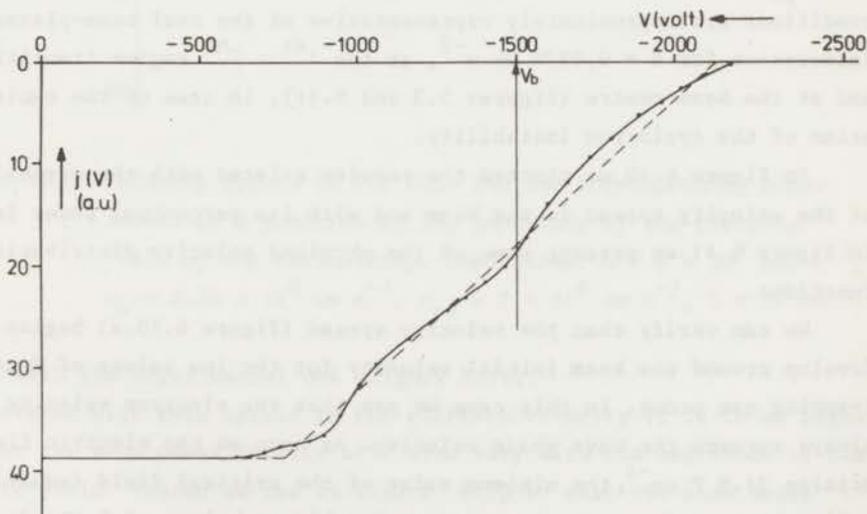


Fig. 6.9. - Theoretical energy analyser characteristic corresponding to the beam distribution function presented in figure 6.8.

mer measurements (figure 5.6.b).

Therefore we should emphasize that the acquisition of data related with the beam distribution function from measurements done with electrostatic energy analysers must not be taken too seriously, as only qualitative results are obtained. Indeed, the unavoidable integration will mask for a big part the fine structure of the velocity distribution. Recently, this same limitation of the electrostatic energy analysers was discussed by LEVITSKII et al. (1970), who could observe a series of small humps in the beam distribution function, using a cylindrical capacitor analyser. However, the use of the conventional retarding field analyser makes the humps on the distribution function unnoticeable.

6.5.3. Generalization of the results obtained when trapping occurs

In this section we will study the influence of the amplitude of the electric field of the beam-plasma instability on the behaviour of the beam electrons which pass through the interaction chamber. For the numerical calculations we used: $\omega = 5 \times 10^9 \text{ rad s}^{-1}$, $v_b = 2.30 \times 10^9 \text{ cm s}^{-1}$, $v_{ph} = 2 \times 10^9 \text{ cm s}^{-1}$, $\Delta v = 0.05 \times 10^9 \text{ cm s}^{-1}$, $L = 75 \text{ cm}$. These conditions are approximately representative of the real beam-plasma interaction for $B = 0.0270 \text{ Wb m}^{-2}$, at the 1st - 2nd regime transition and at the beam centre (figures 5.3 and 5.11), in case of the excitation of the cyclotron instability.

In figure 6.10 we plotted the results related with the extension of the velocity spread in the beam and with its percentual power losses. In figure 6.11 we present some of the obtained velocity distribution functions.

We can verify that the velocity spread (figure 6.10.a) begins to develop around the beam initial velocity for the low values of E as no trapping can occur. In this case we see that the electron velocity always exceeds the wave phase velocity. As soon as the electric field attains 31.8 V cm^{-1} , the minimum value of the critical field (equation 6.9), the trapping mechanism starts. For higher values of E the distribution function will have a tendency to develop symmetrically around the wave phase velocity. This is seen to happen for $E > 60 \text{ V cm}^{-1}$. For still larger values of E the distribution remains practically symmetric around v_{ph} . For $E = 150 \text{ V cm}^{-1}$ the theoretical velocity spread

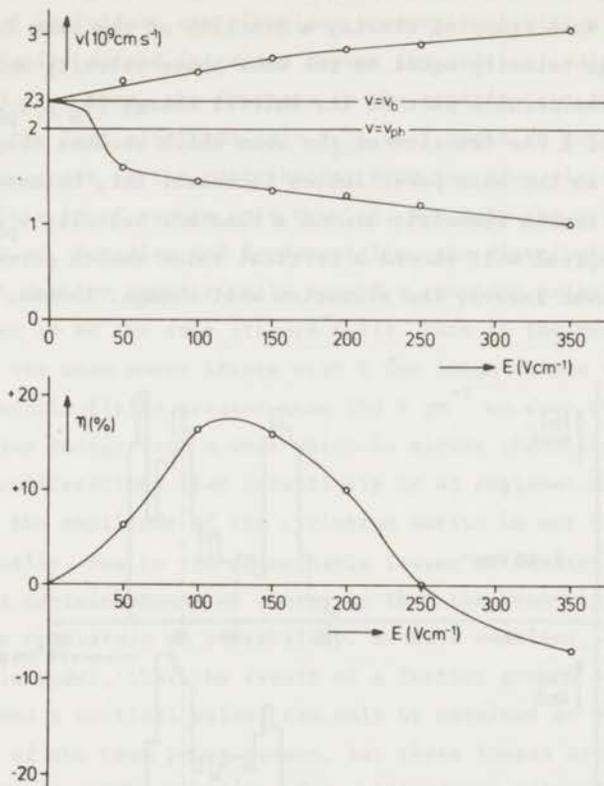


Fig. 6.10. - Velocity spread in the beam and the corresponding power losses as a function of the amplitude of the electric field of the instability. Conditions: $\omega = 5 \times 10^9 \text{ rad s}^{-1}$, $v_b = 2.30 \times 10^9 \text{ cm s}^{-1}$, $v_{ph} = 2 \times 10^9 \text{ cm s}^{-1}$, $L = 75 \text{ cm}$.

agrees with the experimental one (figure 5.11).

Related with this spread in the electron velocity it is to be expected that the beam power density will also vary with the amplitude of the electric field. Indeed we see in figure 6.10.b that the beam loses energy for $E < 250 \text{ V cm}^{-1}$. For higher values of E the beam, on the contrary, gains energy from the wave. This fact can be easily understood if we think that the obtained distributions have in general a "plateau-like" character (figure 6.11), at least in the sense formerly referred (figure 6.9). Therefore the energy balance will be as follows: For very

small values of E the beam will have also very small power losses (figure 6.4). When trapping starts, a fraction of the beam is forced to have an average velocity equal to the wave phase velocity and so it will lose a considerable part of its initial energy ($v_b > v_{ph}$). With the increase of E the fraction of the beam which becomes trapped also increases and so the beam power losses increase. But, because the distributions remain symmetric around a constant velocity v_{ph} , when the velocity spread will exceed a critical value (which corresponds to the maximum power losses) the situation will change. Indeed, the power

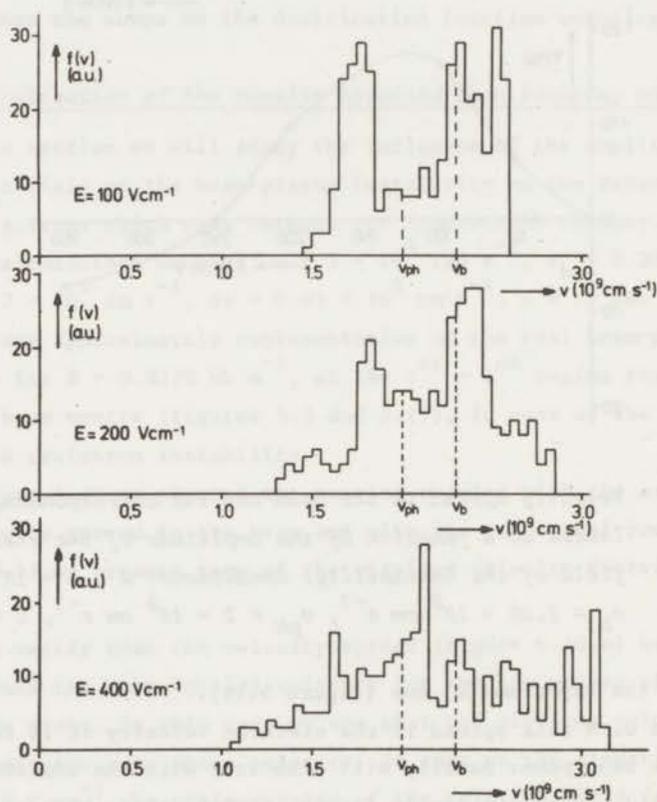


Fig. 6.11. - Some examples of the theoretical beam velocity distribution functions for the condition referred to in figure 6.10.

is made up of individual contributions proportional with v^3 . Therefore, when the velocity spread increases beyond the critical value, symmetrically around v_{ph} , then, the increase in the contribution to the power coming from the fast electrons ($v > v_{ph}$) will begin to surpass the simultaneous decrease in the contribution from the slow electrons ($v < v_{ph}$). This is of course only true if, not only the velocity spread (figure 6.10.a), but also and fundamentally, the distribution function itself, will develop symmetrically around a constant velocity ($v = v_{ph}$), as it is seen to be the case (figure 6.11). This is the reason for the decrease of the beam power losses with E for large values of E.

For electric fields greater than 250 V cm^{-1} we even verify that the beam gains energy from a wave which is slower than itself! These energetic considerations lead intuitively to an explanation for the saturation of the amplitude of the cyclotron bursts in our beam-plasma system. Actually, due to the unavoidable losses of the system, the beam must lose a certain amount of energy so that the beam-plasma system becomes able to sustain an instability. We have verified, with the presented simple model, that the result of a further growth of the instability, beyond a critical value, can only be obtained at the cost of a reduction of the beam power losses. But these losses are just necessary to maintain the instability. For still larger values of the electric field ($E > 250 \text{ V cm}^{-1}$), we arrived at the absurd conclusion that the wave can only grow at the cost of a decrease in its electrostatic energy, as conservation of energy states that the energy that the beam gains must be equal to the energy that the wave loses and vice-versa. We therefore conclude that, for the conditions given above, the maximum electric field of the instability must lie between 125 and 250 V cm^{-1} . This is in rather good agreement with our former measurements (chapter 5) in which we found for E the value of 150 V cm^{-1} at the 1st - 2nd regime transition.

Table 6.1 presents the numerical results, obtained for the different values of E, concerning: a) the percentage β of the beam electrons which becomes trapped; b) the maximum number of half oscillations in the potential well n_{max} , made by the beam electrons during their transit along the interaction chamber; c) the percentual power losses η ; d) the extension of the velocity spread in the beam.

TABLE 6.1

NUMERICAL RESULTS

E (V cm ⁻¹)	50	100	150	200	250	350
β (%)	40.9	62	69	73.5	77	80
n_{\max}	3	6	8	10	11	13
η (%)	6.25	16.40	15.85	10.01	-0.06	-7.06
$(v_M - v_m)$ (10 ⁹ cm s ⁻¹)	0.90	1.15	1.40	1.55	1.70	2.05

Parameters: $\omega = 5 \times 10^9$ rad s⁻¹; $v_b = 2.30 \times 10^9$ cm s⁻¹;

$v_{ph} = 2 \times 10^9$ cm s⁻¹; $L = 75$ cm.

6.6. Final considerations

Concluding this numerical study we should consider one of its fundamental limitations: - We assumed that the electric field can be considered constant along the interaction chamber. This will not be, almost certainly, the experimental situation. Indeed, not only the plasma density and temperature vary significantly with z (LEVITSKII et al., 1967), but and fundamentally, the beam-plasma instabilities, especially the electron plasma ones, can have a convective character. Therefore, if the beam-plasma bursts will be coherent in space, we expect that their amplitude will increase with z . This fact however, does not change the most important results of the present numerical analysis, namely the formation of the "plateau-like" distributions. Anyhow, if the wave amplitude saturates quickly in space, the presented model for the wave-beam interaction can become quite reasonable.

Therefore we stress the importance of future measurements of the correlation length in the plasma for the different beam-plasma instabilities (YAREMENKO et al., 1969, 1970; LAVROSKII et al., 1967, 1970; GASHEVSKI et al., 1969). Only this type of measurements can support or reject the assumed model for the beam-plasma interaction, by furnishing information about the spatial distribution of the instability electric field during a beam-plasma burst. Only measurements of this type can give an answer to the fundamental question: "Are the beam-plasma bursts

local phenomena or are they spread over the entire interaction chamber?"

We have thus seen that the measurements referred to in chapter V can be reasonably described by the trapping mechanism described in this chapter. For the measurements presented in chapter IV we are now faced with the question: "What is the mechanism involved in the development of the instabilities?"

We think that the results obtained in the first regime of the plasma are better explained on basis of the presented model for the interaction. Indeed, the spectrum of oscillations is narrow and fast analysis of the bursts reveal the almost monochromatic character of the instabilities. The width of the spectrum is probably due to the amplitude modulation of the instabilities (bursts) and to the formation of side bands arising from nonlinear wave-particle interaction (trapping). The reason for the saturation of the instabilities at such low values of the electric field and for the sudden disappearance of the instability is still obscure. However, the variation of the internal beam-plasma parameters, which accompany the excitation of these instabilities, can be on the basis of these effects.

For conditions which lead to the 1st-2nd regime we think that the state of the system can be described by a relaxation type oscillation of low frequency (ion instability) which periodically makes possible the excitation of the weak plasma instability and the strong cyclotron one. The model considered in this chapter is assumed to be valid for the instantaneous description of the state of the beam-plasma system.

In strong second regime states the situation can be completely different and this will be the subject for future investigations. Indeed in these states the spectrum of oscillations is rather broad, the radiation of the plasma decreases in relation to that measured at the transition of regime, and the velocity spread is extremely large and without fluctuations. Therefore we think that in these last states the presented model is not applicable. It is possible that the conditions of applicability of the quasilinear theory will become fulfilled. Indeed the existence of a broad spectrum suggests weak turbulence and the fact that we verified experimentally the formation of a plateau in the distribution function, which extends to very low energy values, is in good agreement with the predictions of this theory. As the distribution function does not show appreciable fluctuations and the

radiated power is relatively small, the interaction process must change of character when the plasma enters the second regime.

Finally, we should stress the importance of the recent studies on the behaviour of trapped particles in beam-plasma systems. Indeed, trapped particles can, in general, give rise to some interesting effects (LYAMOV et al., 1968). Among these ones, some can have an important role in beam-plasma systems, like for example:

- the formation of side bands in the spectra of the excited instabilities (WHARTON et al., 1968), due to the nonlinear exchange of energy between the trapped particles and the wave;
- the nonlinear Landau damping of large amplitude plasma waves (DAWSON et al., 1968; RAND, 1968; ELDRIDGE, 1970).
- the excitation of a new type of instability, the so-called trapped particle instability (ZASLAVSKII et al., 1968; KRUEER et al., 1969; SHAPIRO et al., 1970).

CHAPTER VII

MEASUREMENT OF THE TRANSVERSE ENERGY OF THE BEAM ELECTRONS

7.1. Introduction

As we have seen (section 3.8) theory predicts that the development of beam-plasma instabilities resulting from the anomalous Doppler effect will be accompanied by a considerable increase in the beam transverse energy (SHAPIRO et al., 1962, 1968). In fig. 4.3 we can verify that there are two instabilities which arise due to the anomalous Doppler effect: one appearing with a frequency slightly above the electron cyclotron frequency (SMULLIN et al., 1962) and another with a frequency below the electron plasma frequency. These two instabilities have rather small growthrates when compared with the ones related with the excitation of Cerenkov instabilities. However, a significant increase in the beam transverse energy can be attained when the Doppler shifted frequency of the instabilities, as seen by the beam electrons, becomes equal to the electron cyclotron frequency. In this way, the beam electrons will feel the transverse field of the instabilities always in phase and this leads to a coherent increase in their Larmor radius.

Measurements of the transverse energy of the beam electrons only recently began to appear in literature (MORSE, 1969; SCHUSTIN et al., 1969; CABRAL et al., 1969, 1970). In general it is still rather difficult to obtain a clear picture of the radial dependence of the beam transverse velocity distribution function. In our measurements we succeeded in obtaining some information about the beam transverse energy in two particular cases: - The first one deals with measurements made at the beam centre and makes use of a new possibility of our electrostatic energy analyser. The second particular type of measurement was to obtain an estimate for the transverse energy at the beam edge. This method is based on the experimentally observed increase in the beam diameter during the bursts of the beam-plasma instabilities (KHARCHENKO et al., 1962). Let us now consider the last case.

7.2. Measurement of the transverse energy at the beam edge

7.2.1. General considerations

An estimate for the transverse energy of the beam electrons near to the beam edge can be obtained by measuring the increase in beam diameter due to the excitation of the beam-plasma instabilities. For these measurements we have to analyse the beam radial profiles. These ones were obtained with the deflection technique referred to in section 5.3.6. As we remember, the beam diameters were computed from

$$d = 2L \frac{B_{\perp}}{B} \quad (7.1)$$

where L is the interaction length and B_{\perp} is the variation in the transverse magnetic field necessary to deflect the beam, on the energy analyser external wall, over a distance equal to its radius.

Considering the determination of the transverse energy we must relate this quantity with the experimentally observed increase in the beam diameter. Let us assume that, when the instability starts, the beam is cold and has its minimum diameter (measured under optimal conditions in a good vacuum). Let us also admit that the final diameter is attained due to the increase in the transverse energy of the electrons which were initially at the beam edge. Under these circumstances these ones will acquire at least a Larmor radius equal to one half of the measured increase in the beam diameter. These assumptions lead of course to a minimum value for the transverse energy U_{\perp} , which is computed from the Larmor radius assuming that the electrons rotate with the cyclotron frequency.

$$U_{\perp} = \frac{1}{2} m \omega_{ce}^2 r_L^2 \quad (7.2)$$

In this section we will present measurements obtained under conditions similar to those of chapters IV and V.

7.2.2. Time integrated measurements of the transverse energy of the beam electrons during the development of the beam-plasma instabilities

The measurements which will be presented were obtained under the experimental conditions referred to in chapter IV. We remember that we let an electron beam interact with its own created plasma in an interaction chamber of variable length. The beam current, beam potential and the Helium

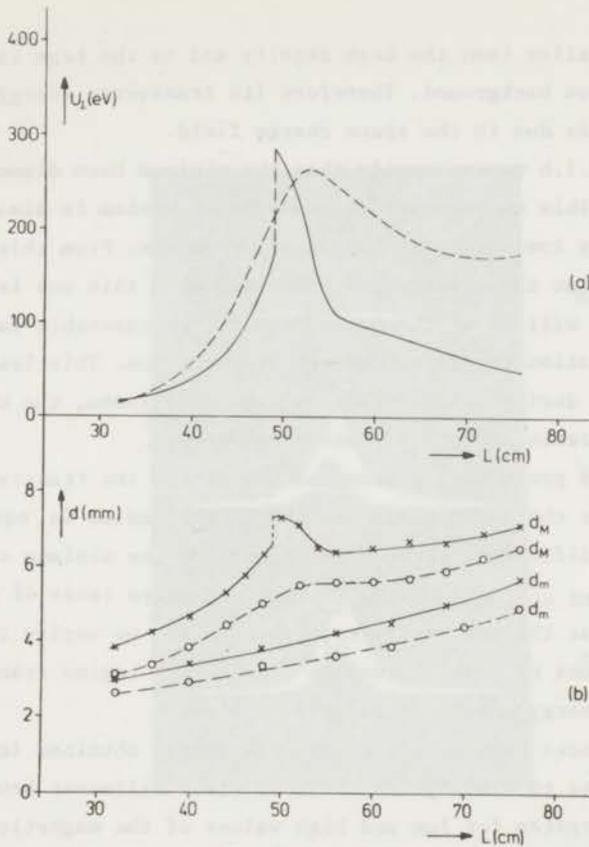


Fig. 7.1. - Final and minimum values of the beam diameter and the associated transverse energy as a function of L for two values of B . Conditions: $V_b = 1500$ V, $i_b = 16$ mA, $p = 4.8 \times 10^{-4}$ Torr. $\circ-\circ-\circ$ $B = 0.0540$ Wb m^{-2} ; $\times-\times-\times$ $B = 0.0325$ Wb m^{-2} .

pressure are kept constant in these measurements in which the main parameters are the interaction length L and the magnetic field B .

Figure 7.1.b presents the measured values of the beam diameter as a function of L for two values of the magnetic field. For each value of L we measured the maximum attained beam diameter as well as its minimum value. The minimum beam diameters were measured by adjusting the background pressure to an optimum value in the neighbourhood of 10^{-6} Torr. It was observed that for still lower values of the pressure the beam diameter increases again. This is possibly due to the fact that, for these rather low values of the pressure ($\sim 10^{-7}$ Torr), the plasma densi-

ty can become smaller than the beam density and so the beam is not neutralized by an ion background. Therefore its transverse energy can take appreciable values due to the space charge field.

In figure 7.1.b we can verify that the minimum beam diameter increases with L . This means that the beam-plasma system is always unstable, even at very low values of the Helium pressure. From this figure we can presume that the diameter of the beam, when this one is injected into the plasma, will be of the order of 2 mm, a reasonable value if we take in consideration the design of our electron gun. This leads to the conclusion that, during its interaction with the plasma, the beam acquires a considerable amount of transverse energy.

Figure 7.1.a presents the computed values for the transverse energy obtained under the assumption that the Larmor radius is equal to one half of the difference between the final and the minimum diameters of the beam, measured at the distance L . This procedure leads of course to minimum values for the transverse energy. Even so, we verify that, especially for values of L which lead to the 1st-2nd regime transition, the transverse energy can be as large as 285 eV.

The dependences on L of the transverse energy obtained in these two cases, permit also to distinguish the completely different behaviour of the beam-plasma system for low and high values of the magnetic field as referred to in chapter IV. Indeed the 1st-2nd regime transition has an abrupt character for low values of B and a continuous character for high values of B . Interesting is the result that the transverse energy in the second regime (high values of L) decreases substantially with L for low values of the magnetic field. We have thus verified that the transverse interaction between the electron beam and the plasma waves is more intense under conditions which lead to the regime transition in the plasma.

7.2.3. Correlated measurements of the transverse energy of the beam electrons at the 1st-2nd regime transition

We now present measurements obtained under the experimental conditions referred to in chapter V. This means that we are interested in the obtention of correlated measurements made at the 1st-2nd regime transition. The beam radial profiles show, under these circumstances, two well defined configurations. Using the correlation technique, described in sec-

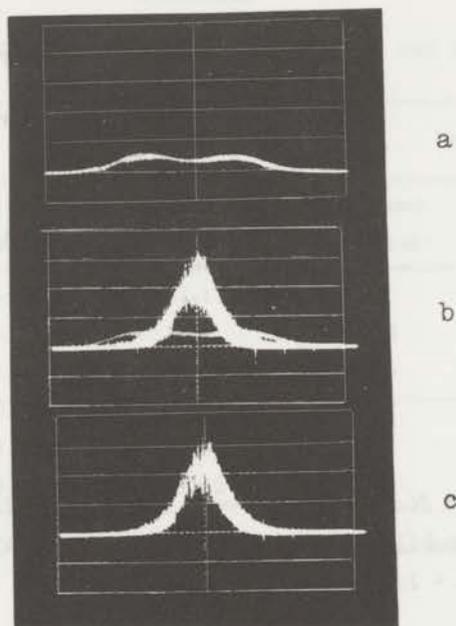


Fig. 7.2. - Example of a correlated measurement of the beam profile (Horizontal scale = 1 mm/div). a) correlated with the cyclotron instability; c) correlated with the plasma instability; b) superposition of both profiles. Conditions: $V_b = 1500$ V; $i_b = 8$ mA; $p = 5 \times 10^{-4}$ Torr; $L = 73$ cm.

tion 5.2, we could distinguish in the beam (figure 7.2) two states observed respectively when the electron plasma and the electron cyclotron instabilities are present.

With a series of similar measurements, made at other values of the magnetic field, we could obtain the results presented in figure 7.3. There we plotted the different values of the beam diameter as a function of the inverse of the magnetic field. For every value of B we determined the minimum value of the beam diameter as well as those obtained respectively in correlation with the plasma and the cyclotron instabilities.

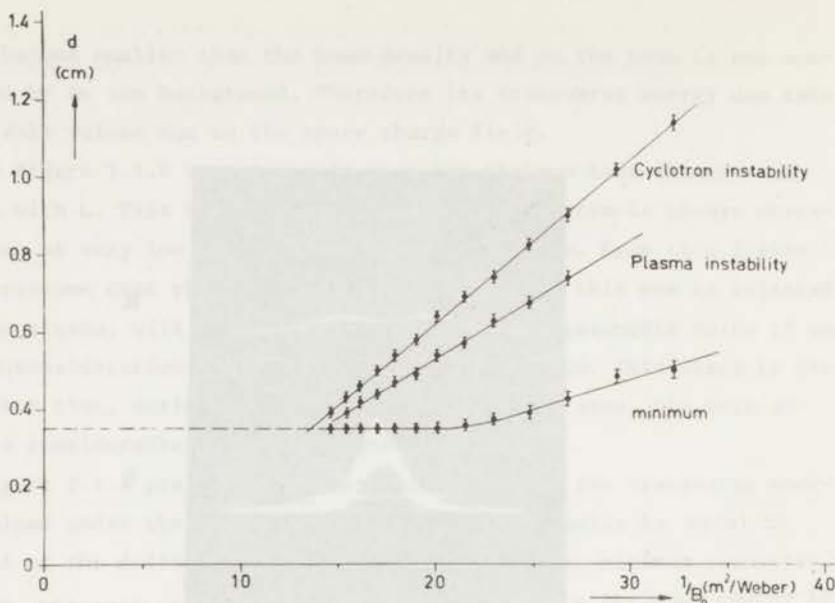


Fig. 7.3. - Beam diameters occurring during the plasma and the cyclotron instabilities. Conditions: $V_b = 1500$ V; $i_b = 8$ mA; $3.9 \times 10^{-4} \leq p \leq 5.4 \times 10^{-4}$ Torr; $L = 73$ cm.

The minimum beam diameters were again obtained by adjusting adequately the Helium pressure ($p \sim 10^{-6}$ Torr).

From figure 7.3 we can conclude:

- a) The minimum diameter remains practically constant for all values of the magnetic field;
- b) The largest beam diameter is attained during the bursts of the cyclotron instability;
- c) The diameters occurring during both instabilities show a linear increase with the inverse of the magnetic field.

According to our former assumptions, the electron Larmor radius is equal to one half of the difference between the final and the minimum beam diameters. Then, using equation (7.2) we arrive at the results presented in Table 7.1, where we can verify that, especially for the case of the excitation of the cyclotron instability, the beam electrons possess rather large transverse energies. This means that if a magnetic mirror would be applied to our experiment, it would be possible to build up a high temperature plasma directly from beam electrons. The formation

of plasmas with a high electron temperature is a well known characteristic of beam-plasma experiments in a magnetic bottle (SMULLIN, 1968).

TABLE 7.1

TRANSVERSE ENERGY OF THE BEAM ELECTRONS AT THE BEAM EDGE

B (10^{-4} Wb m $^{-2}$)	r_L (mm)		U_{\perp} (eV)	
	plasma instab.	cyclotr. instab.	plasma instab.	cyclotr. instab.
270	-	3.15	-	635
324	1.5	2.4	208	530
378	1.25	1.9	196	455
432	0.9	1.35	132	300
485	0.57	0.9	67	168
540	0.3	0.52	23	67
594	-	0.2	-	12

7.3. Measurement of the transverse energy at the beam centre

7.3.1. General considerations

Returning to figure 4.2 we can see that the first collector of the electrostatic energy analyser (plate 5) has also a hole ($\phi = 0.2$ mm) in its centre. Electrons which pass through this hole are then collected on the second collector (plate 6). The assembly of these two internal collectors can be moved into the transverse direction over a maximum distance of 9 mm. This transverse scan of the second hole of the analyser is accomplished by 200 turns of a motordriven axis equipped with a helipot for X-Y recording. This permits a very precise measurement of the "maximum" electron Larmor radius in a direct way. Indeed if we make a plot of the current collected on the second collector as a function of the radial distance r over which the assembly of the two collectors has been displaced, we obtain a curve peaked at $r = 0$ (figure 7.5) and decreasing with the modulus of r . The position $r = 0$ represents the situation in which the two holes of the analyser are aligned with the magne-

tic field lines and with the analyser's retarding field structure. However the leak current between the two collectors ($\sim 10^{-10}$ A), due to the applied potentials, is noisy and so it sets a limit to the accuracy of the measurements. For the determination of the "maximum" transverse energy we assume that we only collect electrons on the second collector if its current is at least a factor 2 higher than the value it has in the absence of the electron beam. Even so we still have a good accuracy in the measurements as this limiting current is always a factor $10^4 - 10^5$ smaller than the maximum collected current (measured at $r = 0$).

Now if we call r_M the distance from the axis at which the collected current decreases to its limiting value, then there must exist at least some electrons which possess a Larmor radius equal to

$$r_L = \frac{1}{2} (2r_M - \delta_1 - \delta_2) \quad (7.3)$$

where δ_1 and δ_2 are the diameters of the two holes on the analyser.

The reason for performing the measurements at the beam centre is that only there we expect rotational symmetry, which is a necessary condition for the validity of expression (7.3).

Our measurements were done with the axial retarding potential continuously swept (50 Hz) between - 100 V (to reflect the plasma electrons) and - 2000 V (to reflect all the electrons). In this way the helical electron path inside the analyser, which has a length of about 12 cm, varies periodically in pitch. Thus we can, in first approximation, expect that when the beam electrons arrive at the first collector (second hole) they will have the same probability of being at any particular position of their transverse circular orbit. This means that, no matter what their parallel velocity is, there will be some instants of time at which the beam electrons will strike the first collector at their maximum distance from the analyser's axis. This is an important point to stress, as without this sweeping technique the measurements of the "maximum" transverse energy would not be trustworthy.

The values of the transverse energy are then determined, by the knowledge of the Larmor radius (equation 7.3) and of the electron cyclotron frequency, according to equation (7.2).

7.3.2. Experimental results

We began by measuring the "maximum" transverse energy possessed by the beam electrons, as a function of the beam current, for several values of the magnetic field. Figure 7.4 presents the obtained results.

In this figure we can verify that:

- For all values of B , the transverse energy begins to increase with the beam current i_b , attains a maximum and then decreases with a further increase in the beam current
- The value of i_b associated with the maximum transverse energy is some 20% lower than the one corresponding to the so-called 1st-2nd regime transition.

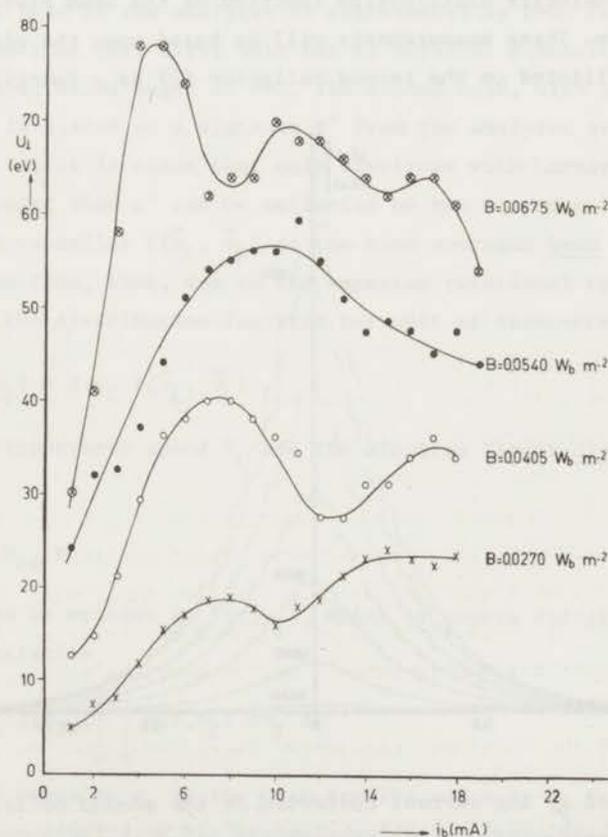


Fig. 7.4. - "Maximum" transverse energy of the beam electrons as a function of the beam current for different values of the magnetic field. Conditions: $V_b = 1500 \text{ V}$; $p = 4.8 \times 10^{-4} \text{ Torr}$; $L = 73 \text{ cm}$.

c) The higher the magnetic field the higher the transverse energy.

It was also verified that the dependences on the beam current of both the transverse energy and the total radiated microwave power (measured with a bolometer) are rather similar. Thus, the transverse energy is almost certainly related with the high frequency instabilities.

7.4. Determination of the 3-dimensional velocity distribution function of the beam electrons at the beam centre.

7.4.1. Theoretical considerations

Let us now try to derive an equation for the measurement of the 3-dimensional velocity distribution function of the beam electrons at the beam centre. These measurements will be based upon the plots of the current collected on the second collector (j) as a function of the

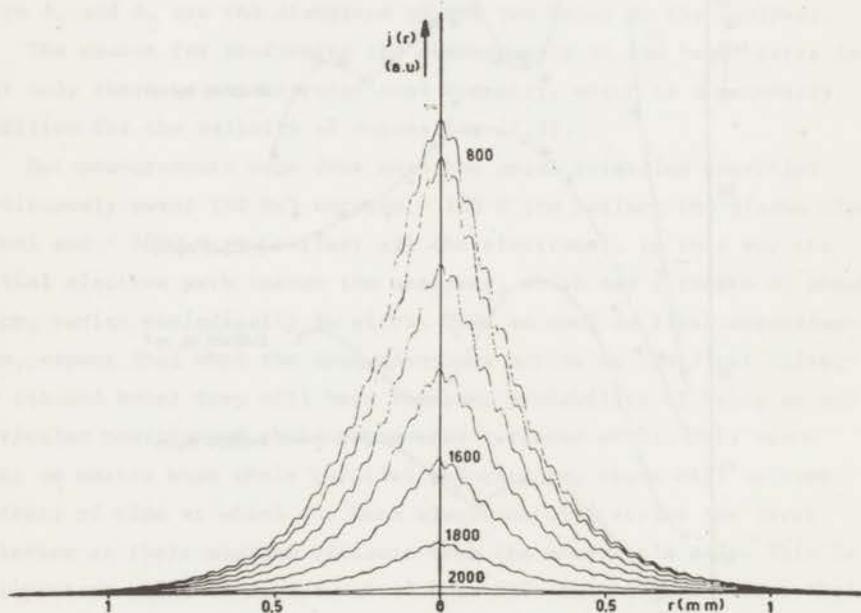


Fig. 7.5. - Plot of the current collected on the second collector as a function of r for different values of the fixed retarding potential in the analyser. This one is varied in steps of 200 V from -800 to -2000 V. Conditions: $V_b = 1500$ V; $i_{b2} = 17$ mA; $p = 4.5 \times 10^{-4}$ Torr; $L = 73$ cm. $B = 0.0675$ Wb m^{-2} .

radial distance (r) over which the collectors assembly is displaced. As we wrote before these plots are curves peaked at $r=0$ and decreasing with the modulus of r . Figure 7.5 presents some examples of these curves related with the measurement of the beam transverse velocity distribution function. The small ripple is due to the rotation of the axis of the driving mechanism of the collectors assembly (about 200 turns for a 9 mm displacement) and represents deviations of the order of 0.02 mm from the ideal rectilinear continuous movement of the analyser second hole. From identical curves we are now interested in obtaining an expression for the determination of the total velocity distribution.

In figure 7.6 we make a sketch of the projection on a transverse plane of some electron trajectories inside the analyser. The position of the first hole of the analyser is represented by $r=0$. For simplicity it is assumed that this first hole has no physical dimensions. So all electron trajectories begin at $r=0$. The second hole, with a diameter equal to δ , is placed at a distance r' from the analyser axis ($\delta \ll r'$). From figure 7.6 it is clear that only electrons with Larmor diameter equal or greater than r' can be collected on the second collector.

Now, if we define $f(\vec{v}_\perp, \vec{v}_\parallel)$ as the time averaged beam velocity distribution function, then, due to the expected rotational symmetry of our system, the distribution function per unit of transverse speed is

$$f(v_\perp, v_\parallel) = 2\pi v_\perp f(\vec{v}_\perp, \vec{v}_\parallel) \quad (7.4)$$

As the transverse speed v_\perp and the electron Larmor diameter r are related by

$$v_\perp = \frac{1}{2} \omega_{ce} r \quad (7.5)$$

$f(v_\perp, v_\parallel)$ can be written as $f(r, v_\parallel)$, which of course satisfies the normalization relation

$$n_b = n_o \frac{1}{2} \omega_{ce} \int_0^\infty \int_0^\infty f(r, v_\parallel) dv_\parallel dr \quad (7.6)$$

In this equation n_b is the beam density and $n_o = n_p + n_b$ is the total electron density of the beam-plasma system (sections 2.1 and 2.3.2). So, we have from (7.4) and (7.5)

$$f(r, v_\parallel) = \pi \omega_{ce} r f(\vec{v}_\perp, \vec{v}_\parallel) \quad (7.4.a)$$

We are now interested in obtaining an expression for the current density $j(r)$ based on the value of $f(r, v_{\parallel})$. This current density is made up of contributions from electrons with Larmor diameter equal or greater than r' . Let us then imagine that we have an annular slit centered at $r=0$ with an average radius equal to r' and a width equal to δ (figure 7.6).

For every trajectory (and this means for every pair of values of \vec{v}_{\perp} and \vec{v}_{\parallel}), the first condition for the entrance of the respective electron through the second hole of the analyser is that its intersection point with the plane of plate 5 (figure 4.2) will fall inside this slit. The probability for this to happen is, due to the formerly referred sweeping technique (modulation of \vec{v}_{\parallel}), simply given by

$$p_1 = \frac{2\Delta(r)}{\pi r} \quad (7.7)$$

where $2\Delta(r)$ is the portion of the electron transverse orbit comprised between $r' - \frac{\delta}{2}$ and $r' + \frac{\delta}{2}$. Now, due to rotational symmetry and because actually we do not have a slit but rather a hole with a diameter δ , there is another probability factor p_2 , for the electron passage through

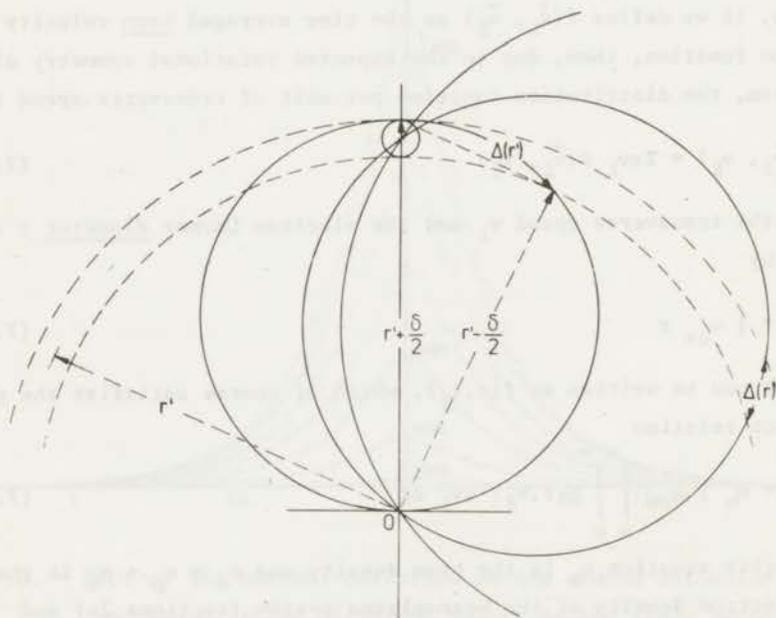


Fig. 7.6. - Projection on a transverse plane of some electron trajectories inside the analyser.

the hole, which is independent of its Larmor diameter. This one is

$$P_2 \approx \frac{\delta}{2 \pi r'} \quad (7.8)$$

Now we must analyse how do electrons with a certain axial energy contribute to the current measured at plate 6. We remember that the retarding potential in the analyser (plate 3) was continuously swept from -100 to -2000 V by a 50 Hz sinusoidal voltage. Then during a fraction $\alpha(U_{\parallel})$ of the sweeping period (20 ms), electrons can not reach the collector as they are reflected by the potential barrier of the analyser. $\alpha(U_{\parallel})$ is of course a decreasing function of U_{\parallel} . So we verify that fast electrons are favoured in relation to the slower ones, in what concerns the build up of the collected current, by two reasons: First, by the greater fraction of time in which they can be collected and second, simply because they are faster.

Under these circumstances, we can finally write the expression for the current density to be measured at a distance $r=r'$ from the analyser axis:

$$j(r') = \frac{\omega_{ce} n_0 e \delta}{2\pi r'} \int_{r'}^{\infty} \int_0^{\infty} \pi \omega_{ce} r f(\vec{v}_{\perp}, \vec{v}_{\parallel}) \frac{\Delta(r)}{\pi r} v_{\parallel} [1 - \alpha(v_{\parallel})] dv_{\parallel} dr \quad (7.9)$$

Without any prescription for the total velocity distribution function it is not possible to derive $f(\vec{v}_{\perp}, \vec{v}_{\parallel})$ from the knowledge of $j=j(r)$. Anyhow, if there is no correlation between the transverse and the axial velocities of the beam electrons, the total distribution can be written as a product of two terms (MORSE, 1969; SEIDL, 1970)

$$f(\vec{v}_{\perp}, \vec{v}_{\parallel}) = f(\vec{v}_{\perp}) \times f(\vec{v}_{\parallel}) \quad (7.10)$$

In this case we can simplify equation (7.9) to

$$j(r') = \frac{n_0 e \delta \omega_{ce}^2}{2\pi r'} \int_{r'}^{\infty} f(\vec{v}_{\perp}) \Delta(r) dr \times \int_0^{\infty} f(\vec{v}_{\parallel}) v_{\parallel} [1 - \alpha(v_{\parallel})] dv_{\parallel} \quad (7.11)$$

As the last integral is independent of r' , we obtain, by differentiation

$$\frac{d}{dr'} [r' j(r')] \sim \Delta(r') f(\vec{v}_{\perp})_{v_{\perp} = \frac{1}{2} \omega_{ce} r'} \quad (7.12)$$

Thus, we can determine the transverse distribution function if we

know $\Delta(r')$. Looking again at figure 7.6 we verify that $\Delta(r)$, which is approximately equal to δ for $r \gg r'$, increases when r approaches r' . When $r=r'$, $\Delta(r)$ will be of the order of

$$\delta(r') \approx (2r'\delta)^{\frac{1}{2}} \quad (7.13)$$

Thus, the final expression for the transverse velocity distribution function can be written, in general, as

$$f(\vec{v}_{\perp}) \sim r^{-\frac{1}{2}} \times \frac{d}{dr} [r \times j(r)] \quad (7.14)$$

We recall that expression (7.14) is only valid if the three fundamental assumptions are satisfied:

- 1) There is no correlation between \vec{v}_{\perp} and \vec{v}_{\parallel} .
- 2) The system is rotationally symmetric.
- 3) There is an equal probability to find the beam electrons at any particular position on their transverse circular orbit (sweeping technique).

A particular case of the first assumption (equation 7.10) is the case in which the beam is axially monoenergetic. In this case its distribution function can be written as

$$f(\vec{v}_{\perp}, \vec{v}_{\parallel}) = f(\vec{v}_{\perp}) \times \delta(\vec{v}_{\parallel} - \vec{v}_b) \quad (7.15)$$

where $\delta(\vec{v}_{\parallel} - \vec{v}_b)$ is a Dirac function, and so equation (7.14) is valid.

7.4.2. Experimental results

7.4.2.1. Proof that there is no correlation between the transverse and the axial beam velocities in strong second regime states of our beam-plasma system

Under our experimental conditions the beam usually shows rather large velocity spreads. So, the determination of its transverse velocity distribution function can not be obtained directly from the analysis of the plots of the total collected current as a function of r . Anyhow we still have the possibility to investigate if, under our experimental situation, the transverse velocity of the beam electrons is or is not correlated with their axial velocity. To this end we use the following technique: - We choose states of our beam-plasma system in which the

axial velocity spread is large (second regime states). Then we reflect from the analyser electrons with axial energies smaller than a certain value U_{\parallel} , without disturbing the contribution of the faster ones to the collected current. In other words, we are interested in having $\alpha(U_{\parallel}) = 1$ (permanent reflection) for $U < U_{\parallel}$ while keeping unchanged the values of $\alpha(U_{\parallel})$ for electrons with $U > U_{\parallel}$. This is simply done by applying to plate 2 (figure 4.2) a fixed negative potential V_{\parallel} , and operating plate 3 under the formerly referred manner (sweeping technique). The positive potential for reflection of the plasma ions is applied to plate 4. With this technique we cut from the collected current the contribution of electrons with $U < U_{\parallel}$ without changing the contribution of the faster ones.

This procedure leads to a family of curves with U_{\parallel} as parameter like in figure 7.5. In this figure U_{\parallel} was varied in steps of 200 eV. From this type of measurements we can determine the differential contribution to the total collected current arising from electrons with a well defined axial energy (between U_{\parallel} and $U_{\parallel} + \Delta U$). These differential plots represent the collected current originated by an almost axially monoenergetic beam of average energy equal to $U_{\parallel} + \frac{1}{2} \Delta U$.

So, we verify that, although we can not use expression (7.14) a priori to the total curve $j=j(r)$, at least we can apply it to the differential curves $\Delta j = \Delta j(r, U_{\parallel})$. We have normalized these last curves to the same level ($\Delta j(r=0) = Cte$), and we have presented them on a single graph as a function of r (figure 7.7). We see that the radial dependence of $\Delta j(r, U_{\parallel})$ is practically independent of U_{\parallel} . Therefore, as similar measurements made for other values of the magnetic field lead to the same conclusions, it seems that in our experiment the beam transverse velocity at the beam centre, is not correlated with its axial velocity.

In chapter 5, we explained the extension of the axial velocity spread at the 1st-2nd regime transition, in terms of trapping of the beam electrons in the cyclotron wave potential well. If this trapping mechanism is also valid for the second regime of the plasma, then why should indeed the transverse velocity of a particular electron depend on the phase of its trapping oscillatory movement, which as we verified has a period short compared to the electron transit time?! On the contrary, the experimental observation of a strong dependence of v_{\perp} on v_{\parallel} ,

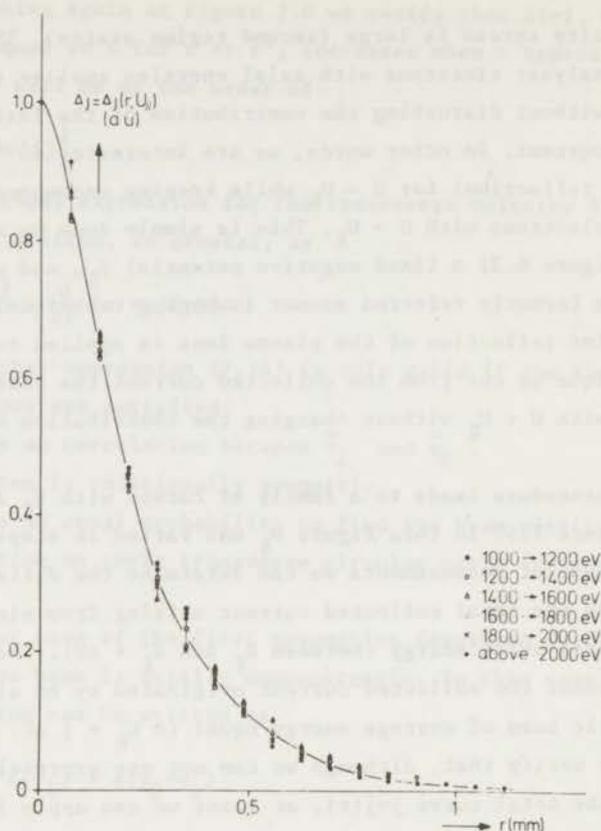


Fig. 7.7. - Proof that the transverse velocity distribution function is independent of the axial velocity. Conditions presented in figure 7.5.

as predicted by theory (SHAPIRO et al., 1968), would immediately lead to a severe criticism about the assumed trapping mechanism. These last measurements are therefore in agreement with the considerations made in chapters V and VI.

7.4.2.2. Quantitative results

In figure 7.7 we plotted six differential dependences of the type $\Delta_j = \Delta_j(r, U_{||})$. The curve traced on this figure represents the average variation of Δ_j with the Larmor diameter r . This curve permits the obtention of the beam transverse velocity distribution function. Indeed,

for each of the six dependences summarized by this single curve, the axial velocity was practically constant and equation (7.14) is therefore valid.

We verified that the so obtained distribution is constituted by a cold bulk of electrons and a hot tail which is found to be Maxwellian. With the conditions of figures 7.5 and 7.7, the temperature of the hot tail is as large as 31 eV and electrons are found with transverse energies of the order of 125 eV.

Similar measurements were done, as we wrote before, to other values of the magnetic field. We verified that the shape of the distribution function was in every case always the same, with the cold bulk of electrons and the hot Maxwellian tail. Figure 7.8 presents the obtained distribution functions for the case of $B = 0.0270 \text{ Wb m}^{-2}$, with the beam current as a parameter. This figure is quite representative of the behaviour of $f(\vec{v}_1)$ as a function of the beam current, and so we can conclude:

- The temperature of the hot tail begins to increase with i_b , reaches a maximum and then begins to decrease with a further increase on the beam current. This current dependence is similar to that of the "maximum" transverse energy (figure 7.4) and of the total radiated microwave power measured with a bolometer as referred to in section 7.3.2. Therefore we see that the transverse temperature is directly related with the average (time integrated) electrostatic energy of the beam-plasma waves.

- The ratio ξ between the density of heated electrons and their total density increases however monotonically with the beam current. This ratio seems to be related with the percentage of time occupied by the beam-plasma instabilities, which as we know appear in bursts. ξ varies from the small value of 3.8%, shown in figure 7.8, up to 45% for $B = 0.054 \text{ Wb m}^{-2}$ and $i_b = 20 \text{ mA}$. In this last case, fast analysis of the r.f. signals coming from the probes reveal that the time is almost filled with instabilities. On the contrary, in the case of low magnetic field (small ξ) instabilities are very few and well defined in time (isolated bursts) and most of the time the plasma is silent.

- The temperature of the cold bulk of particles is always very low, in the range 0.5 - 4 eV.

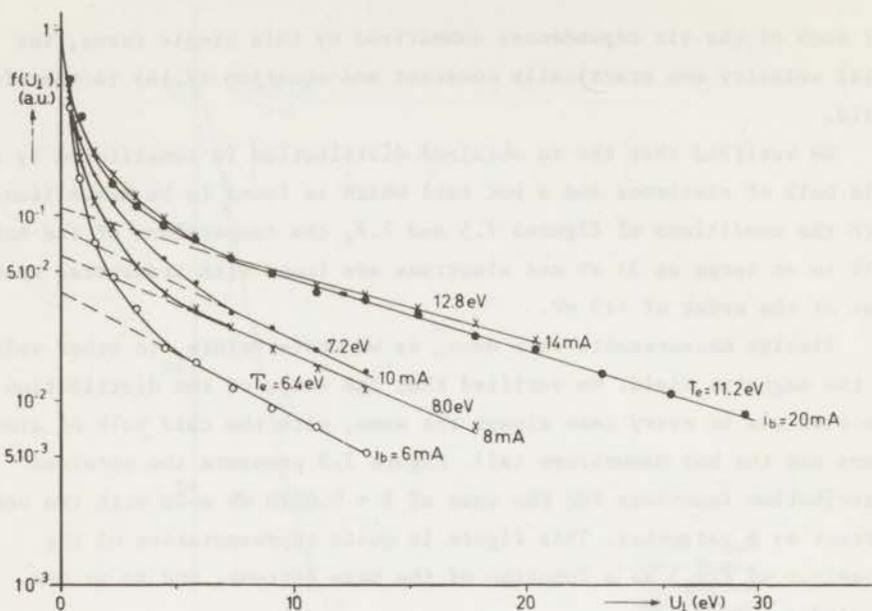


Fig. 7.8. - The influence of the beam current on the transverse velocity distribution function of the beam electrons for a given value of the magnetic field. Conditions: $V_b = 1500$ V; $B = 0.027$ Wb m^{-2} ; $p = 4.8 \times 10^{-4}$ Torr; $L = 73$ cm.

- The fact that we find Maxwellian distributions probably reveals the stochastic nature of beam-plasma instabilities. Indeed the amplitude of the beam-plasma instabilities (bursts) seems to be randomly distributed in time (LAVROVSKII et al., 1970). As the measurements of the transverse energy were heavily time integrated ($RC \sim 1$ ms), the obtained distributions are averages taken over many instabilities as well as over various amplitudes.

- At last we notice that the transverse temperatures of the beam electrons, although of the same order of magnitude, usually seem to be larger than the temperatures of the plasma electrons when measured under similar conditions (Table 4.1).

- The numerical results obtained for other values of the magnetic field are summarized in Table 7.2, where we can verify that both ξ and the transverse temperature increase with the magnetic field.

TABLE 7.2

TRANSVERSE TEMPERATURE OF THE BEAM ELECTRONS AT THE BEAM CENTRE

B	i_b	ξ	T
(10^{-4} Wb m $^{-2}$)	(mA)	(%)	(eV)
270	6	3.8	6.4
270	8	6.0	8.0
270	10	8.4	7.2
270	14	10.4	12.8
270	20	11.0	11.2
405	8	6.6	20.5
405	20	17.5	15.6
540	8	20.0	20.7
540	20	45.0	22.2
675	17	27.2	31.0

7.5. Conclusions

From the presented results we can verify that the electron beam acquires a considerable amount of transverse energy during the interaction with its own created plasma. Indeed we were able to observe in our experiment the presence of electrons with transverse energy as high as 635 eV.

Especially for the case of the lower values of the magnetic field, the transverse energy is seen to be much larger at the beam edge than at the beam centre. In section 5.4 we mentioned the fact that theory predicts radial variations of the electric field of the instabilities according to a J_0 Bessel function for the axial field and to a J_1 Bessel function for the transverse field. In chapter V we could present measurements which sustain the hypothesis of the existence of a J_0 Bessel function dependence of E_{\parallel} on the radius. In this chapter we could only observe that the transverse energy is rather small at the beam centre and that it can attain large values at the beam edge. These results are therefore in qualitative agreement with theory and we can expect that E_{\perp} will have a dependence on the radius which will not differ much from a J_1 Bessel function. These results are in good agreement with those published by EGOROV et al. (1970), who also verified

that the axial electric field has a maximum at the axis of the plasma column and that the transverse electric field has the maximum close to the boundary of the plasma waveguide.

At the beam centre, we could determine the transverse velocity distribution function. We verified that the distribution is a monotonically decreasing function of the transverse velocity. According to SEIDL (1970), this is a sufficient condition for the excitation of the Anomalous Doppler effect instabilities. Therefore we can relate the acquisition of transverse energy by the beam electrons to the excitation of these instabilities.

We have also verified that, at the beam centre, there is no correlation between the transverse and the axial velocity of the beam electrons. Thus, we think that the axial velocity spread in the beam is determined by the intensity of the Cerenkov instabilities, which eventually can originate the trapping of a fraction of the beam in the wave potential well. Accordingly, we also think that the transverse energy of the beam electrons is directly related with the excitation of Anomalous Doppler effect instabilities. Presumably, during its passage through the interaction chamber, a beam electron can experience the effects due to the excitation of these two types of instabilities.

In section 3.8 we referred to a paper by SHAPIRO and SHEVCHENKO (1968), in which it is theoretically predicted that the acquisition of transverse energy by the beam electrons should be accompanied by a decrease in their axial energy. We verify that this is in contradiction with our experimental observations made at the beam centre. However, at the beam edge, our results are in agreement with this theoretical study as we verified (figure 5.8) that the electrons found outside the minimum beam diameter always experienced an axial deceleration. We therefore conclude that, in the regions of the beam in which the transverse electric field is supposed to be large (beam edge), there is indeed a conversion of axial into transversal energy. This process of energy conversion is presumably not a straightforward one. The beam electrons can, for example, lose axial energy to the build up of the Cerenkov instabilities, which in turn can change the beam-plasma parameters in a way which permits the excitation of the Anomalous Doppler effect instabilities. Finally, these last instabili-

ties can give back to the beam electrons a fraction of the energy lost before, now under the form of transverse energy.

Concluding we can remind that the observed variation in the beam diameter can lead to an appreciable change of the growthrate of the different instabilities (SEIDL, 1970), and so it can be related to the quick alternation of the different beam-plasma instabilities.

Finishing this study it is interesting to mention that the transverse energy distribution function of the plasma ions, measured by FUMELLI et al. (1969), in a Penning Discharge in a magnetic bottle, has precisely the same shape as the distributions presented by us in figure 7.8. The temperature of the hot tail also increases with the magnetic field, but, opposite to our results, the percentage of heated particles ξ decreases with B.

REFERENCESCHAPTER I

- AKHIEZER, A.I., FAINBERG, Ya.B. (1949); Dokl.Akad.Nauk.SSSR 64, 555
(1951) JETP 21, 1262.
- BOHM, D., GROSS, E.P. (1949); Phys.Rev. 75, 1851, 1964.
- BOHM, D., GROSS, E.P. (1950); Phys.Rev. 79, 992.
- CRAWFORD, F.W., KINO, G.S. (1961); Proc.IRE 49, 1767.
- CRAWFORD, F.W. (1965); Nuclear Fusion 5, 73.
- DRUMMOND, W.E., PINES, D. (1962); Nucl.Fusion Suppl.Part 3, 1049.
- DUSHIN, L.A., KUZNETSOV, Yu.K., PAVLICHENKO, O.S. (1969); Soviet Phys. Techn.Phys. 13, 1030.
- EINAUDI, F., SUDAN, R.N. (1969); Plasma Physics 11, 359.
- FAINBERG, Ya.B. (1968); Czechoslovak J.Phys. B18, 652.
- FEDORCHENKO, V.D., MURATOV, V.I., RUTKEVICH, B.N. (1967); Soviet Phys. Techn.Phys. 11, 1462.
- GABOVICH, M.D., PASECHNIK, L.L. (1959); Soviet Phys. JETP 9, 727.
- HOPMAN, H.J. (1969); Invited Lecture - 9th Int.Conf.Phen.Ionized Gases, Bucharest - To be published.
- JANCARIK, J., KOPECKY, V., PIFFL, V., POHANKA, J., PREINHAELTER, J., SEIDL, M., SUNKA, P., ULLSCHMIED, J. (1969) - "Plasma Physics and Controlled Nuclear Fusion Research", Vienna, 733.
- KADOMTSEV, B.B., POGUTSE, O.P. (1970); Internat.Centre for Theoret.Phys. - Miramare-Trieste - Repport IC/70/45.
- KADOMTSEV, B.B., POGUTSE, O.P. (1970); Phys.Rev.Letters 25, 1155.
- KHARCHENKO, I.F., FAINBERG, Ya.B., NIKOLAEV, R.M., KORNILOV, E.A., LUTSENKO, E.I., PEDENKO, N.S. (1960); Soviet Phys. JETP 11, 493.
- KHARCHENKO, I.F., FAINBERG, Ya.B., NIKOLAEV, R.M., KORNILOV, E.A., LUTSENKO, E.I., PEDENKO, N.S. (1962); Soviet Phys. Techn.Phys. 6, 551.
- KLIMONTOVICH, Yu.L. (1959); Soviet Phys. JETP 9, 999.
- KOGAN, M.I., SAKHAROV, I.E. (1968); Soviet Phys. Techn.Phys. 12, 1599.
- KRIVORUCHKO, S.M., MEDVEDEV, Yu.V. (1968); Soviet Phys. Techn.Phys. 13, 61.
- LANGMUIR, I. (1925); Phys.Rev. 26, 585.
- LANGMUIR, I., TONKS, L. (1929); Phys.Rev. 33, 195.

- LEVITSKII, S.M., SHAPOVAL, V.Z., SHASHURIN, I.P. (1969); Soviet Phys. Techn.Phys. 14, 343.
- MALMBERG, J.H., WHARTON, C.B., GOULD, R.W., O'NEIL, T.M. (1968); Phys. Fluids, 11, 1147.
- MERRILL, H.J., WEBB, H.W. (1939); Phys.Rev. 55, 1191.
- MIKHAILOVSKII, A.B., JUNGWIRTH, K. (1966); Soviet Phys. JETP 23, 689.
- NEIDIGH, R.V., ALEXEV, I., GUEST, G.E., JONES, V.D., MONTGOMERY, D.C., ROSE, D.J., STIRLING, W.L. (1969); "Plasma Physics and Controlled Nuclear Fusion Research", I.A.E.A., Vienna, 693.
- NEZLIN, M.V., SAPOZHNIKOV, G.I., SOLNTSEV, A.M. (1966); Soviet Phys. JETP 23, 232.
- PENNING, F. (1926); Physica 6, 241.
- PIERCE, J.R. (1948); J.Appl.Phys. 19, 231.
- ROMANOV, Yu.A., FILIPOV, G.F. (1961); Soviet Phys. JETP 13, 87.
- SHAPIRO, V.D., SHEVCHENKO, V.I. (1962); Soviet Phys. JETP 15, 1053.
- SMULLIN, L.D., GETTY, W.D. (1966); Proc.Conf.Plasma Phys.Contr.Nuclear Fusion Research, I.A.E.A., Vienna, II, 815.
- VEDENOV, A.A., VELIKHOV, E., SAGDEEV, A. (1962); Nucl.Fusion Suppl.Part 2, 465.

CHAPTER II

- ALLIS, W.P. (1967)-(1958); "Electrons, Ions and Waves" - M.I.T., 269.
- BRIGGS, R.J. (1964); "Electron stream interaction with plasmas" - M.I.T., 17, 48.
- DAWSON, J. (1961); Phys.Fluids 4, 869.
- DELCROIX, J.L. (1963); "Physique des Plasmas" - Dunod, 126, 177.
- KLIMONTOVICH, Yu.L. (1967); "The statistical theory of non-equilibrium processes in a plasma" - M.I.T., 88, 99.
- LANDAU, L. (1946); Journal of Physics, USSR 10, 25.
- PENROSE, O. (1960); Physics of Fluids, 3, 258.
- SAGDEEV, R.Z., GALEEV, A.A. (1969); "Non-linear plasma theory" - W.A. Benjamin Inc., 37.
- SIMON, A. (1965); Plasma Physics IAEA - Vienna, 163, 175, 181.
- STIX, T.H. (1962); "The theory of plasma waves"- McGraw-Hill, 143.
- VAN KAMPEN, N.G. (1955); Physica 21, 949.
- VAN KAMPEN, N.G., FELDERHOF, B.U. (1967); "Theoretical Methods in Plasma Physics" - North-Holland Publ.Comp., 153.

CHAPTER III

- AL'TSHUL', L.M.; KARPMAN, V.I. (1966) Soviet Phys. JETP 22, 361.
- BASS, F.G.; FAINBERG, Ya.B.; SHAPIRO, V.D. (1966) Soviet Phys. JETP 22, 230.
- BERNSTEIN, I.B.; ENGELMANN, F. (1966) Phys.Fluids 9, 937.
- BREIZMAN, B.N.; RYUTOV, D.D. (1970) Soviet Phys. JETP 30, 759.
- BRIGGS, R.J. (1964) Electron-Stream Interaction with Plasmas, M.I.T. 47.
- CARNEVALE, M.; CROSIGNANI, B.; ENGELMANN, F. (1967) Phys.Fluids 10, 436.
- DAWSON, J. (1965) Phys.Fluids 4, 869.
- DRUMMOND, W.E.; PINES, D. (1962) Nucl.Fusion Suppl., Part 3, 1049.
- DRUMMOND, W.E. (1964) Phys.Fluids 7, 816.
- EINAUDI, F.; SUDAN, R.N. (1969) Plasma Physics 11, 359.
- FAINBERG, Ya.B.; SHAPIRO, V.D. (1965) Soviet Phys. JETP 20, 937.
- FAINBERG, Ya.B.; SHAPIRO, V.D.; SHEVCHENKO, V.I. (1970) Soviet Phys. JETP 30, 528.
- IVANOV, A.A.; RUDAKOV, L.I. (1967a) Soviet Phys. JETP 24, 1027.
- IVANOV, A.A.; MARKEEV, B.M.; RUDAKOV, L.I. (1967b) Soviet Phys. JETP 25, 389.
- KADOMTSEV, B.B. (1965) Plasma turbulence, Academic Press London, 15.
- KLOZENBEG, J.P.; BERNSTEIN, I.B. (1970) Journal of Plasma Physics, vol. 4, part 3, 595.
- KOVRIZHNYKH, L.M. (1967) Soviet Phys. JETP 24, 608.
- ROWLANDS, J.; SHAPIRO, V.D.; SHEVCHENKO, V.I. (1966) Soviet Phys. JETP 23, 651.
- RYUTOV, D.D. (1967) Soviet Phys. JETP 25, 916.
- RYUTOV, D.D. (1970) Soviet Phys. JETP 30, 131.
- SAGDEEV, R.Z.; GALEEV, A.A. (1969) Nonlinear Plasma Theory, W.A. Benjamin Inc., New York, 37.
- SEIDL, M. (1970) Phys.Fluids 13, 966.
- SHAPIRO, V.D.; SHEVCHENKO, V.I. (1962) Soviet Phys. JETP 15, 1053.
- SHAPIRO, V.D. (1963) Soviet Phys. 17, 416.
- SHAPIRO, V.D.; SHEVCHENKO, V.I. (1968) Soviet Phys. JETP 27, 635.
- SIZONENKO, V.L.; STEPANOV, K.N. (1966) Soviet Phys. JETP 22, 832.
- STIX, T.H. (1962) The Theory of Plasma Waves, McGraw-Hill, New York, 137.

- VEDENOV, A.A., VELIKHOV, E., SAGDEEV, A. (1962); Nucl.Fusion Suppl. part 2, 465.
- VEDENOV, A.A., VELIKHOV, E.P. (1963); Soviet Phys. JETP 16, 682.
- VEDENOV, A.A. (1967); "Reviews of Plasma Physics", Leontovich (editor), New York, Vol.3, 229.
- VÖLK, H.J. (1967); Phys.Fluids 10, 2629.
- WHARTON, C.B., MALMBERG, J.H., O'NEIL, T.M. (1968); Phys.Fluids 11, 1761.
- ZASLAVSKII, G.M., FILONENKO, N.N. (1968); Soviet Phys. JETP 25, 851.

CHAPTER IV

- APEL, J.R. (1969.a); Phys.Fluids 12, 291.
- APEL, J.R. (1969.b); Phys.Fluids 12, 640.
- ARTEMOV, V.M., LEONT'EV, N.I., TIMOSHENKO, A.P., UDOVICHENKO, Yu.K. (1968); Soviet Phys. Techn.Phys. 12, 1615.
- ASTRELIN, V.T., BUCHELNIKOVA, N.S., KUDRYAVTSEV, A.M. (1969); 3rd Europ. Conf.Control.Fusion - Plasma Physics, Utrecht, 92.
- BEREZIN, A.K., BEREZINA, G.P., BOLOTIN, L.I., FAINBERG, Ya.B. (1964); Plasma Physics 6, 173.
- BRIGGS, R.J. (1964); "Electron stream interaction with plasmas" - M.I.T.
- BUCHSBAUM, S.J., MOWER, L., BROWN, S.C. (1960); Phys.Fluids 3, 806.
- BUCHSBAUM, S.J., MOWER, L., BROWN, S.C. (1962); Phys.Fluids 5, 1545.
- CABRAL, J.A., HOPMAN, H.J., VAN WAKEREN, J.H.A. (1969); 9th Int.Conf. Phenom.Ionized Gases, Bucharest, 559.
- ETIEVANT, C. (1964); Report CEA-R 2456, Fontenay-aux-Roses.
- HOPMAN, H.J., MATITTI, T., KISTEMAKER, J. (1968); Plasma Physics 10, 1051.
- HOPMAN, H.J., CABRAL, J.A. (1969); "Nonlinear Effects in Plasmas", Kalman and Feix (editors), 503.
- HOPMAN, H.J. (1969); "The electron cyclotron instability in a beam-plasma system", Thesis, Amsterdam.
- IVANOV, A.A., RUDAKOV, L.I. (1967); Soviet Physics JETP 24, 1027.
- JANKARIC, J., KOPECKY, V., PIFFL, V., POHANKA, J., PREINHAELTER, J., SEIDL, M., SUNKA, P., ULLSCHMIED, J. (1969); Plasma Physics and Controlled Nuclear Fusion Research, IAEA, Vienna, 733.
- KHARCHENKO, I.F., FAINBERG, Ya.B., KORNILOV, E.A., PEDENKO, N.S. (1964); Soviet Phys. Techn.Phys. 9, 798.
- KOGAN, M.I., SHAKHAROV, I.E. (1968); Soviet Phys. Techn.Phys. 12, 1599.

- LEVITSKII, S.M., SHASHURIN, I.P. (1966); Sov.Phys. Techn.Phys. 10, 915.
- LEVITSKII, S.M., SHASHURIN, I.P. (1967.a); Sov.Phys. Techn.Phys. 11, 1018.
- LEVITSKII, S.M., SHASHURIN, I.P. (1967.b); Sov.Phys. JETP 25, 227.
- LEVITSKII, S.M., SHASHURIN, I.P. (1967.c); 8th Int.Conf.Phenom.Ionized Gases, Vienna, 382.
- LEVITSKII, S.M., SHASHURIN, I.P. (1969); 9th Int.Conf.Phenom.Ionized Gases, Bucharest, 566.
- MALMBERG, J.H., WHARTON, C.B. (1969); Phys.Fluids 12, 2600.
- MORSE, D.L. (1969); Plasma Physics 11, 175.
- RYUTOV, D.D. (1970); Sov.Phys. JETP 30, 131.
- SEIDL, M., SUNKA, P. (1967); Nuclear Fusion 7, 237.
- SEIDL, M. (1970); Phys.Fluids 13, 966.
- SHAPIRO, V.D., SHEVCHENKO, V.I. (1962); Sov.Phys. JETP 15, 1053.
- SHASHURIN, I.P. (1967); Soviet Phys. JETP Letters 6, 245.
- SHUSTIN, E.G., POPOVICH, V.P., KHARCHENKO, I.F. (1969); Sov.Phys. Techn. Phys. 14, 745.
- SMULLIN, L.D., GETTY, W.D. (1962); Phys.Review Letters 9, 3.
- VERMEER, A., HOPMAN, H.J., MATITTI, T., KISTEMAKER, J. (1966); 7th Int. Conf.Phenom.Ionized Gases, Belgrade, Vol.2, 386.
- VERMEER, A. (1968); "Excitation of ion oscillations by beam-plasma interaction", Thesis, Delft.

CHAPTER V

- APEL, J.R. (1969.a); Phys.Fluids 12, 291.
- APEL, J.R. (1969.b); Phys.Fluids 12, 640.
- BOTTIGLIONI, F. (1969); 3rd Europ.Conf.Contr.Fusion and Plasma Phys., Symp. Beam-Plasma Interactions, Utrecht, 24.
- CABRAL, J.A., HOPMAN, H.J., INSINGER, F.G., OTT, W. (1969.a); "Plasma Physics and Controlled Nuclear Fusion Research", IAEA, Vienna, 749.
- CABRAL, J.A., HOPMAN, H.J., VITALIS, F. (1969.b); 9th Int.Conf.Phenom. Ionized Gases, Bucharest, 553.
- CABRAL, J.A., HOPMAN, H.J. (1970); Plasma Physics 12, 759.
- DAWSON, J.M., SHANNY, R. (1968); Phys.Fluids 11, 1506.
- EGOROV, A.M., KIVSHIK, A.F. (1970); Sov.Phys. Techn.Phys. 15, 392.
- FEDORCHENKO, V.D., MURATOV, V.I., RUTKEVICH, B.N. (1967); Sov.Phys. Techn.Phys. 11, 1462.

- FRANK, R. (1968); Nucl.Fusion 8, 351.
- HOPMAN, H.J., OTT, W. (1968.a); Plasma Physics 10, 315.
- HOPMAN, H.J., MATITTI, T., KISTEMAKER, J. (1968.b); Plasma Physics 10, 1051.
- JANCARIK, J., PIFFL, V., SEIDL, M., ULLSCHMIED, J. (1969); 3rd Europ. Conf.Contr.Fusion Plasma Phys. - Symp. Beam-Plasma Interactions, Utrecht, 28.
- LEVITSKII, S.M., SHAPOVAL, V.Z., SHASHURIN, I.P. (1969); Sov.Phys. Techn.Phys. 14, 343.
- NEZLIN, M.V., SAPOZHNIKOV, G.I., SOLNTSEV, A.M. (1966); Sov.Phys. JETP 23, 232.
- O'NEIL, T. (1965); Phys.Fluids 8, 2255.
- SEIDL, M., SUNKKA, P. (1967); Nuclear Fusion 7, 237.
- STIX, T.H. (1962); "The Theory of Plasma Waves" - McGraw-Hill, New York, 137.
- VAN WAKEREN, J.H.A., HOPMAN, H.J., CABRAL, J.A. (1969); 9th Int.Conf. Phenom.Ionized Gases, Bucharest, 571.
- VERMEER, A., MATITTI, T., HOPMAN, H.J., KISTEMAKER, J. (1967); Plasma Physics, 9, 241.
- WHARTON, C.B., MALMBERG, J.H., O'NEIL, T.M. (1968); Phys.Fluids 11, 1761.

CHAPTER VI

- BAILEY, V.L., DENAVIT, J. (1970); Phys.Fluids 13, 451.
- BARTLETT, C.J. (1968); Phys.Fluids 11, 822.
- BEST, R.W.B. (1968); Physica 40, 182.
- CABRAL, J.A., HOPMAN, H.J., VITALIS, F. (1969); 9th Int.Conf.on Phenom. in Ionized Gases, Bucharest, 553.
- DAWSON, J.M., SHANNY, R. (1968); Phys.Fluids 11, 1506.
- DRUMMOND, W.E., MALMBERG, J.H., O'NEIL, T.M., THOMPSON, J.R. (1970); Phys.Fluids 13, 2422.
- ELDRIDGE, O. (1970); Phys.Fluids 13, 738.
- GASHEVSKI, V.A., KOVTUN, R.I. (1969); 9th Int.Conf.on Phenom. in Ionized Gases, Bucharest, 568.
- IVANOV, A.A., RUDAKOV, L.I. (1967); Soviet Phys. JETP 24, 1027.

- KRUEER, W.L., DAWSON, J.M., SUDAN, R.N. (1969); Plasma Physics Laboratory, Princeton University, Report MATT-725.
- LAVROVSKY, V.A., DEYEV, V.M., ROGASHKOV, S.A., YAREMENKO, Yu.G., KHARCHENKO, I.F. (1967); 8th Int.Conf.on Ionized Gases, Vienna, 375.
- LAVROVSKY, V.A., DEEV, V.M., ROGASHKOV, S.A., YAREMENKO, Yu.G., KHARCHENKO, I.F. (1970); Sov.Phys. Techn.Phys. 14, 1190.
- LEVITSKY, S.M., SHASHURIN, I.P. (1967); Sov.Phys. Techn.Phys. 11, 1018.
- LEVITSKY, S.M., NURIEV, K.Z. (1970); JETP Letters 12, 119.
- LYAMOV, V.E., SAPOGIN, L.G. (1968); Soviet Phys. Techn.Phys. 12, 449.
- O'NEIL, T. (1965); Phys.Fluids 8, 2255.
- RAND, S. (1968); Phys.Fluids 11, 1168.
- SHAPIRO, V.D., SHEVCHENKO, V.I. (1970); Sov.Phys. JETP 30, 1121.
- WHARTON, C.B., MALMBERG, J.H., O'NEIL, T.M. (1968); Phys.Fluids 11, 1761.
- YAREMENKO, Yu.G., DEEV, V.M., EREMIN, S.M., KOVTUN, R.I., KHARCHENKO, I.F. (1969); 9th Int.Conf.Phenom.Ionized Gases, Bucharest, 580.
- YAREMENKO, Yu.G., DEEV, V.M., EREMIN, S.M., KHARCHENKO, I.F. (1970); Sov.Phys. Techn.Phys. 14, 1158.
- ZASLAVSKII, G.M., FILONENKO, N.N. (1968); Sov.Phys. JETP 25, 851.

CHAPTER VII

- CABRAL, J.A., HOPMAN, H.J., INSINGER, F.G., OTT, W. (1969); "Plasma Physics and Controlled Nuclear Fusion Research", IAEA, Vienna, 749.
- CABRAL, J.A., HOPMAN, H.J., VAN WAKEREN, J.H.A. (1970); "Fourth Europ. Conf.on Controlled Fusion and Plasma Physics", Rome, 69.
- FUMELLI, M., DEI-CAS, R., GIRARD, J.P., VALCKX, F.P.G. (1969); 3rd Europ.Conf.Controlled Fusion and Plasma Phys. - Symp.Beam-plasma Interactions, Utrecht, 112.
- KHARCHENKO, I.F., FAINBERG, Ya.B., NIKOLAEV, R.M., KORNILOV, E.A., LUTSENKO, E.I., PEDENKO, N.S. (1962); Sov.Phys. Techn.Phys. 6, 551.
- LAVROVSKII, V.A., DEEV, V.M., ROGASHKOV, S.A., YAREMENKO, Yu.G., KHARCHENKO, I.F. (1970); Sov.Phys. Techn.Phys. 14, 1190.
- MORSE, D.L. (1969); Plasma Physics 11, 175.
- SCHUSTIN, E.G., POPOVICH, V.P., KHARCHENKO, I.F. (1969); 9th Int.Conf. on Phenomena in Ionized Gases, Bucharest, 565.
- SEIDL, M. (1970); Phys.Fluids 13, 966.
- SMULLIN, L.D., GETTY, W.D. (1962); Phys.Review Letters 9, 3.

SMULLIN, L.D. (1968); 8th Int.Conf.on Phenomena in Ionized Gases,

Invited papers, IAEA, Vienna, 129.

SHAPIRO, V.D., SHEVCHENKO, V.I. (1962); Soviet Phys. JETP 15, 1053.

SHAPIRO, V.D., SHEVCHENKO, V.I. (1968); Soviet Phys. JETP 27, 635.

SUMMARY

We begin this thesis by giving, in chapter I, a short survey of the development of the theory of beam-plasma interaction as well as of the most salient aspects of the experimental research on this subject.

Chapter II is a review of the linear theory of plasma oscillations. A dispersion equation is derived for pure longitudinal electrostatic oscillations in an infinite and homogeneous collisionless plasma. Particular solutions of the dispersion equation are analysed. Namely, we establish the unstable character of beam-plasma systems and we consider the problem of Landau damping. The damping (or growth) rate of the plasma oscillations is then related with the velocity gradient of the distribution function of the plasma electrons. The existence of unstable states is predicted and a criterium for instability is presented.

In chapter III we treat the quasilinear approximation in the dynamics of a collisionless plasma. The quasilinear equations are deduced following A.A. Vedenov, and applied to the study of the development of the velocity space instabilities. The conditions of applicability of the theory are analysed. The problem of the adiabatic diffusion of the nonresonant electrons is considered. We also obtain an estimate for the relaxation time of the quasilinear interaction process. Finally a review of the recent development of the quasilinear theory is made, and three publications are analysed with some detail, as they make a bridge between the exposed theory and our experimental situation.

In chapter IV a short description of our beam-plasma experiment and of some conventional diagnostic methods is made. A dispersion diagram for the beam-plasma waves is presented and the most important instabilities are theoretically identified. Varying the length of the interaction chamber, while keeping the other external parameters constant, we simulate the spatial development of the beam-plasma instabilities. We verify that the increase in the interaction strength is accompanied by an increase in the beam velocity spread, in the width of the excited spectrum of oscillations and in the plasma density. These variations in the beam-plasma internal parameters characterize the passage of the plasma from a weak first regime to a deep second regime. The 1st-2nd regime transition occurs abruptly for low values of the magnetic field and smoothly for higher values of B. In the latter case an

exponential spatial increase of the total radiated microwave power of the beam-plasma oscillations is observed (convective instabilities). For the case of low values of B the radiated power remains practically constant along the interaction chamber. It is verified that the general evolution of the interaction does not depend on the way by which we increase its strength. A typical evolution of the beam axial velocity spread as well as of the excited spectrum of oscillations is described. The temperature of the plasma electrons is measured. Finally, we compare the obtained results with the predictions of the quasilinear theory of beam-plasma interaction. The plateau of the beam velocity distribution function and the value of the relaxation length for the interaction are results which are in good agreement with theoretical predictions.

In chapter V the 1st-2nd regime transition is studied as a function of the axial magnetic field. The beam-plasma system is characterized by time resolved measurements of the excited frequency spectrum, plasma density and beam axial velocity spread. These parameters show strong fluctuations with a repetition frequency of about 30 KHz. Correlation measurements permit us to identify in the plasma, despite the continuous operation of the experiment, two completely different states, observed respectively when the electron plasma and the electron cyclotron instabilities, which occur in bursts, are excited. These two instabilities alternate in time. Special attention is paid to the beam velocity distribution function which always has a "plateau-like" character. The largest velocity spread in the beam is attained during the excitation of the electron cyclotron instability. In this case the velocity plateau is explained by the trapping of the beam electrons in the potential well of the cyclotron wave. Under these conditions, the electric field, at the beam centre, is found to be independent of the magnetic field. A radial analysis of the extension of the axial velocity spread in the beam is made for the case of the excitation of the cyclotron instability. Theoretical J_0 Bessel function dependences on the radius are verified for the axial component of the electric field. The beam axial power losses are calculated. These losses are found to decrease with the magnetic field. On the basis of the referred trapping mechanism an explanation is given for this fact as well as for the saturation of the cyclotron instability at an amplitude which is independent of B .

In chapter VI we make a numerical study of the nonlinear interaction between a monoenergetic electron beam and a large amplitude monochromatic traveling wave, in a beam-plasma system of finite length. This study is made to test the validity of the trapping mechanism referred to in chapter V. The main purpose of this numerical analysis is the obtention of both the velocity distribution function of the beam electrons, when leaving the interaction chamber, and the associated value of the beam power losses. We can verify that, even with low values of the electric field (absence of trapping), the velocity distribution function, at the end of the interaction chamber, has always a "plateau-like" character, in agreement with our measurements of chapter IV. For the larger values of the electric field, for which a great percentage of the beam electrons becomes trapped in the wave potential well, we verify that the velocity distribution function is practically symmetric in relation to the wave phase velocity. A good agreement is found between the theoretical and the experimental results concerning the beam velocity distribution function and the beam axial power losses. Therefore the trapping mechanism assumed in chapter V is reasonably supported by this study. Finally it is theoretically proved, just by a simple power balance, that the growth of the wave, at the cost of a part of the kinetic energy of the beam, can not surpass a certain value.

We finish this thesis by presenting, in chapter VII, some measurements of the transverse energy of the beam electrons. The first part of the chapter deals with measurements of the transverse energy at the beam edge. We verify that the transverse energy is maximum at the 1st-2nd regime transition. Correlation measurements made at this regime transition permit us to verify that the transverse energy attained during the electron cyclotron instability bursts is larger than that attained during the electron plasma bursts. The transverse energy is seen to attain relatively large values (of the order of 40% of the beam initial energy). In the second part of this chapter we are concerned with measurements of the transverse energy at the beam centre. Also here we verify that this energy is maximum for conditions leading to the 1st-2nd regime transition. The acquisition of transverse energy by the beam electrons is seen to be directly related with the excitation of the beam-plasma instabilities. The 3-dimensional beam velocity distribution function, at the beam

centre, is determined. We verify that, the transverse velocity of the beam electrons is uncorrelated with their axial velocity. The transverse velocity distribution function of the beam electrons, at the beam centre is found to be constituted by a cold bulk of electrons and a hot Maxwellian tail. The percentage of heated electrons, as well as their temperature, are seen to increase with the magnetic field. The theoretical prediction of a J_1 Bessel function dependence of the transverse electric field on the radius of the plasma column is qualitatively verified.

ACKNOWLEDGEMENTS

It is my pleasant duty to express here my gratitude to all those, who, in one way or another, have contributed to the elaboration of this thesis.

A special acknowledgement is due to Professor dr J. Kistemaker, director of the "FOM-Instituut voor Atoom- en Molecuulfysica" in Amsterdam. Indeed, without his great comprehension and his continuous stimulation this thesis would not yet have been written. To work under his supervision, during more than five years, has been a fruitful experience, which very much contributed to my scientific formation.

I am also very grateful to Professor dr J. Los, for accepting to be "medelezer" of my thesis and for his stimulating interest in my activity in the Institute.

Thankfulness is also due to Dr. H.J. Hopman for his collaboration in almost all my scientific work as well as for his careful reading of the thesis and his sharp criticism.

I am very obliged to Dr. T. Matitti, Dr. E.P. Barbian, Dr. F.G. In-singer, Ir. J.G. Bannenberg and Drs. J.H.A. van Wakeren for the valuable discussion of my experimental results.

The technical help of A.A. Ravenstein, W.G.M. Koperdraad, H.G. Ficke, J.P. van der Fluit, H.J. Timmer and T. Dijkhuis, was highly appreciated and indeed quite indispensable for the perfect working conditions of the experiment.

Thanks are also due to F. Vitalis for his cooperation in the numerical study presented in chapter VI, by developing the associated computer program.

To the personal of the workshop and of the Electronics Laboratorium, respectively directed by A.F. Neuteboom and P.J. van Deenen, my gratitude for their assistance in some specialized problems.

The kindness of the secretary of Professor Kistemaker, Miss A. Klapmuts, who was always ready to help me, as a foreigner, whenever necessary, can not be forgotten.

Finally, in what concerns the materialization of this thesis, I am glad to acknowledge the excellent work of Mrs. C.J. Köke-van der Veer (typing of the text), F.L. Monerie and Th. van Dijk (photographic work and size reduction) and H. Luyten (off-set printing).

AGRADECIMENTOS

Ao concluir os meus estudos na Holanda, queria reconhecidamente agradecer ao Professor M.J. de Abreu Faro todo o interesse que tem manifestado pela minha formação cultural. Como Director do Centro de Estudos de Electrónica e especialmente como Professor do Instituto Superior Técnico, grande tem de facto sido a sua influência na minha carreira científica.

Ao Doutor J.F. Poñe Figanier os meus agradecimentos pelas proveitosas discussões que tivemos sobre alguns assuntos tratados nesta tese.

Agradeço ao Instituto de Alta Cultura a prolongada bolsa de estudos que me foi concedida, condição essencial à realização da presente tese de doutoramento.

CURRICULUM VITAE

With the purpose of satisfying the requirements of the "Faculteit der Wiskunde en Natuurwetenschappen", of the University of Leiden, here follows a short survey of my studies.

After four years of primary school and seven years of secondary studies (Liceum) done at Lourenço Marques, I entered, in 1955, the "Universidade Técnica de Lisboa".

In the "Instituto Superior Técnico" of this University I followed a six-year course on Electrotechnical Engineering.

Immediately after getting my University diploma, in 1962, I was invited to work at the "Centro de Estudos de Electrónica" of the "Comissão de Estudos de Energia Nuclear" of the "Instituto de Alta Cultura", in Lisbon.

Under the supervision of Professor M.J. de Abreu Faro, I worked at this department, during the next three years, being mainly concerned with electronics and its applications to physical research.

In 1965, accepting a scholarship from the "Instituto de Alta Cultura", I came to the Netherlands with the main purpose of getting a specialization on the field of Plasma Physics, at the "FOM-Instituut voor Atoom- en Molecuulfysica" in Amsterdam.

At this Institute I began to work, under the supervision of Professor dr J. Kistemaker, on beam-plasma interaction. This led to the obtention of the "doctorandus" degree from the University of Leiden in 1967.

THE UNIVERSITY OF CHICAGO

with the purpose of studying the development of the "University of Chicago" in the "University of Chicago" of the University of Chicago. The University of Chicago was founded in 1837 and has since that time been one of the leading universities in the world. It has a long and distinguished history and has produced many of the world's leading scholars and scientists. The University of Chicago is a member of the Association of American Universities and is one of the most prominent universities in the United States. It has a large and diverse student body and a wide range of academic programs. The University of Chicago is committed to the highest standards of academic excellence and to the advancement of knowledge and learning. It is a place where students and faculty alike are encouraged to explore the frontiers of knowledge and to make significant contributions to their fields. The University of Chicago is a place where the pursuit of knowledge is a way of life. It is a place where the past meets the future and where the best of both worlds are brought together. The University of Chicago is a place where the future is being shaped and where the world is being made a better place. The University of Chicago is a place where the dream of a better world is being realized. The University of Chicago is a place where the future is bright and where the world is full of hope. The University of Chicago is a place where the future is being written and where the world is being made a better place. The University of Chicago is a place where the dream of a better world is being realized. The University of Chicago is a place where the future is bright and where the world is full of hope. The University of Chicago is a place where the future is being written and where the world is being made a better place.

the 1990s, the number of people in the UK who are aged 65 and over has increased from 10.5 million to 13.5 million, and the number of people aged 75 and over has increased from 4.5 million to 6.5 million (Office for National Statistics 2000).

There is a growing awareness of the need to address the needs of older people, and the need to ensure that the health care system is able to meet the needs of older people. The Department of Health (2000) has published a strategy for older people, which sets out the government's commitment to older people and the need to ensure that the health care system is able to meet the needs of older people.

The strategy for older people is based on the following principles: (1) older people should be able to live independently and actively; (2) older people should be able to access the health care services they need; (3) older people should be able to live in their own homes; (4) older people should be able to participate in the community; (5) older people should be able to live in a safe and secure environment; (6) older people should be able to live in a caring and supportive environment; (7) older people should be able to live in a healthy and safe environment; (8) older people should be able to live in a peaceful and quiet environment; (9) older people should be able to live in a clean and hygienic environment; (10) older people should be able to live in a well-maintained environment.

The strategy for older people is based on the following principles: (1) older people should be able to live independently and actively; (2) older people should be able to access the health care services they need; (3) older people should be able to live in their own homes; (4) older people should be able to participate in the community; (5) older people should be able to live in a safe and secure environment; (6) older people should be able to live in a caring and supportive environment; (7) older people should be able to live in a healthy and safe environment; (8) older people should be able to live in a peaceful and quiet environment; (9) older people should be able to live in a clean and hygienic environment; (10) older people should be able to live in a well-maintained environment.

The strategy for older people is based on the following principles: (1) older people should be able to live independently and actively; (2) older people should be able to access the health care services they need; (3) older people should be able to live in their own homes; (4) older people should be able to participate in the community; (5) older people should be able to live in a safe and secure environment; (6) older people should be able to live in a caring and supportive environment; (7) older people should be able to live in a healthy and safe environment; (8) older people should be able to live in a peaceful and quiet environment; (9) older people should be able to live in a clean and hygienic environment; (10) older people should be able to live in a well-maintained environment.

The strategy for older people is based on the following principles: (1) older people should be able to live independently and actively; (2) older people should be able to access the health care services they need; (3) older people should be able to live in their own homes; (4) older people should be able to participate in the community; (5) older people should be able to live in a safe and secure environment; (6) older people should be able to live in a caring and supportive environment; (7) older people should be able to live in a healthy and safe environment; (8) older people should be able to live in a peaceful and quiet environment; (9) older people should be able to live in a clean and hygienic environment; (10) older people should be able to live in a well-maintained environment.

The strategy for older people is based on the following principles: (1) older people should be able to live independently and actively; (2) older people should be able to access the health care services they need; (3) older people should be able to live in their own homes; (4) older people should be able to participate in the community; (5) older people should be able to live in a safe and secure environment; (6) older people should be able to live in a caring and supportive environment; (7) older people should be able to live in a healthy and safe environment; (8) older people should be able to live in a peaceful and quiet environment; (9) older people should be able to live in a clean and hygienic environment; (10) older people should be able to live in a well-maintained environment.

The strategy for older people is based on the following principles: (1) older people should be able to live independently and actively; (2) older people should be able to access the health care services they need; (3) older people should be able to live in their own homes; (4) older people should be able to participate in the community; (5) older people should be able to live in a safe and secure environment; (6) older people should be able to live in a caring and supportive environment; (7) older people should be able to live in a healthy and safe environment; (8) older people should be able to live in a peaceful and quiet environment; (9) older people should be able to live in a clean and hygienic environment; (10) older people should be able to live in a well-maintained environment.

